

AD-A020 941

**BOMB DAMAGE REPAIR (BDR) DAMAGE PREDICTION. VOLUME I.
TECHNICAL DISCUSSION**

George W. Brooks, et al

Martin Marietta Aerospace

Prepared for:

Air Force Civil Engineering Center

October 1975

DISTRIBUTED BY:

NTIS

**National Technical Information Service
U. S. DEPARTMENT OF COMMERCE**

058159

AFCEC-TR-75-24



**BOMB DAMAGE REPAIR (BDR)
DAMAGE PREDICTION**

VOLUME I, - TECHNICAL DISCUSSION

MARTIN MARIETTA CORPORATION
ORLANDO DIVISION
ORLANDO, FLORIDA 32805

OCTOBER 1975



FINAL REPORT: FEBRUARY 1975 - OCTOBER 1975

Distribution unlimited; approved for public release.



AIR FORCE CIVIL ENGINEERING CENTER
(AIR FORCE SYSTEMS COMMAND)
TYNDALE AIR FORCE BASE
FLORIDA 32805

Reproduced by
**NATIONAL TECHNICAL
INFORMATION SERVICE**
U S Department of Commerce
Springfield VA 22151

ADA020941

UNCLASSIFIED

SECURITY CLASSIFICATION OF THIS PAGE (When Data Entered)

REPORT DOCUMENTATION PAGE		READ INSTRUCTIONS BEFORE COMPLETING FORM
1. REPORT NUMBER AFCEC-TR-75-24	2. GOVT ACCESSION NO.	3. RECIPIENT'S CATALOG NUMBER
4. TITLE (and Subtitle) BOMB DAMAGE REPAIR (BDR) DAMAGE PREDICTION Volume I - Technical Discussion		5. TYPE OF REPORT & PERIOD COVERED Final Report 15 Feb 1975 - 15 Oct 1975
7. AUTHOR(s) George W. Brooks John E. Cunningham Paul W. Mayer		6. PERFORMING ORG. REPORT NUMBER
9. PERFORMING ORGANIZATION NAME AND ADDRESS Martin Marietta Corporation Orlando Division Orlando, Florida 32805		8. CONTRACT OR GRANT NUMBER(s) F3960- F2901-75-C-0053
11. CONTROLLING OFFICE NAME AND ADDRESS Air Force Civil Engineering Center (AFSC) Tyndall AFB, Florida 32401		10. PROGRAM ELEMENT, PROJECT, TASK AREA & WORK UNIT NUMBERS Program Element 63723F Project 21042B16
14. MONITORING AGENCY NAME & ADDRESS (if different from Controlling Office)		12. REPORT DATE October 1975
		13. NUMBER OF PAGES 139 139
		15. SECURITY CLASS. (of this report) UNCLASSIFIED
		15a. DECLASSIFICATION/DOWNGRADING SCHEDULE
16. DISTRIBUTION STATEMENT (of this Report) Approved for public release; distribution unlimited.		
17. DISTRIBUTION STATEMENT (of the abstract entered in Block 20, if different from Report) DDC RECEIVED FEB 24 1976 REGULATORY C		
18. SUPPLEMENTARY NOTES Available in DDC		
19. KEY WORDS (Continue on reverse side if necessary and identify by block number) Civil Engineering Weapon Effects Soil Mechanics		
20. ABSTRACT (Continue on reverse side if necessary and identify by block number) Several test programs have been conducted in recent years to define the level of damage sustained by airfield pavement systems which are subjected to conventional weapon detonations. Knowledge of airfield damage and the capability to predict damage from possible hostile attack are required to allow Bomb Damage Repair (BDR) personnel to plan base recovery activity and rapid runway repair. The objective of the effort reported herein was to collect existing data on airfield pavement effects, as functions of pavement and weapon parameters, identify those		

DD FORM 1 JAN 73 1473

EDITION OF 1 NOV 65 IS OBSOLETE

UNCLASSIFIED

SECURITY CLASSIFICATION OF THIS PAGE (When Data Entered)

20. ABSTRACT (Concluded)

parameters having a significant effect on pavement damage, repair time and effort, and generate damage prediction relationships for use by BDR engineers. During this effort the collected data were placed in a consistent format in a computerized data file. By plotting the data and subjecting them to various analytical procedures, significant parameters affecting damage were identified. Mathematical relationships were developed between the data, and damage prediction nomographs were generated for the three repair levels considered. These prediction relationships are in a format readily usable by field personnel and enable rapid damage prediction computations and subsequent runway repair planning operations. Recommendations are presented for expanding the data base and for completing additional analysis to further enhance applicability of the developed methodology.

ACQUISITION BY
NTIS
DPO
MAY 1980
JULY 1980
BY
EX
AVAILABILITY GROUP
M 311

A

FOREWORD

This final report was prepared by the Martin Marietta Corporation, Orlando, Florida, and documents work completed under Contract Number F29601-75-C-0053 with the Air Force Civil Engineering Center, Tyndall Air Force Base, Florida. The effort originated with the Air Force Weapons Laboratory, Kirtland Air Force Base, New Mexico, which had program responsibility prior to reorganization and transfer to AFCEC.

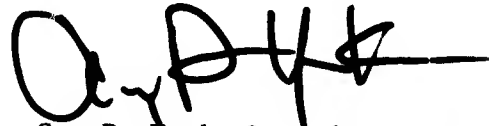
This document was prepared by Messrs. George W. Brooks, John E. Cunningham, and Paul W. Mayer, under the direction of Mr. William R. Porter, Chief of Warhead Technology for Martin Marietta Corporation, Orlando, Florida. The authors are indebted to several persons and organizations for their assistance in completing the reported effort, particularly for help in locating pertinent data. These sources include Lt. Raymond S. Rollings of AFCEC, who was the Project Officer in-charge and is currently responsible for much BDR development work; Captain L. D. Hokanson, AFIT, Wright-Patterson Air Force Base, Ohio, who has been involved with BDR for several years and who supplied much data and insight into the problems; Mr. L. K. Davis, U.S. Army Engineer Waterways Experiment Station, Vicksburg, Mississippi who provided data and valuable discussions concerning pavement damage analysis; numerous persons at the Air Force Armament Laboratory, Eglin Air Force Base, Florida, who are associated with airfield vulnerability and analysis of munition effects (including Government/Contractor personnel at the Nonnuclear Munitions Information Analysis Center); and personnel of the Air Force Flight Dynamics Laboratory, Wright-Patterson Air Force Base, Ohio, who supplied data on runway roughness effects.

This report is published in two volumes; the first contains the main technical discussion, and the second consists of two appendices presenting supporting technical data.

This technical report has been reviewed and is approved for publication.



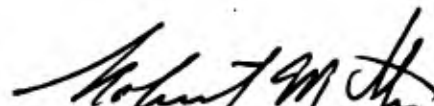
Raymond S. Rollings, 1Lt USAF
Project Officer



Guy P. York, Lt Col USAF
Director, Engrg Materials



Robert E. Brandon
Technical Director



Robert M. Iten, Col USAF
Commander

TABLE OF CONTENTS

Section	Title	Page
I	INTRODUCTION	10
	1. Background	10
	2. Objective	12
	3. Approach	12
II	PAVEMENT REPAIR PROCEDURES	13
	1. Repair Procedure Requirements	13
	2. Repair Procedures	15
III	DATA COLLECTION AND CLASSIFICATION	20
	1. Data Sources and Availability	20
	2. Data File	35
	3. Significant Parameter Identification	48
IV	ANALYSIS AND CORRELATION OF DATA	54
	1. Analytical Methodology	54
	2. Reduced Plots - Functional Relationships	57
	3. Fuzing Reliability and Penetration Capability	100
V	DAMAGE PREDICTION RELATIONSHIPS	104
	1. Derivation and Use of Nomographs	104
	2. Damage Prediction Nomographs	106
VI	CONCLUSIONS AND RECOMMENDATIONS	131
	1. Conclusions	131
	2. Recommendations	132
	REFERENCES	135

LIST OF ILLUSTRATIONS

Figure	Title	Page
1	Crater Dimension Definitions	16
2	Camouflet Dimension Definitions	16
3	Typical Runway Crater and Illustration of Available Photographic Data	28
4	Reproduction of Damage Sketch Provided by AFWL for Hays and Fort Sumner Tests	29
5	Pavement Removal Area Definition	30
6	Volume of Earth Removed Definition	31
7	Illustrations of Methods of Estimating Apparent Crater Volume When Only Depth and Radius Were Available	33
8	Volume of Earth Replaced Definitions	34
9	Schematic of Computerized Data Manipulation System	36
10	Data File Record Illustration	42
11	Pavement Crater Types (WES Format)	44
12	Illustration of BDRPLOT Output Format	49
13	Weapon Weight Distribution for Hays and Fort Sumner Tests	52
14	Depth of Burst Distribution for Hays and Fort Sumner Tests	52
15	Pavement Thickness Distribution for Hays and Fort Sumner Tests	53
16	Soil Type Distribution for Hays and Fort Sumner Tests	53
17	Comparison of Second-Order and Exponential Curve Fits to Reduced Earth Replacement Volume for Organic Clay Subbase	59
18	Comparison of Second-Order and Exponential Curve Fits to Reduced Earth Replacement Volume for Silty, Clayey Sand Subbase	60
19	Residual Distribution for Second-Order Approximation, Semipermanent Earth Replacement Volume, Organic Clay Subbase	62

LIST OF ILLUSTRATIONS (Continued)

Figure	Title	Page
20	Residual Distribution for Exponential Approximation, Semipermanent Earth Replacement Volume, Organic Clay Subbase	63
21	Residual Distribution for Second-Order Approximation, Semipermanent Earth Replacement Volume, Silty, Clayey Sand Subbase	64
22	Residual Distribution for Exponential Approximation, Semipermanent Earth Replacement Volume, Silty, Clayey Sand Subbase	65
23	Reduced Ejecta Volume Versus Reduced Depth of Burst; Organic Clay Subbase	67
24	Reduced Ejecta Volume Versus Reduced Depth of Burst; Silty, Clayey Sand Subbase	68
25	Reduced Earth Replacement Volume for Semipermanent Repair Versus Depth of Burst; Organic Clay Subbase	69
26	Reduced Earth Replacement Volume for Semipermanent Repair Versus Depth of Burst; Silty, Clayey Sand Subbase	70
27	Reduced Earth Removal Volume for Semipermanent Repair Versus Depth of Burst; Organic Clay Subbase	71
28	Reduced Earth Removal Volume for Semipermanent Repair Versus Depth of Burst; Silty, Clayey Sand Subbase	72
29	Reduced Earth Removal Volume for Expedient Repair Versus Depth of Burst; Organic Clay Subbase	73
30	Reduced Earth Removal Volume for Expedient Repair Versus Depth of Burst; Silty, Clayey Sand Subbase	74
31	Reduced Earth Removal Volume for Permanent Repair Versus Depth of Burst; Organic Clay Subbase	75
32	Reduced Earth Removal Volume for Permanent Repair Versus Depth of Burst; Silty, Clayey Sand Subbase	76
33	Reduced Pavement Repair Area for Expedient Repair Versus Depth of Burst; Organic Clay Subbase	77

LIST OF ILLUSTRATIONS (Continued)

Figure	Title	Page
34	Reduced Pavement Repair Area for Expedient Repair Versus Depth of Burst; Silty, Clayey Sand Subbase	78
35	Reduced Pavement Repair Area for Semipermanent Repair Versus Depth of Burst; Organic Clay Subbase	79
36	Reduced Pavement Repair Area for Semipermanent Repair Versus Depth of Burst; Silty, Clayey Sand Subbase	80
37	Reduced Pavement Repair Area for Permanent Repair Versus Depth of Burst; Organic Clay Subbase	81
38	Reduced Pavement Repair Area for Permanent Repair Versus Depth of Burst; Silty, Clayey Sand Subbase	82
39	Reduced Earth Replacement Volume for Expedient Repair Versus Depth of Burst; Organic Clay Subbase	83
40	Reduced Earth Replacement Volume for Expedient Repair Versus Depth of Burst; Silty, Clayey Sand Subbase	84
41	Reduced Earth Replacement Volume for Permanent Repair Versus Depth of Burst; Organic Clay Subbase	85
42	Reduced Earth Replacement Volume for Permanent Repair Versus Depth of Burst; Silty, Clayey Sand Subbase	86
43	Reduced Pavement Removal Area for Expedient Repair Versus Depth of Burst; Organic Clay Subbase	87
44	Reduced Pavement Removal Area for Expedient Repair Versus Depth of Burst; Silty, Clayey Sand Subbase	88
45	Reduced Pavement Removal Area for Semipermanent Repair Versus Depth of Burst; Organic Clay Subbase	89
46	Reduced Pavement Removal Area for Semipermanent Repair Versus Depth of Burst; Silty, Clayey Sand Subbase	90
47	Reduced Pavement Removal Area for Permanent Repair Versus Depth of Burst; Organic Clay Subbase	91

LIST OF ILLUSTRATIONS (Concluded)

Figure	Title	Page
48	Reduced Pavement Removal Area for Permanent Repair Versus Depth of Burst; Silty, Clayey Sand Subbase	92
49	Semipermanent Earth Replacement Volume Function; Exponential Approximation Residuals as a Function of Pavement Thickness	97
50	Fourth-Root Reduced Semipermanent Earth Replacement Volume	99
51	Bomb Damage Repair Nomograph; Instructional Example	105
52	Bomb Damage Repair Nomograph; Ejecta Volume	107
53	Bomb Damage Repair Nomograph; Earth Replacement Volume, Expedient Repair	109
54	Bomb Damage Repair Nomograph; Earth Replacement Volume, Semipermanent Repair	111
55	Bomb Damage Repair Nomograph; Earth Replacement Volume, Permanent Repair	113
56	Bomb Damage Repair Nomograph; Earth Removal Volume, Expedient Repair	115
57	Bomb Damage Repair Nomograph; Earth Removal Volume, Semipermanent Repair	117
58	Bomb Damage Repair Nomograph; Earth Removal Volume, Permanent Repair	119
59	Bomb Damage Repair Nomograph; Pavement Repair Area, Expedient Repair	121
60	Bomb Damage Repair Nomograph; Pavement Repair Area Semipermanent Repair	123
61	Bomb Damage Repair Nomograph; Pavement Repair Area, Permanent Repair	125
62	Bomb Damage Repair Nomograph; Pavement Removal Area, Semipermanent Repair	127
63	Bomb Damage Repair Nomograph; Pavement Removal Area, Permanent Repair	129

LIST OF TABLES

Table	Title	Page
1	Repair Parameter List Showing Parameters and Repair Level(s) to Which They are Pertinent	19
2	Available BDR Data Sources	21
3	Data Available for All Tests Having Good or Fair Estimated Reliabilities	25
4	Data File Storage Location Keys	38
5	Data File Reference List	45
6	Curve Fitting Functions	47
7	Weapon Parameters	51
8	Target Parameters	51
9	Hays and Fort Sumner Test Parameters (115 Tests)	51
10	Earth Replacement Volume, Semipermanent Repair; Comparison of Approximating Functions	61
11	Bomb Damage Repair Prediction Relationships, Exponential Function Approximation	94
12	Example Soil and Nose Constants	101
13	Equivalent Weight of TNT for Selected Explosives	106

SECTION I
INTRODUCTION

1. BACKGROUND

The United States Air Force has become increasingly concerned with the repair of bomb damaged airfield pavements, due to the critical role of the pavement in maintaining an air operations capability following a possible enemy attack. In such a situation, Air Force personnel would be required to repair bomb damaged runway surfaces in minimal time to allow high-speed aircraft with high gross takeoff configurations to resume operations. Thus, it is necessary to accurately predict expected damage levels to known pavement systems from applicable weapon parameters, so that efficient and adequate bomb damage repair (BDR) procedures can be established and repair times estimated.

Until recently there had been little effort in the general area of BDR, and no programs were designed specifically to enable quick and accurate prediction of expected damage levels from hostile attack against airfield pavement systems. Most early work was concerned with cratering effects in various soils, without pavement overlays, and was done either to predict damage to targets other than pavement or for scaling to nuclear weapon yields. The limited early pavement cratering work which was done (ref. 1 - 4) emphasized the repair activities; the recording of cratering data was sparse, with the crater generated merely to have a damaged area to repair. Most of these tests involved large explosive weights. The first planned experimental program to define pavement damage from small, penetrating weapons (ref. 5) was conducted by the Air Force Weapons Laboratory (AFWL) in support of a weapons development program at the Air Force Armament Laboratory, Eglin Air Force Base, Florida. Only after 1971, when the Air Force Weapons Laboratory was assigned responsibility for BDR activities, was there a direct systematic development program to define damage to pavement systems from various weapons, by combining weapon parameters with pavement design elements.

Since it was not clear whether the test results from these earlier small-scale tests based on 1 1/2 pounds of explosive could be reliably extrapolated to larger weapons, additional experimental programs were accomplished. The first was a full-scale field test utilizing existing

abandoned runways at Ft. Sumner, New Mexico, and Hays (Walker Air Base), Kansas, as test sites. The second effort was a small scale modeling study conducted at the Civil Engineering Research Facility (CERF) located at Kirtland Air Force Base, New Mexico. The results of these tests (ref. 6) were expected to show a possible relationship between the small-scale and full-scale tests but were unfortunately inconclusive and indicated a need for further testing and analysis. Succeeding work included a similitude analysis to define the influence of pavement on crater size (ref. 7) and an evaluation of soil parameter effects on pavement cratering (ref. 8). Additional test work to help define the effects of pavement design on damage was completed (ref. 9), and additional field testing of BDR procedures and methods (ref. 9 - 12) was conducted at the Air Force Civil Engineering Center, Tyndall Air Force Base, Florida.

During this period an analysis of runway vulnerability (from the offensive viewpoint) was conducted by the U.S. Army (ref. 13), providing additional analytical methodology for evaluating the BDR problem. A pavement damage test program was also conducted by the contractor during this period (ref. 14) as a portion of IR&D runway penetrator development effort. Other related activity includes pavement material properties studies by the Naval Weapons Center, various munitions development programs by the Air Force Armament Laboratory, and pavement roughness effects analyses done by the Air Force Flight Dynamics Laboratory.

Air Force base civil engineers are responsible for maintaining capability to recover bomb damaged airfields in a minimal time frame; currently this is interpreted to be completion of expedient repair* of three 750-pound bomb craters within 4 hours (ref. 15). Based on test results obtained by AFWL, the level of damage from many small, penetrating weapons is expected to be several times that of the standard threat (ref. 11). Thus, revision to the rapid runway repair procedure to include the effects of a range of weapon sizes on various pavements, as well as upgrading in other areas, is needed. Damage prediction techniques are the key factors for defining expected levels of damage from possible attack and for determining the requirements for different types of pavement repair. In general they are also needed in order to plan required base recovery activities and bomb damage repair techniques.

* Expedient repair: in this case consists of removing damaged pavement, filling the crater, and covering with landing mat.

2. OBJECTIVE

The objective of this program was to collect existing data on the damage to airfield pavement systems generated by conventional weapons, analyze the data to determine significant parameters, and generate either mathematical or graphical relationships between expected damage parameters and weapon and pavement properties. Relationships generated were to be in a form readily usable by field personnel.

3. APPROACH

In approaching this three-phase effort - data collection and classification, analysis and correlation of data (significant relationship identification), and damage prediction relationship generation - the immediate problem was to sort through the large amount of existing data and put these data in a readily retrievable form. The data were collected by various organizations for many objectives, and there was a general lack of consistency in the way data were presented. To avoid pitfalls of using data previously manipulated by others, or which had been analyzed based on different definitions and assumptions, raw data were used whenever possible. All data collected were placed in a computerized data bank, carefully referenced, and made available in a consistent format for later analysis. Parameters were plotted and evaluated, and those for which a significant effect on damage levels could be identified were so labeled. Damage levels, repair procedures, and roughness criteria were established, and appropriate relationships were generated between them and their causative effects. Specific details of the program are discussed in the following sections of this report, and the field-usable damage prediction relationships generated are presented. The collected data and significant parameter relationships are presented in raw data form, in the appendices, as basic data plots.

SECTION II
PAVEMENT REPAIR PROCEDURES

1. REPAIR PROCEDURE REQUIREMENTS

During previous efforts to reduce runway crater data, various criteria (often unstated) were used to define damage magnitudes. For example, the values of such parameters as "pavement upheaval," "pavement blown out," "pavement fractured," and "pavement severely damaged" were used in describing runway surface damage. Exact criteria for determination of these values were not defined in detail. The initial survey of available information determined that values reported for these terms were not sufficiently consistent to be used throughout compilation of data. Raw data were, therefore, used to the maximum possible degree to obtain consistency. Therefore, an additional study requirement as reported herein was to define damage corresponding to three different repair levels:

- (1) Expedient - Runway to be marginally serviceable for immediate aircraft operations, further repair to be effected as soon as conditions permit;
- (2) Semipermanent - Runway to be made serviceable in an intermediate period of time and remain serviceable for the duration of a particular operation;
- (3) Permanent - Runway to be restored to its original condition.

None of the earlier test data collection was accomplished using criteria consistent with three separate damage levels, further emphasizing the necessity to use raw data when available.

Reduction of raw test data to damage values which fit the three defined repair levels resulted in a requirement to define runway defeat criteria for each level. Extensive discussions were held with the Air Force Weapons Laboratory (AFWL) BDR project office personnel and with several other organizations involved in BDR-related activities to determine runway defeat criteria. Organizations contacted included, in addition to AFWL, the U.S. Army Engineer Waterways Experiment Station (WES), Air Force Flight Dynamics Laboratory (AFFDL), and Air Force Armament Laboratory (AFATL).

As a result of these discussions, it was learned that no firm data were available to define runway damage limits for aircraft operations. Work was underway both at AFWL and WES to establish such criteria, but results were not yet available. WES suggested using a pavement elevation differential of 1.5 inches over a 70 foot span as the point at which aircraft begin to experience operational difficulty. This was based on results of a British evaluation of the runway roughness problem. WES arbitrarily tripled this elevation differential (to 4.5 inches) to define a certain defeat criterion for fighter aircraft. Limited data on runway roughness have been computed (ref. 16, 17) using a computer code (TAXI) developed for AFWL by AFFDL (ref. 18). These efforts were concerned with aircraft response to a BDR patch (1.5 inches in height) and tended to support the 1.5-inch elevation differential as being a point where aircraft could experience some operational problems.

On the basis of the above discussions, the following definitions of repair requirements for each repair level were established:

- a. Expedient repair - Loose, spalled, or fractured pavement must be repaired; slightly damaged pavement which is upheaved less than 4.5 inches over the span of one slab need not be replaced. No effort to excavate or rebuild the pavement subbase will be made, other than to fill the apparent crater.
- b. Semipermanent repair - Loose, spalled or fractured pavement must be repaired along with all pavement upheaved more than 1.5 inches over the span of one slab. Some excavation and repair of the subbase will be accomplished, but a permanent repair will still be required at some later time.
- c. Permanent repair - Pavement, base, and subbase must be restored to their original condition. All damaged pavement must be replaced. (Damaged pavement is defined as that which is upheaved or separated by explosively induced cracks which divide the pavement into 6 or more sections, per AFR 93-5.)

These repair criteria were based on the limited information available and, although not firmly substantiated by existing roughness data, they provide a basis for evaluation of crater data. When firm roughness data become

available, the range of criteria selected here will provide a means of interpolation to estimate repair effort requirements.

The final objective of this program was to develop mathematical or graphical relationships for prediction of pavement damage. The relationships were to be in forms most usable for repair effort estimation, so it was necessary to select specific damage parameters which best characterized the magnitude of a repair effort. It was therefore helpful to relate each repair level to a specific repair procedure in order to identify the damage parameters of interest. A discussion of the assumed procedure used to effect each level of runway repair is contained in the next subsection.

2. REPAIR PROCEDURES

Major steps in a procedure to effect each level of repair were assumed for the purpose of identifying damage parameters which are most pertinent to BDR repair time estimation. Procedures assumed were based on available information on current or projected methods used for BDR work, obtained from technical reports (ref. 11 - 15), from review of photographs and movie films of BDR exercises, and from technical discussions held with the AFWL project office. In Figure 1 a view of a generic subpavement crater is presented to introduce crater dimension nomenclature used in this report. Figure 2 presents a cross-section of a typical camouflet showing similar dimensional information. The assumed procedures are enumerated below, followed by a list of damage parameters with values pertinent to repair time estimation.

Expedient repair procedure:

- a. Remove any pavement material which is loose, spalled, or badly fractured, or which is upheaved to an elevation differential of over 4.5 inches over the span of one slab;
- b. Sweep remaining surface clear of all ejecta;
- c. Backfill crater to original level of bottom of pavement with any available fill, or;
- d. Fill camouflet with wet sand or similar compactable material;
- e. Compact with available equipment and top with resin concrete, quick-set cement, or other repair material, or backfill to original pavement surface with select fill and cover with mat.

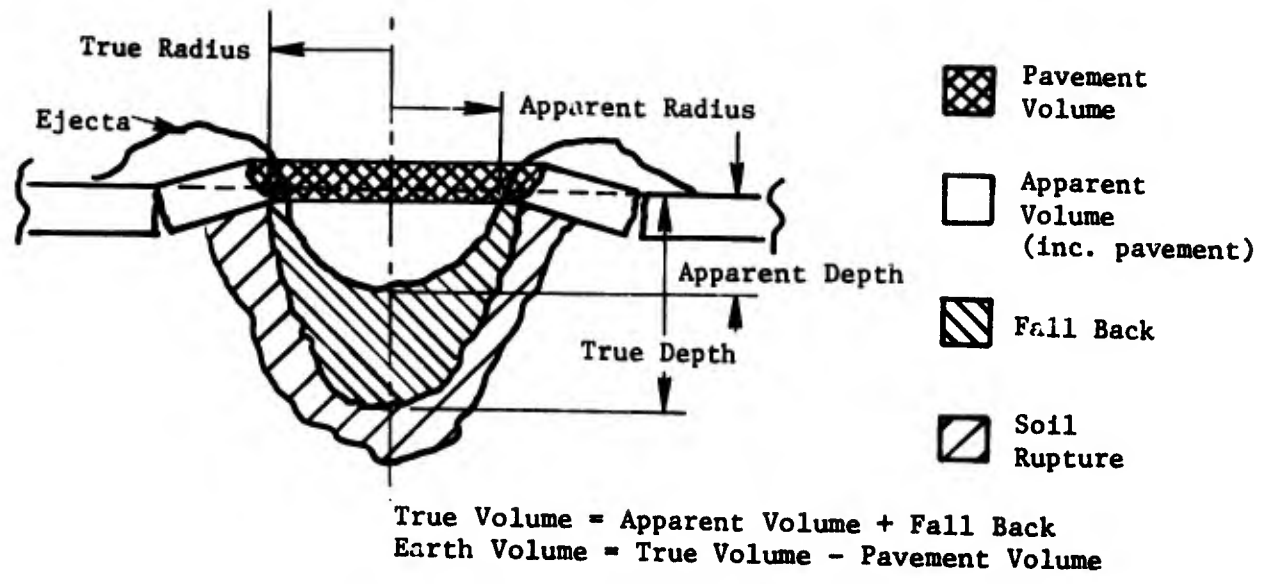


Figure 1. Crater Dimension Definitions

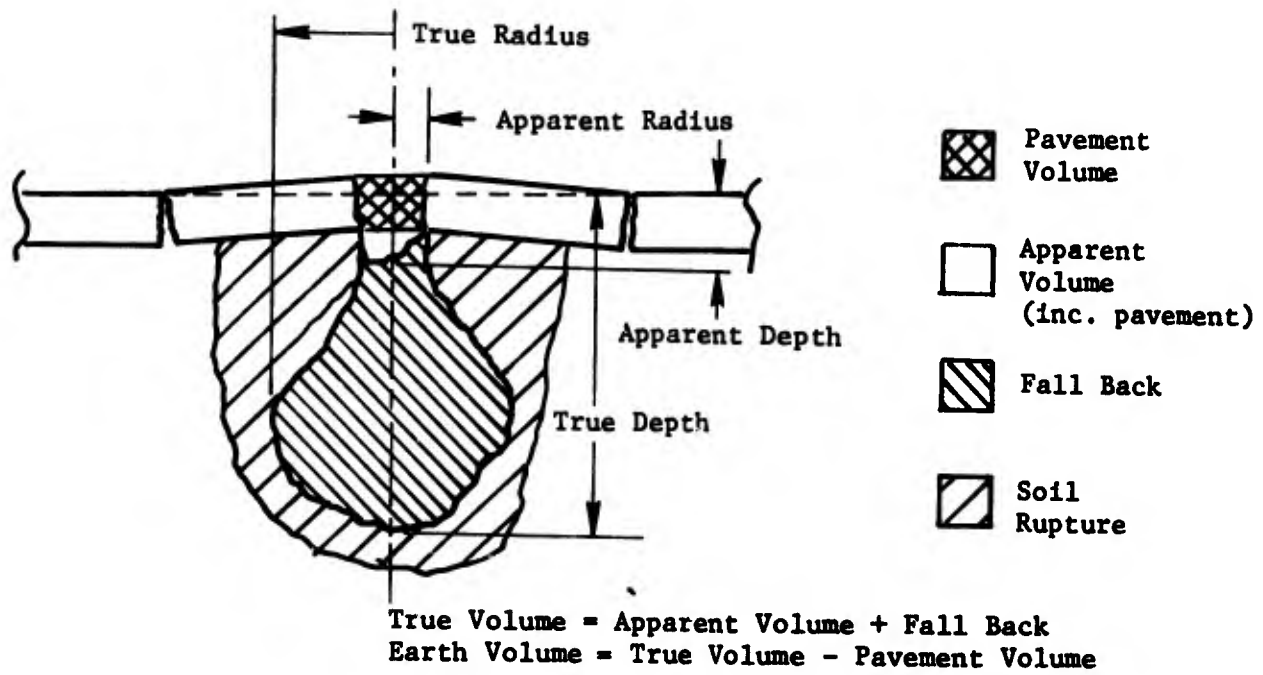


Figure 2. Camouflet Dimension Definitions

Knowledge of the magnitudes of the following parameters would be required to estimate the time required to effect an expedient repair using the above procedure:

- a. Pavement removal area;
- b. Ejecta volume;
- c. Ejecta distribution;
- d. Volume of subbase (earth) material replaced;
- e. Pavement repair area.

Semipermanent repair procedure:

- a. Remove any pavement slab which contains loose, spalled, or badly fractured material which covers a camouflet or which is upheaved such that the elevation differential is more than 1.5 inches over its span;
- b. Sweep remaining surface clear of all ejecta.
- c. Excavate crater, removing fall-back volume;
- d. Fill true crater with select fill and compact by machine;
- e. Replace pavement.

Knowledge of the magnitudes of the following parameters would be required to estimate the time required to effect a semipermanent repair using the above procedure:

- a. Pavement removal area;
- b. Ejecta volume;
- c. Ejecta distribution;
- d. Volume of earth removed to clear the fall-back;
- e. Volume of fill required to fill the true earth crater;
- f. Pavement repair area.

Permanent repair procedure:

- a. Remove all damaged pavement (the limit of undamaged pavement is slabs which have cracks but are not upheaved or cracked in such a way that 6 separate pieces of pavement exist);
- b. Sweep remaining surface clear of all ejecta;

- c. Excavate crater, removing all ruptured material;
- d. Rebuild base and subbase;*
- e. Replace pavement.

Knowledge of the magnitudes of the following parameters would be required to estimate the time required to effect a permanent repair using the above procedure:

- a. Pavement removal area;
- b. Ejecta volume;
- c. Ejecta distribution;
- d. Volume of earth removed to excavate crater;
- e. Base and subbase repair volume;
- f. Pavement repair area.

Using the damage parameter lists which were identified from the assumed procedure for each repair level, a list of all parameters which affect BDR time estimation was compiled. Table 1 lists the damage parameters which were identified as significant and for which prediction relationships would be meaningful to BDR field personnel.

* The following terms are used to describe the runway foundation in this report:

Base - Specially prepared material, usually gravel or stone, placed directly under pavement in a thin (6 - 12 inch) layer.

Subbase - Material which directly underlies the pavement or base when applicable (may be prepared or in-situ).

Soil - Material underlying the subbase if a definite strata exists, always in-situ.

TABLE 1. REPAIR PARAMETER LIST SHOWING PARAMETERS
AND REPAIR LEVEL(S) TO WHICH THEY ARE PERTINENT

Parameter	Level of Repair		
	Expedient Repair	Semipermanent Repair	Permanent Repair
Ejecta Volume	X	X	X
Ejecta Distribution	X	X	X
Expedient Pavement Removal Area	X		
Semipermanent Pavement Removal Area		X	
Permanent Pavement Removal Area			X
Expedient Earth Removal Volume	X		
Semipermanent Earth Removal Volume		X	
Permanent Earth Removal Volume			X
Expedient Pavement Repair Area	X		
Semipermanent Pavement Repair Area		X	
Permanent Pavement Repair Area			X
Expedient Earth Replacement Volume	X		
Semipermanent Earth Replacement Volume		X	
Permanent Earth Replacement Volume			X

SECTION III
DATA COLLECTION AND CLASSIFICATION

1. DATA SOURCES AND AVAILABILITY

The initial phase of the BDR Damage Prediction effort involved a literature survey directed toward collection of all available test data regarding damage to runway pavement systems caused by explosive blasts. These efforts resulted in identification of 11 known sources of test data from which information was obtained. Table 2 lists these sources by test site and number of test cases available. Tests at Hays, Kansas; Fort Sumner, New Mexico; and the Civil Engineering Research Facility, Kirtland Air Force Base, New Mexico, were conducted under the direction of AFWL specifically to collect bomb damage data. Other tests were conducted primarily for different purposes, with some damage data collected.

a. Hays, Kansas

These tests (ref. 6 and 8) produced much raw data, including field notes, computer printout of crater profiles, and photographs (supplied by AFWL). The test site was an abandoned World War II Portland cement concrete (PCC) runway. Slabs, poured in place, were about 20 feet long by 12.5 feet wide and from 8.0 to 11.0 inches thick. There was no prepared runway base, but slabs were poured directly on a 5-foot thick organic clay subbase. Beneath this was a 12-foot silty clay soil layer overlying 3 feet of sand. Beneath the sand was a deep layer of shale and lime sandstone. A limited number of test borings were made to define the subbase soil, and no attempts were made to describe the properties of these materials for each individual cratering test. The pavement was more than 20 years old. Test cylinders indicated it had a high compressive strength; concrete properties were not measured for individual slabs under which cratering tests were performed. Weapons tested included 5-, 15-, and 25-pound bare composition C4 charges along with MK 81, MK 82 and M117 GP bombs having explosive weights of 100, 192, and 386 pounds of TNT, respectively. All weapons were hand emplaced at a zero degree (vertical) obliquity near the center of the runway slabs. Depths of burst ranged from 10 to 120

TABLE 2. AVAILABLE BDR DATA SOURCES

	Number of Test Cases Available
Hays, Kansas	79
Fort Sumner, New Mexico	36
Civil Engineering Research Facility, New Mexico (1.5 Pound Tests)	21
Civil Engineering Research Facility, New Mexico (15/45 Pound Tests)	28
Tyndall Air Force Base, Florida	13
Martin Marietta, Orlando, Florida	5
Fort Bragg, North Carolina	1 (5)*
Eglin Air Force Base, Florida (Static) 1963	3
Eglin Air Force Base, Florida (Static) 1965	1 (?)
Eglin Air Force Base, Florida (Air Drop) 1965	1 (2)
Naval Civil Engineering Laboratory	5

* Numbers in parentheses indicate actual number of tests fired; data were averaged and considered as one case to prevent biasing overall file toward less reliable information.

inches for the C4 charges and 9 to 21 feet for the bombs. Information available to characterize damage included the true crater profile and its depth, radius and volume. Apparent crater radius, depth and volume were available for some tests. Additionally, earth and pavement crater volumes were reported.

b. Fort Sumner, New Mexico

Information about these tests was from Reference 6 and AFWL raw data. This was another World War II vintage runway. The pavement slabs were PCC having a planform 20 feet long and 10 feet wide and a thickness of 7 inches. There was no prepared base and the subbase was a 10-foot thick layer of a medium silty, clayey sand overlying a layer of medium dense sand, followed by gravelly and silty sand. Some pockets of a lean clay material were reported at depths of about 4 to 9 feet; however, which tests this material may have affected was not reported. Other test conditions and data reports were similar to those at Hays except that no GP bombs were tested.

c. Civil Engineering Research Facility 1.5 Pound Tests

Bare composition C4 charges weighing 1.5 pounds were tested at a 30-inch depth of burst (ref. 5). Specifically constructed 25-foot square PCC slabs were laid over a gravel base which varied in thickness from 6 to 12 inches. Slabs, having thicknesses of from 8 to 14 inches, were cured at least 28 days and had strengths around 4000 psi. Some had a 4-inch asphaltic cement concrete (ACC) overlayment. Various joint types were tested. Two subbase configurations were tested, one consisting of 6 feet of prepared clay overlying silty sand soil, and the other in-situ silty sand.

d. Civil Engineering Research Facility 15/45 Pound Tests

Twenty-six tests were conducted to determine the effects of various pavement constructions on cratering effects (ref. 9). Slab planforms were 10 by 10 feet and 30 by 30 feet, with thicknesses of 8 and 12 inches. All 10-foot slabs were PCC, with some having overlays of ACC and PCC. Thirty-foot (continuous) slabs were PCC, continuously reinforced concrete (CRCP) or fiber reinforced concrete (FRCP). The PCC section had an overlay of CRCP separated from the PCC layer by 2 inches of ACC. Several joint types were incorporated in construction of test pads; these

included dowel and key, sawcut, and construction joints. All slabs were 28-day cure concrete laid on a 6- to 12-inch thick prepared gravel base. The two subbases (clay over silty sand, and silty sand) used in the CERF 1.5 pound tests were also employed in these experiments. Test charges were 15 pounds of bare composition C4 explosive buried 84 inches beneath the pavement surface. Test pads for the 10-foot slab systems were 5 slabs wide by 11 long, and experiments were in every other slab, making it difficult to isolate the results of particular tests in some cases.

Additionally, two 45-pound C4 charges were detonated under the continuous pavement systems. These tests reused previously-tested slabs and were thus not considered very reliable. No original field data were available for any of the CERF tests; however, considerable raw data were given in the reference reports. Thus, the reliability of information obtained was estimated to be fairly good.

e. Tyndall Air Force Base

Fourteen pavement cratering tests were performed at Tyndall Air Force Base, Florida, (ref. 11) with the primary purpose of creating craters for BDR exercises. The pavement system was various sizes of 8 and 12 inch thick PCC slabs with an ACC overlay. All slabs were placed on a prepared gravel base overlying either clay or sand subbase.

Cratering charges were 15- and 25-pound bare charges and statically detonated M117 GP bombs containing 386 pounds of TNT. Only limited crater data including the apparent crater dimensions, ejecta volume, and pavement repair area were reported. In addition, in several test cases, a very large excavation was made to place the charge, and in one case an M117 bomb was detonated under a previous repair patch. For these reasons, the reliability of data obtained from these tests was estimated to be only fair. The case where a bomb was detonated under a previous patch was not included in the data compilation; therefore, only 13 cases were obtained.

f. Martin Marietta

Five runway cratering tests were conducted by the Martin Marietta Corporation in support of a runway penetrator munition development program (ref. 14). The pavement system consisted of 28-day cure

doubly-reinforced PCC runway slabs, 12 inches thick and approximately 13 feet long by 5 feet wide. The slabs were placed over a 12-inch prepared limerock base which overlaid a sand subbase. Explosive charges were 3.7 and 5 pounds of composition B explosive in high-length-to-diameter-ratio steel tubes. Only limited subsurface crater data were collected; however, pavement damage was well documented and all field data were available so reliability was estimated to be good.

- g. Fort Bragg, U.S. Navy Civil Engineering Laboratory (USNCEL), and Eglin Air Force Base

Several runway cratering tests were conducted at Fort Bragg, North Carolina (ref. 1); USNCEL (ref. 3); and Eglin Air Force Base, Florida (ref. 2 and 4) to create craters for repair exercises. Only very limited data were reported on any of these tests, which were shot in 6-inch concrete (Fort Bragg) and 4- to 6-inch thick ACC (others). The cratering charges were 40-pound demolition charges (Fort Bragg), air-dropped MK 81 and MK 82 bombs (USNCEL), and static and air dropped M117 bombs and AN-M65A bombs (572 pounds of tritonal explosive) (Eglin). To prevent biasing of more reliable data during analysis, only average data were recorded in the Fort Bragg tests and the Eglin M117 bomb tests. The reliability of these data was estimated to be poor due to the lack of information about the target configuration.

- h. Available Data - Conclusion

In general, the information listed in Table 3 was available for all tests in which the reliability of data was estimated to be either good or fair (these include about 94 percent of the test cases collected). All data which could be pertinent to bomb damage repair analyses were collected whenever values were reported. These data were all tabulated and punched onto computer cards to facilitate implementation of an electronic data storage file.

1. Crater Repair Data

Summary tabulation of crater repair parameters which were determined to significantly affect repair time are presented in Table 1. These data were not specifically measured in any of the available test cases; therefore, it was necessary to develop a consistent set of

TABLE 3. DATA AVAILABLE FOR ALL TESTS HAVING
GOOD OR FAIR ESTIMATED RELIABILITIES

Data Item Description	Range of Values for Weapon and Target Data
- Weapon Data -	
Weapon Explosive Weight	1.5 - 386 Pounds
Weapon Length to Diameter Ratio	1.67 - 6.25
Weapon Weight	1.5 - 750 Pounds
Depth of Burst (Below Pavement Surface)	0 - 252 Inches
Impact Obliquity Angle (Vertical = 0°)	0 - 50 Degrees
Impact Velocity	0 Feet Per Second
Explosive Composition	TNT, Comp. B, Comp. C4
How Weapon Emplaced	By Hand
Fuzing Method	Static
- Pavement Data -	
Thickness	7 - 16 Inches
Slab Area	100 - 900 Square Feet
Slab Aspect Ratio (Width/Length)	0.324 - 1.0
Pavement Compressive Strength	4000 - 10,000 PSI
Test Area Dimensions (Pad)	65 x 25 - 5600 x 150 Feet
Pavement Type	PCC, ACC, CRCP, FRCP
Reinforcement Type	None, Rods, Fiber
Age	28 Day - Old
Overlayment	None, ACC, PCC, CRCP
Joint Type	Doweled, Keyed, Sawcut, Welded, Expansion, Contraction
Construction	Poured in place, Prefabricated
Pavement Design	Slabs, Continuous
- Base Data -	
Thickness	6 - 12 Inches
Base Type	None, Gravel, Gravelly Sand Crushed Rock

TABLE 3. DATA AVAILABLE FOR ALL TESTS HAVING
GOOD OR FAIR ESTIMATED RELIABILITIES (CONCLUDED)

Data Item Description	Range of Values for Weapon and Target Data
<p>- Subbase Data -</p> <p>Subbase Thickness</p> <p>Subbase Type</p> <p>Subbase Soil Classification</p> <p>- Soil Data -</p> <p>Soil Classification</p> <p>- Crater Data -</p> <p>Apparent Crater Dimensions</p> <p>True Crater Dimensions*</p> <p>Pavement Crater Volume</p> <p>Ejecta Volume</p> <p>Fall-Back Volume</p> <p>Crater Type</p>	<p>62 - 1000+ Inches</p> <p>Sand, Silty Sand, Medium Silty Clayey Sand, Clay, Organic Clay</p> <p>SM, SP, SC, SMSP, CH, CL, CHCL</p> <p>Unknown, SM, SP, SPSM, CH, CHCL, GW</p> <p>Depth, Radius, Volume</p> <p>Depth, Radius, Volume</p>

* The dimensions of the True Craters were not available for CERF tests having Silty Sand Subbases.

definitions by which their values could be computed from available data.

Data which were available in most test cases are listed in Table 3. Figure 3 illustrates a typical runway crater created by a small penetrating munition. This figure is typical of photographic data which were supplied by AFWL for the Hays and Fort Sumner tests and which were presented in Reference 9 for the 15-pound CERF tests. In addition, sketches such as the one reproduced in Figure 4 were supplied for Hays and Fort Sumner. Using these data, it was possible to estimate the pavement removal areas for expedient, semipermanent, and permanent repairs, as shown in Figure 5. This work was based on the defeat criteria presented in Section II and the assumption that partial slabs would be replaced only in the case of an expedient repair. Thus, by observation of photographic records, it was determined that the center slab was badly fractured and would be replaced in any case. Also, a small section (area estimated from Figure 4) was estimated to be upheaved more than 4.5 inches and required removal for an expedient repair. For a semipermanent repair, the entire left-hand slab required removal (in addition to the center slab), and for a permanent repair, the bottom center slab also required removal since it was cracked in such a way as to form six or more pieces. Removal areas were then computed as the number of slabs removed times slab area minus area of concrete already blown out (estimated from Figure 4) plus estimated area of partial slabs removed. Pavement repair areas were estimated using similar methodology, except that the concrete blown out was not subtracted from the total area.

Accuracy of the technique used to determine pavement removal and repair areas was strongly dependent on the accuracy with which upheaval could be estimated. In most cases, this was accomplished with fairly high confidence, since pavement thickness was known and edges of slabs could be seen in the photographs. This allowed estimation of upheaval height based on a fraction of pavement thickness.

Figure 6 illustrates the algorithms applied to compute expedient, semipermanent, and permanent earth removal volumes. All information needed to compute these values was available for all Hays and Fort Sumner tests

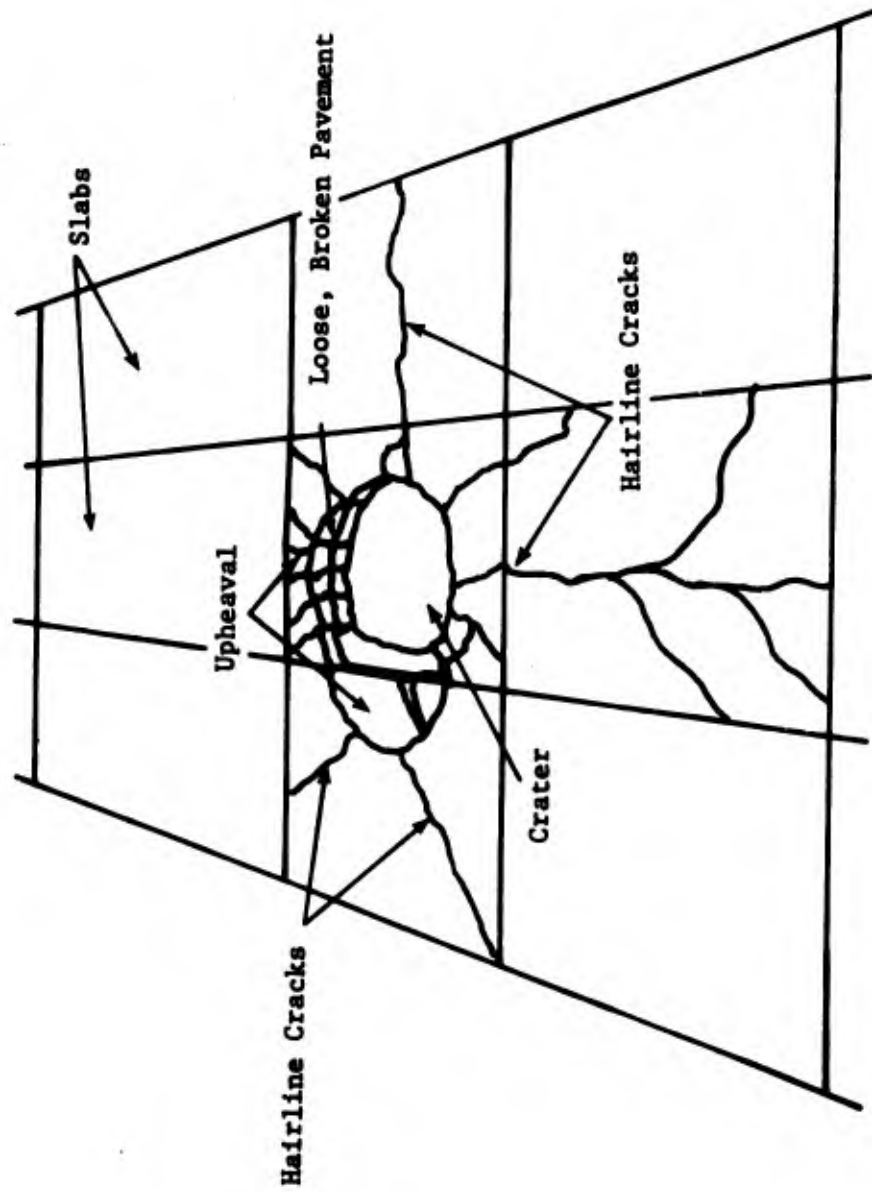
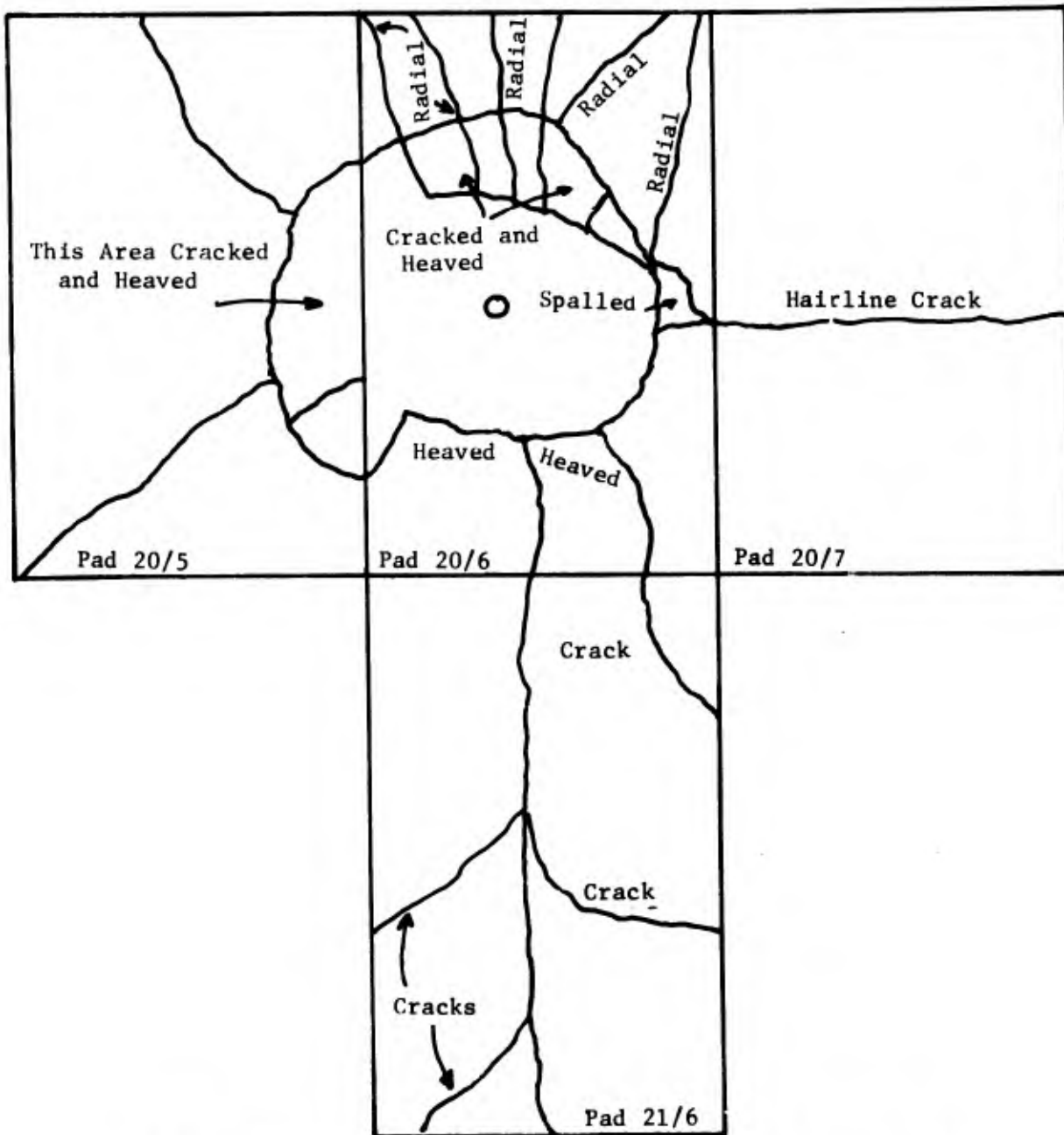
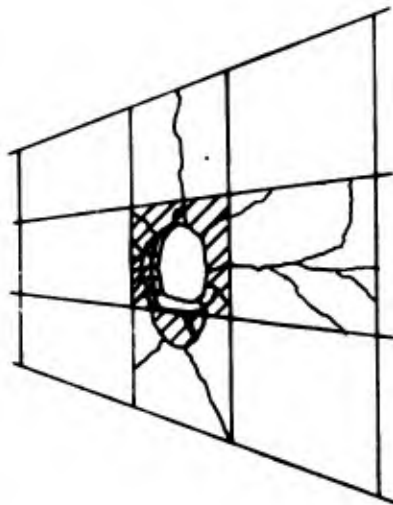


Figure 3. Typical Runway Crater and Illustration of Available Photographic Data



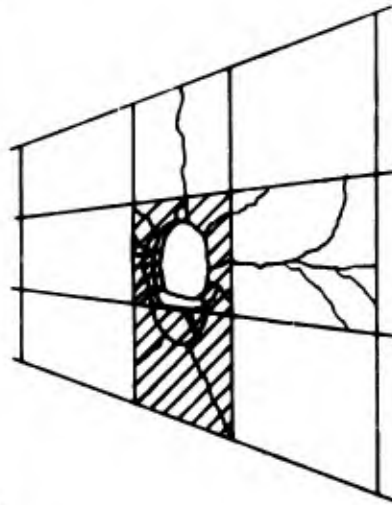
NOTE: Actual Sketches had 6-Inch Square Grid Divisions

Figure 4. Reproduction of Damage Sketch Provided by AFWL for Hays and Fort Sumner Tests



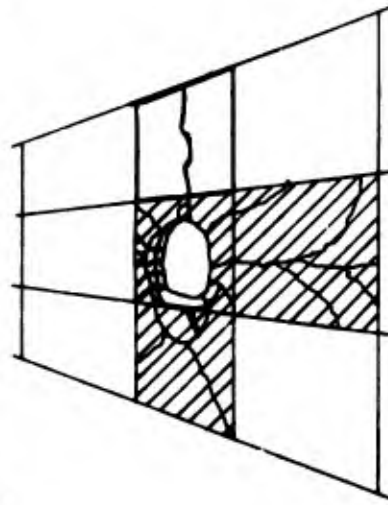
Expedient

No. Slabs Replaced = 1



Semi-Permanent

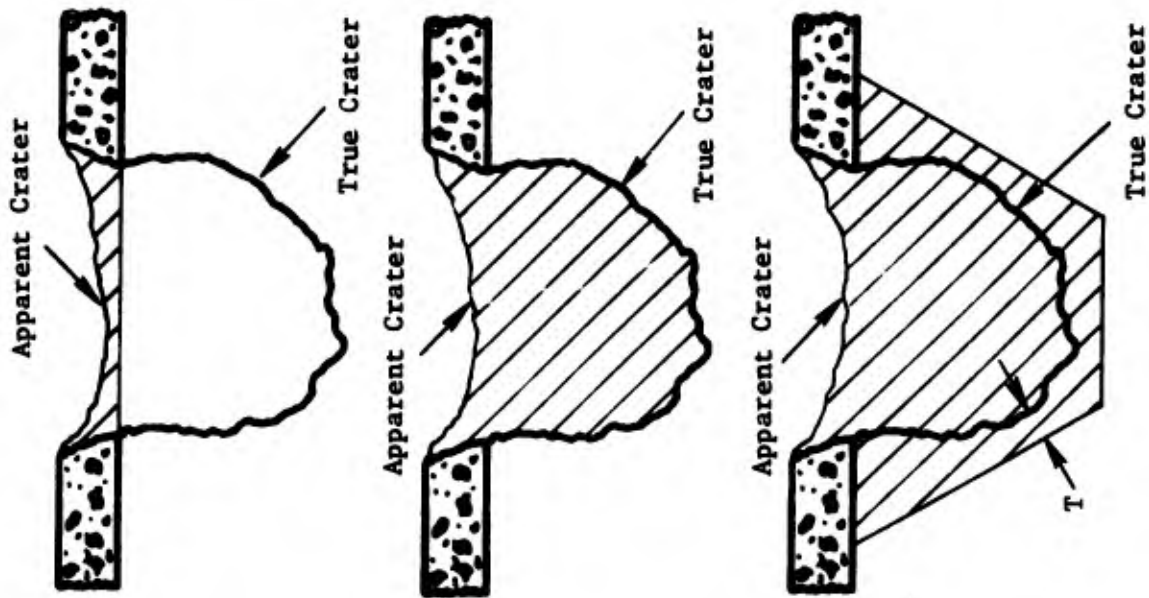
No. Slabs Replaced = 2



Permanent

No. Slabs Replaced = 3

Figure 5. Pavement Removal Area Definitions



$$V_E = \begin{cases} \text{Expedient} \\ 0 & \text{if } V_p < V_A \\ V_p - V_A & \text{if } V_p > V_A \end{cases}$$

where V_A = Apparent Crater Volume,
 V_p = Pavement Crater Volume

$$V_{SP} = \begin{cases} \text{Semi-Permanent} \\ \text{True Crater Volume} & \text{Minus} \\ \text{Apparent Crater Volume} \end{cases}$$

$$V_P = \begin{cases} \text{Permanent} \\ \text{Volume of Truncated } 30^\circ \text{ Cone} \\ \text{Minus Earth Crater Volume} & \text{Plus} \\ \text{True Crater Volume} & \text{Minus} \\ \text{Apparent Crater Volume} \end{cases}$$

$T = 12$ Inches for Charges < 25 Pounds
 $T = 24$ Inches for Charges > 25 Pounds

Figure 6. Volume of Earth Removed Definition

and for the CERF tests having clay subbase configurations with the exception of, in some cases, the apparent crater volume which was then computed as

$$V_A = \frac{1}{6} \pi D_A (D_A^2 + 3R_A^2); \text{ for } D_A \leq R_A; \quad (1)$$

$$V_A = \pi R_A^2 (D_A - R_A) + \frac{2}{3} \pi R_A^3; \text{ for } D_A > R_A \quad (2)$$

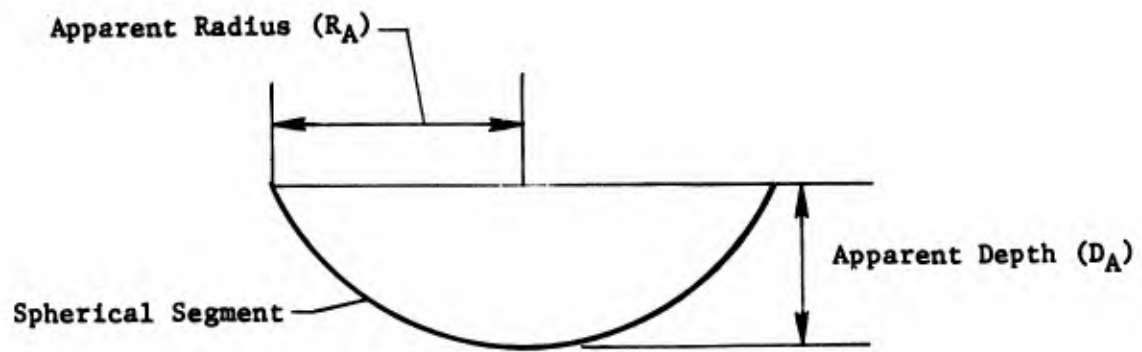
where D_A , R_A , and V_A are apparent crater depth, radius, and volume. Volumes computed by Equations (1) and (2) are illustrated in Figure 7. For the permanent earth removal area it was assumed that removal of a minimum of 1 foot of material beyond the true crater wall would ensure removal of the plastic rupture zone for craters created by 25 pounds or less of explosive. This dimension was increased to two feet for charges larger than 25 pounds. Crater profile plots supplied by AFWL were used to evaluate the size of the truncated cone.

Similar methodology was used to determine the earth replacement volumes which are illustrated in Figure 8.

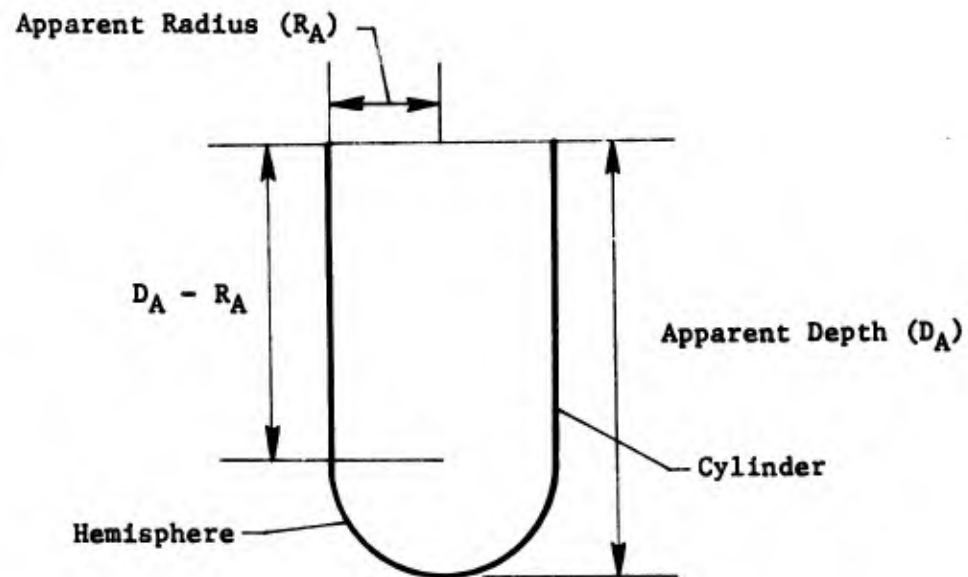
The two other repair parameters identified were ejecta volume and distribution, neither of which was reported extensively in the available information (both were reported for the Tyndall tests only). The law of conservation of mass was used to justify the assumption that ejecta volume was equal to apparent crater volume. No method, however, could be found to estimate ejecta distribution, and this parameter had to be deleted from the parameter list.

Accuracy of the volume data was as good as the accuracy of reported information used in the computations except in the cases where Equations (1) and (2) were used to estimate the apparent volumes. The computed apparent crater volumes compared favorably with actual reported values where they were available and could be checked, except in the case of very shallow craters with large radii and extensive concrete surface spall. For shallow craters, the profile plots supplied by AFWL were used to correct the apparent crater volume values.

Computed ejecta volumes are probably somewhat low because it cannot be expected that fallback material which forms the apparent crater inside the true crater is compacted as tightly as the original material, or that

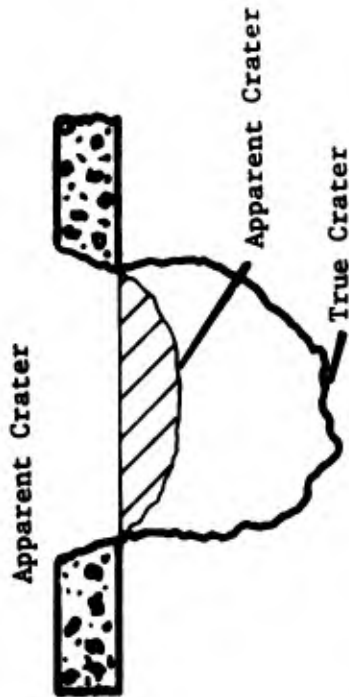


Approximation used when Apparent Depth
was less than or equal to Apparent Radius



Approximation used when Apparent Depth
was greater than Apparent Radius

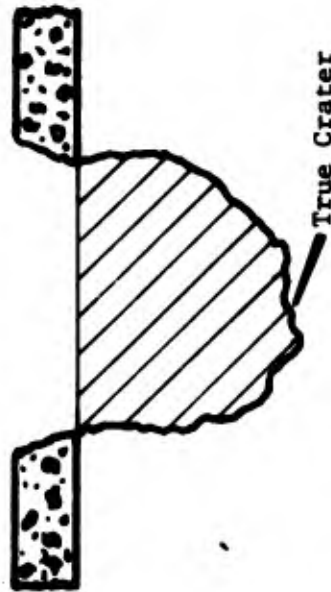
Figure 7. Illustrations of Methods of Estimating Apparent Crater
Volume When Only Depth and Radius were Available



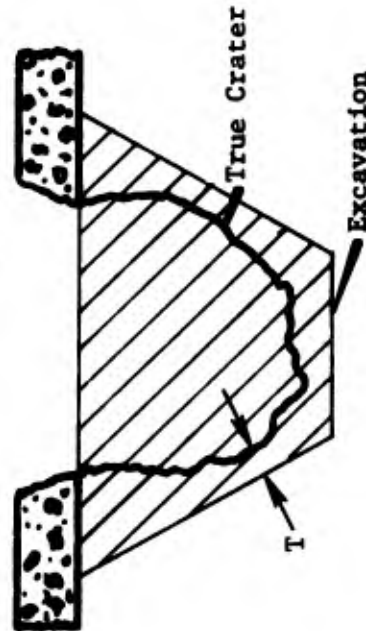
$$V_E = \begin{cases} 0 & \text{if } V_A < V_P \\ V_A - V_P & \text{if } V_A > V_P \end{cases}$$

Expedient

where V_A = Apparent Crater Volume,
 V_P = Pavement Crater Volume



Semi-Permanent
 V_{SP} = Earth Crater Volume



Permanent
 V_P = Volume Removed Plus Apparent Crater
 Volume Minus Pavement Crater Volume

$T = 12$ Inches for Charges ≤ 25 Pounds
 $T = 24$ Inches for Charges > 25 Pounds

Figure 8. Volume of Earth Replaced Definitions

ejecta on the runway is compacted as tightly, either. Therefore two statements can be made which indicate ejecta volumes higher than computed values:

- (1) Less material fills the fallback space in the true crater; thus, the surface ejecta volume is actually larger than the apparent crater volume.
- (2) The ejecta is less compacted on the surface and thus occupies more space there.

No information was available to substantiate these statements, so it is suggested that ejecta volumes used in this report be used only with caution and that they be assumed non-conservative.

It is felt that the repair parameter descriptions discussed above provided a reasonably accurate characterization of the information required. They supply consistent, reliable estimates of essential data for estimating bomb damage repair times if used without disregarding the cautions discussed above. No attempt was made to compute values where insufficient data were available, either as reported raw data or from photographs or field notes, because it was felt that this would unsatisfactorily reduce the reliability of final damage prediction relationships.

2. DATA FILE

The problem of collecting, storing, and accurately manipulating the large amount of available experimental data was solved by developing a computerized data manipulation system. As data from the various sources were received, they were converted to a consistent set of units and stored on a computer permanent file. Software was also developed to manipulate, print, and/or plot desired information. Figure 9 shows an overview of the system which consists of four related FORTRAN 4 computer programs and the storage file. Program BDRINIT initializes the file, setting it up to accept data from punch cards. Program BDREDIT performs input functions and creates lists of all data by test case. Program BDRTABL performs the output function of tabulating data according to specified format, and program BDRPLOT creates plots of data, performs various mathematical functions, and generates and plots curve fits.

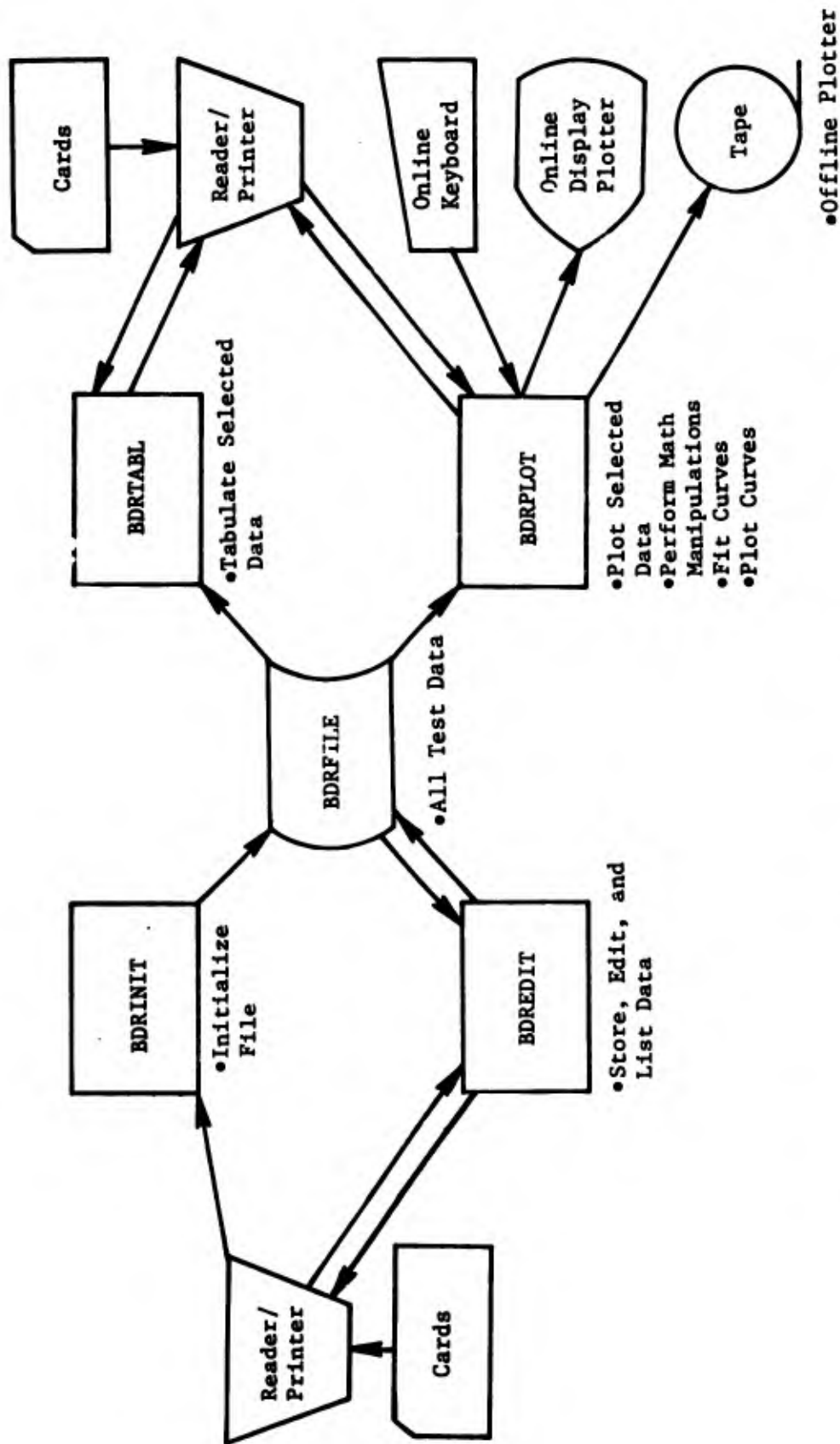


Figure 9. Schematic of Computerized Data Manipulation System

The data file contains locations for 160 separate pieces of information for each test case, of which 114 were identified and are given in Table 4 along with their units. Locations are referred to by their "key" numbers which are also shown in the table. Each test case is contained in one record of the file (there are currently 193 records); Figure 10 illustrates the information contained in a typical record. The first several lines printed contain historical data about the record. Record number locates the slot in the file which the test case occupies. Test site identifies the geographical location where test data were obtained, creation date is the date on which the data were initially filed, and revision number and date last updated tells how many times the data have been revised and when the last revision took place. Crater type refers to the nomenclature shown in Figure 11. The comments are a short description of general test conditions. These title data are also contained in a special index record which can be displayed to provide a synopsis of the contents of the data file. Both the index and a complete listing of the current data file are contained in Appendix A of this report.

Following the title data, individual test data are listed by their respective category (i.e. weapon data, damage data, etc.). Information presented along with the data values are:

- a. "Key" location (the number used to retrieve data);
- b. Type (whether the information is in alphabetic (A) or numeric (N) format);
- c. Name (24 character abbreviated descriptions of the data contained);
- d. Units;
- e. Reference (one or two digit number which references the specific source of the information, see Table 5).

Data for which no information is available are not listed, although a location is reserved in the file. For example, in the test case illustrated, the only information available to describe the runway subbase were those shown. Data such as the compressive strength (Key 65 from Table 4) were not available and are therefore not listed.

TABLE 4. DATA FILE STORAGE LOCATION KEYS

Key Number	Type	Name	Units	Remarks
		- WEAPON DATA -		
1	Numeric	EXPLOSIVE WEIGHT	Pounds	
2	Numeric	EXPLOSIVE DENSITY	Pounds per cubic inch	
3	Numeric	ENERGY RELEASE	Inch Pounds per pound	Heat of explosion
4	Numeric	LENGTH/DIAMETER (WH)	Inches	Ratio of length divided by diameter of explosive device
5	Numeric	DEVICE WEIGHT	Pounds	Total weight of weapon
6	Numeric	AVG CASE THICKNESS	Inches	(Device weight minus explosive weight) divided by surface area of a cylinder having given L/D and explosive weight
7	Numeric	FOCUS DIRECTION	Degrees	Primary direction of warhead focus measured from zero = vertical
8	Numeric	DEPTH OF BURST	Inches	Measured from warhead center of gravity to pavement surface
9	Numeric	IMPACT OBLIQUITY	Degrees	Measured from zero = vertical
10	Numeric	IM. POS. FR LONG EDG	Inches	Distance from long edge of slab to warhead impact point
11	Numeric	IM. POS. FR SHORT EDG	Inches	Distance from short edge of slab to warhead impact point
12	Numeric	IMPACT VELOCITY	Feet per second	
13	Numeric	TNT EQUIVALENT EXPLOSIVE	Pounds	Equivalent weight of TNT required to produce same energy release
211	Alphanumeric	EXPLOSIVE NAME	-	TNT, Comp B, Comp C4, etc.
212	Alphanumeric	EMPLACEMENT	-	How weapon placed under pavement
213	Alphanumeric	FUZING	-	How weapon fuzed
		- PAVEMENT DATA -		
21	Numeric	PAVEMENT THICKNESS	Inches	Including any overlay
22	Numeric	SLAB AREA	Square Inches	
23	Numeric	SLAB ASPECT RATIO	-	Width divided by length
24	Numeric	PAVEMENT DENSITY	Pounds per cubic inch	

TABLE 4. DATA FILE STORAGE LOCATION KEYS (CONTINUED)

Key Number	Type	Name	Units	Remarks
		- PAVEMENT DATA (Cont) -		
25	Numeric	PAV. COMP. STRENGTH	PSI	Compressive strength of pavement material
26	Numeric	PAV. COMP. MODULUS	PSI	
27	Numeric	JOINT STRENGTH	Pounds	
28	Numeric	NO. JOINTS PER SLAB	-	
29	Numeric	SURFACE TEMPERATURE	Degrees F	Temperature of pavement material before test shot
30	Numeric	PENT. HOLE DIAMETER	Inches	Diameter of hole drilled to emplace weapon
31	Numeric	REBAR DENSITY	Inch ² per inch ²	Portion of an average crosssection of pavement containing reinforcement
32	Numeric	REBAR DIAMETER	Inches	
33	Numeric	REBAR ASPECT RATIO	-	
34	Numeric	DEPTH FIRST REBAR LAYER	Inches	
35	Numeric	DEPTH SECOND REBAR LAYER	Inches	
36	Numeric	DEPTH THIRD REBAR LAYER	Inches	
37	Numeric	PAV VOID CONTENT	% Void	
38	Numeric	TEST AREA LENGTH	Feet	
39	Numeric	TEST AREA WIDTH	Feet	
201	Alphanumeric	PAV CONSTRUCTION	-	Poured, prefab, etc.
202	Alphanumeric	PAVEMENT DESIGN	-	Slabs, continuous, etc.
214	Alphanumeric	PAVEMENT TYPE	-	PCC, ACC, CRCP, etc.
215	Alphanumeric	REINFORCEMENT	-	None, rods, fiber, etc.
216	Alphanumeric	CONDITION	-	New, good, cracked, etc.
217	Alphanumeric	AGE	-	28 day, old, etc.
218	Alphanumeric	OVERLAYMENT	-	PCC, ACC, etc.
219	Alphanumeric	JOINT TYPE	-	Dowel, key, etc.
		- BASE/SUBBASE/SOIL DATA -		
41/61/81	Numeric	THICKNESS	Inches	
42/62/82	Numeric	DENSITY	Pounds per cubic inch	
43/63/83	Numeric	COMP. STRENGTH	PSI	
44/64/84	Numeric	COMP. MODULUS	PSI	
45/65/85	Numeric	SHEAR STRENGTH	PSI	
46/66/86	Numeric	SHEAR MODULUS	PSI	
47/67/87	Numeric	SOUND SPEED	Inches per second	

TABLE 4. DATA FILE STORE LOCATION KEYS (CONTINUED)

Key Number	Type	Name	Units	Remarks
		- BASE/SUBBASE/SOIL DATA - (Continued)		
48/68/88	Numeric	MOISTURE (BY V)	% Water	Moisture content of sub-grade material by volume
49/69/89	Numeric	DISENTION	-	Dry density divided by fully compacted density (provides measure of compaction)
50/70/90	Numeric	AVG. PART. SIZE	Inches	Average size of subbase material particles
51/71/91	Numeric	SOLID DENSITY	Pounds per cubic inch	Density of fully compacted subgrade materials
220/222/-	Alphanumeric	TYPE	-	Clay, sand, etc.
221/223/224	Alphanumeric	CLASSIFICATION	-	According to unified soil classification system (MIL-STD-619B)
		- DAMAGE DATA -		
98	Numeric	CRATER ASPECT RATIO	-	True crater depth divided by true crater radius
99	Numeric	SURFACE CRATER RADIUS	Inches	Square root of (pavement crater volume divided by pavement thickness)
100	Numeric	RUBBLE VOL (EJECTA)	Cubic Inches	
101	Numeric	APPARENT CTR DEPTH	Inches	
102	Numeric	APPARENT CTR RADIUS	Inches	
103	Numeric	APPARENT CTR VOLUME	Cubic Inches	
104	Numeric	TRUE CRATER DEPTH	Inches	
105	Numeric	TRUE CRATER RADIUS	Inches	
106	Numeric	TRUE CRATER VOLUME	Cubic Inches	
107	Numeric	EARTH CRATER VOLUME	Cubic Inches	
108	Numeric	PAVEMENT CRATER VOLUME	Cubic Inches	
109	Numeric	CRACK RADIUS	Inches	Maximum extent of cracking from impact position
110	Numeric	MAX UPHEAVAL HEIGHT	Inches	
111	Numeric	FALL BACK VOLUME	Cubic Inches	
225	Alphanumeric	CRATER TYPE (WES)	-	Standard, blow-out, camo-heave, camo-spall, camouflet, spall, heave

TABLE 4. DATA FILE STORAGE LOCATION KEYS (CONCLUDED)

Key Number	Type	Name	Units	Remarks
		- REPAIR DATA -		
112	Numeric	V EARTH REMOVED (E)	Cubic Inches	Expedient earth removal volume
113	Numeric	V EARTH REMOVED (SP)	Cubic Inches	Semipermanent earth removal volume
114	Numeric	V EARTH REMOVED (P)	Cubic Inches	Permanent earth removal volume
115	Numeric	NO. SLABS REPL (E)	-	Number of full slabs replaced in making an expedient repair
116	Numeric	NO./SLABS REPL (SP)	-	
117	Numeric	NO. SLABS REPL (P)	-	
118	Numeric	PAV REPAIR AREA (E)	Square Inches	Expedient pavement repair area
119	Numeric	PAV REPAIR AREA (SP)	Square Inches	Semipermanent pavement repair area
120	Numeric	PAV REPAIR AREA (P)	Square Inches	Permanent pavement repair area
121	Numeric	V EARTH REPL (E)	Cubic Inches	Expedient earth replacement volume
122	Numeric	V EARTH REPL (SP)	Cubic Inches	Semipermanent earth replacement volume
123	Numeric	V EARTH REPL (P)	Cubic Inches	Permanent earth replacement volume
124	Numeric	PAV REMOVAL AREA (E)	Square Inches	Expedient pavement removal area
125	Numeric	PAV REMOVAL AREA (SP)	Square Inches	Semipermanent pavement removal area
126	Numeric	PAV REMOVAL AREA (P)	Square Inches	Permanent pavement removal area
		- EXTRA INFORMATION -		
226	Alphanumeric	DATA SOURCE	-	Abbreviation of the document number which contains test information
227	Alphanumeric	EST DATA RELIABILITY	-	Good, Fair, Poor
228	Alphanumeric	TEST SITE	-	Hays, CERF, etc.

NEW RECORD CREATED DURING EDIT NO. 2 ADDED TO HDR PERMANENT DATA FILE.

RECORD REV. TEST TEST CREATION DATE LAST COMMENTS
 NO. NO. SITE NO. DATE DATE UPDATED
 54 0 MAYS M63 04/30/75 04/30/75 25 LB. C4, 95 IN. DOR BAND IN PAVEMENT

KEY	TYPE	NAME	VALUE	UNITS	REF	KEY	TYPE	NAME	VALUE	UNITS	REF
*** WEAPON DATA ***											
1N	-	EXPLOSIVE WEIGHT	25.0000	LBS	1	2N	-	EXPLOSIVE DENSITY	.578000E-01	LB/CU-IN	98
4N	-	LENGTH/DIAMETER (WH)	1.75000	IN	10	5N	-	DEVICE WEIGHT	25.0000	LBS	10
6N	-	AVG CASE THICKNESS	0.	IN	10	8N	-	DEPTH OF BURST	95.0000	IN	1
9N	-	IMPACT ORLIQUITY	00.0000	DEGREES	10	10N	-	IN. POS. FR LONG EDG	75.0000	IN	10
11N	-	IN. POS. FR SHRT EDG	75.0000	IN	10	12N	-	IMPACT VELOCITY	120.000	FT/SEC	10
13N	-	TNT EQUIVALENT EXPL.	27.3000	LBS	9A	211A	-	EXPLOSIVE NAME	COMP C4		10
212A	-	EMPLACEMENT	HAND		10	213A	-	FUZZING	B4PC		10
*** PAVEMENT DATA ***											
21N	-	PAVEMENT THICKNESS	9.00000	IN	1	22N	-	SLAB AREA	36000.0	SQ-IN	10
23N	-	SLAB ASPECT RATIO	.625000		10	24N	-	PAVEMENT DENSITY	.852000E-01	LB/CU-IN	13
25N	-	PAV. COMP. STRENGTH	10022.0	PSI	13	26N	-	PAV. COMP. MODULUS	.590000E+07	PSI	13
30N	-	PENT. HOLE DIAMETER	8.00000	IN	10	31N	-	REBAR DENSITY	0.	IN/SQ-IN	10
39N	-	TEST AREA LENGTH	5000.00	FEET	10	39N	-	TEST AREA WIDTH	150.000	FEET	10
214A	-	PAVEMENT TYPE	PORT CEM		10	215A	-	REINFORCEMENT	NONE		10
217A	-	AGE	OLD		10	218A	-	OVERLAYMENT	NONE		10
219A	-	JOINT TYPE	PEG		10	201A	-	PAV CONSTRUCTION	POURED		10
202A	-	PAVEMENT DESIGN	PAUS		10						
*** BASE DATA ***											
41N	-	BASE THICKNESS	60.0000	IN	10	42N	-	BASE DENSITY	.654000E-01	LB/CU-IN	19
48N	-	BASE MOISTURE (RY V)	24.1500	% WATER	19	49N	-	BASE DISTENTION	.680000		19
51N	-	BASE SOLID DENSITY	.965000E-01	LB/CU-IN	10	220A	-	BASE TYPE	ORG CLAY		10
221A	-	BASE SOIL CLASS	CHCL		16						
*** SUBBASE DATA ***											
61N	-	SUR. THICKNESS	144.000	IN	10	62N	-	SUB. DENSITY	.705000E-01	LB/CU-IN	19
66N	-	SUR. MOISTURE (RY V)	18.2800	% WATER	16	69N	-	SUR. DISTENTION	.720000		19
71N	-	SUR. SOLID DENSITY	.576000E-01	LB/CU-IN	19	222A	-	SUBBASE TYPE	SILTY CY		10
223A	-	SURBASE SOIL CLASS	CHCL		16						
*** SOIL DATA ***											
81N	-	SOIL THICKNESS	36.0000	IN	10	224A	-	SOIL CLASSIFICATION	SW		10
*** CRATER DATA ***											
99N	-	CRATER ASPECT RATIO	21.6000		40	99N	-	SURFACE CTR RADIUS	6.00000	IN	80
100N	-	RURFL VOL (EJECTA)	643.100	CU-IN	40	101N	-	APPARENT CTR DEPTH	8.04000	IN	2
102N	-	APPARENT CTR RADIUS	6.00000	IN	51	103N	-	APPARENT CTR VOLUME	643.100	CU-IN	52
104N	-	TRUF CRATER DEPTH	129.000	IN	1	105N	-	TRUE CRATER RADIUS	40.0000	IN	1
106N	-	TRUF CRATER VOLUME	299600.	CU-IN	1	107N	-	EARTH CRATER VOLUME	298800.	CU-IN	1
108N	-	PAVEMENT CTR VOLUME	864.000	CU-IN	1	110N	-	MAX UPPEVAL HEIGHT	8.00000	IN	12
111N	-	FALL-BACK VOLUME	299000.	CU-IN	59	225A	-	CRATER TYPE (MES)	CAMO-HEAVE		14

Figure 10. Data File Record Illustration

RECORD NO. 56 EDIT NO. 2 CONTINUED.

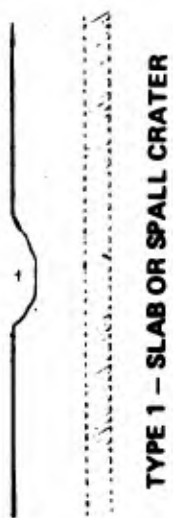
KEY	TYPE - NAME	VALUE	UNITS	HFF	KEY	TYPE - NAME	VALUE	UNITS	REF
112N	V EARTH REMOVED (E)	140.900	CU-IN	61	113N	V EARTH REMOVED (SP)	299000.	CU-IN	62
114N	V EARTH REMOVED (P)	.924900E+07	CU-IN	64	115N	NO. SLABS REPL (E)	0.		54
116N	NO. SLABS REPL (SP)	1.00000		52	117N	NO. SLABS REPL (P)	5.00000		56
118N	PAV REPAIR AREA (E)	32510.0	SO-IN	63	119N	PAV REPAIR AREA (SP)	36000.0	SO-IN	63
120N	PAV REPAIR AREA (P)	180000.	SO-IN	63	121N	V EARTH REPL (E)	0.	CU-IN	65
122N	V EARTH REPL (SP)	299600.	CU-IN	57	123N	V EARTH REPL (P)	.925000E+07	CU-IN	65
124N	PAV REMOVAL AREA (E)	32400.0	SO-IN	57	125N	PAV REMOVAL AREA (SP)	35890.0	SO-IN	58
126N	PAV REMOVAL AREA (P)	179900.	SO-IN	5A					
100N	RURBLE VOL (EJECTA)	683.100	CU-IN	60					
227A	EST DATA RELIABILITY	9000		99					
					226A	DATA SOURCE	AFWLTR7261		99
					228A	TEST SITE	MAYS		10

*** REPAIR DATA ***
 61 CU-IN
 64 CU-IN
 52
 63 SO-IN
 63 SO-IN
 57 CU-IN
 57 SO-IN
 5A

*** EXTRA INFORMATION ***
 60 CU-IN
 99

TEST PERFORMED AT MAYS, KANSAS ON 15 JUN 1971. BY THE AFWL OF
 SLAB NO. 111/10 STATION 24. 119 FEET FROM THE LEFT EDGE OF
 THE RUNWAY TEST SECTION.

Figure 10. Data File Record Illustration (Concluded)



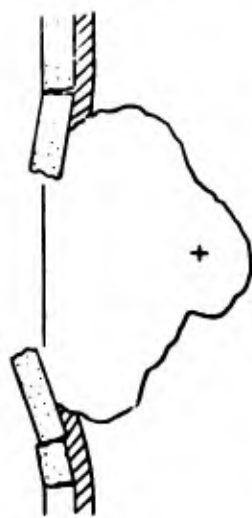
TYPE 1 - SLAB OR SPALL CRATER



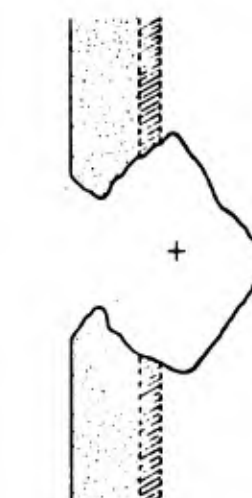
TYPE 2 - BLOW-OUT CRATER



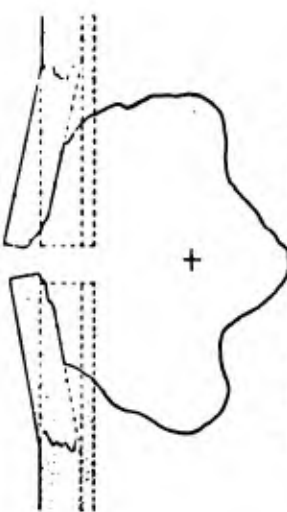
TYPE 3 - STANDARD CRATER



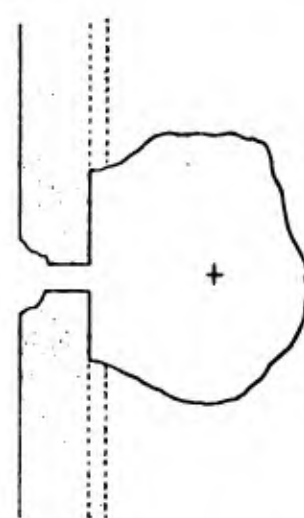
TYPE 4 - HEAVE CRATER



TYPE 5 - CAMOUFLET WITH SPALL CRATER



TYPE 6 - CAMOUFLET WITH HEAVE MOUND



TYPE 7 - CAMOUFLET

Figure 11. Pavement Crater Types (WES Format)

TABLE 5. DATA FILE REFERENCE LIST

Reference Number	Source
1	Crater Profile Field Data Supplied by AFWL
2	Field Notes and Sketches Supplied by AFWL
3	Estimated From Motion Pictures Supplied by AFWL
4	Estimated From Still Photographs Supplied by AFWL
10	Data from Text of Reference 6
11	Tabulated Data from Reference 6
12	Scaled from Graphical Presentations in Reference 6
13	Average of Data Contained in Reference 6
14	Crater Type Inferred from Data Contained in Reference and/or Photographs
15	Data from Text of Reference 8
16	Tabulated Data from Reference 8
17	Scaled from Graphical Presentations in Reference 8
18	Average of Data Contained in Reference 8
19	Unified Soil Classification Data Defined According Military Standard 619B and Obtained from Reference 8
20	Data from Reference 9
21	Data from Reference 1
23	Data from Reference 4
25	Data from Reference 3
26	Data from Reference 14
27	Data from Reference 5
28	Data from Reference 2
29	Data Obtained Via Computer Terminal Interface with Nonnuclear Munitions Information Analysis Center
33	Data from References 11 and 12
51	Estimated Number of Full Slabs Requiring Replacement to Meet the Expedient Repair Criteria
52	Estimated Numbers of Slabs Requiring Replacement to Meet the Semipermanent Repair Criteria

TABLE 5. DATA FILE REFERENCE LIST (CONCLUDED)

Reference Number	Source
53	Estimated Number of Slabs Requiring Replacement to Meet the Permanent Repair Criteria
54	Computed Expedient Pavement Removal Area
55	Computed Apparent Crater Volume
56	Computed Permanent Pavement Removal Area
57	Fall Back Volume Computed as True Crater Volume Minus Apparent Crater Volume
58	Computed Ejecta Volume
59	Computed Expedient Earth Removal Volume
60	Computed Semipermanent Earth Removal Volume
61	Computed Expedient Pavement Repair Area
62	Computed Semipermanent Pavement Repair Area
63	Computed Permanent Pavement Repair Area
64	Computed Permanent Earth Removal Volume
65	Computed Expedient Earth Replacement Volume
66	Computed Semipermanent Earth Replacement Volume
67	Computed Permanent Earth Replacement Volume
68	Expedient Pavement Removal Area for Hays Bomb Tests Computed as True Crater Concrete Repair Volume Minus True Crater Concrete Crater Volume Divided by Pavement Thickness Where Data were Tabulated in Reference 6
69	Apparent Crater Volume for Shallow Depth of Burst Tests at Hays and Fort Sumner - Estimated from Crater Profile Data Supplied by AFWL

All filed information was stored using the inch-pound-second system of units so that conversion of units would not be required during data manipulation. Both output programs are capable of converting data to other systems so that more universally recognized units can be displayed on output lists or plots. Both programs are capable of searching the entire data file and selecting data according to input specifications. Additionally, BDRPLOT can plot information directly from the file or functions containing data from one or more filed locations and specified input constants. It also performs curve fitting functions using least squares methodology to develop curves fitting any of the mathematical forms shown in Table 6.

Deletion of deviant data can be accomplished during curve fitting. If this option is used, an initial curve is established and its RMS error is computed; the program then computes the deviation of each data point from the curve and compares its value with the RMS error. If the deviation exceeds n times the RMS error (where n is an input constant), the point is identified as deviant. A new curve is then fit to the data which were not identified as deviant.

TABLE 6. CURVE FITTING FUNCTIONS

- Polynomial
$Y = a_0 + a_1X$ Straight Line (First Order)
$Y = a_0 + a_1X + a_2X^2$ Quadratic Curve (Second Order)
$Y = a_0 + a_1X + a_2X^2 + a_3X^3$ Cubic Curve (Third Order)
- Exponential
$Y = a \cdot b^X$ or $\log Y = a + (\log b)X$
- Power Function (Geometric)
$Y = a \cdot X^b$ or $\log Y = \log a + b \log X$
- Logarithmic Curve
$Y = a + b \log X$

Figure 12 is an illustration of the standard plot output format, which is used for all data plots presented in this report. The figure illustrates a graph of true crater radius versus depth of burst for several conditions. Each set of conditions is annotated by a different plot character which is keyed to qualifications stated in the notes column. Thus the \square plot characters are true crater radius (Key 105) versus depth of burst (Key 8) only for test cases where 5-pound explosive charges (Key 1) were detonated beneath runways having pavements (Key 21) between 7 and 8.5 inches thick and organic clay subbases (Key 222). Additionally only test cases where the damage did not result in a camouflet or camouflet with heave (Key 225) crater are plotted using the \square . All points shown, in fact, represent 5-pound charges under 7- to 8.5-inch thick pavements; other characters, however, represent medium silty clayey sand subbases and non-camouflet craters (X) as well as camouflet craters in the two subbase types (Δ and \diamond). Second order curves fit using least squares methodology are shown for both sets of non-camouflet points, and the dotted line represents the positive standard deviation (RMS error) for the non-camouflet craters in organic clay subbases. Plots such as the one illustrated here were used extensively for identification of weapon and target parameters which affected crater formation. This plot clearly illustrates the effect of depth of burst and subbase constitution on both crater radius and camouflet formation for 5-pound explosive charges. A complete set of plots which show the relationships of depth of burst, weapon weight, subbase type, and pavement thickness to the various damage parameters are contained in Appendix B of this report.

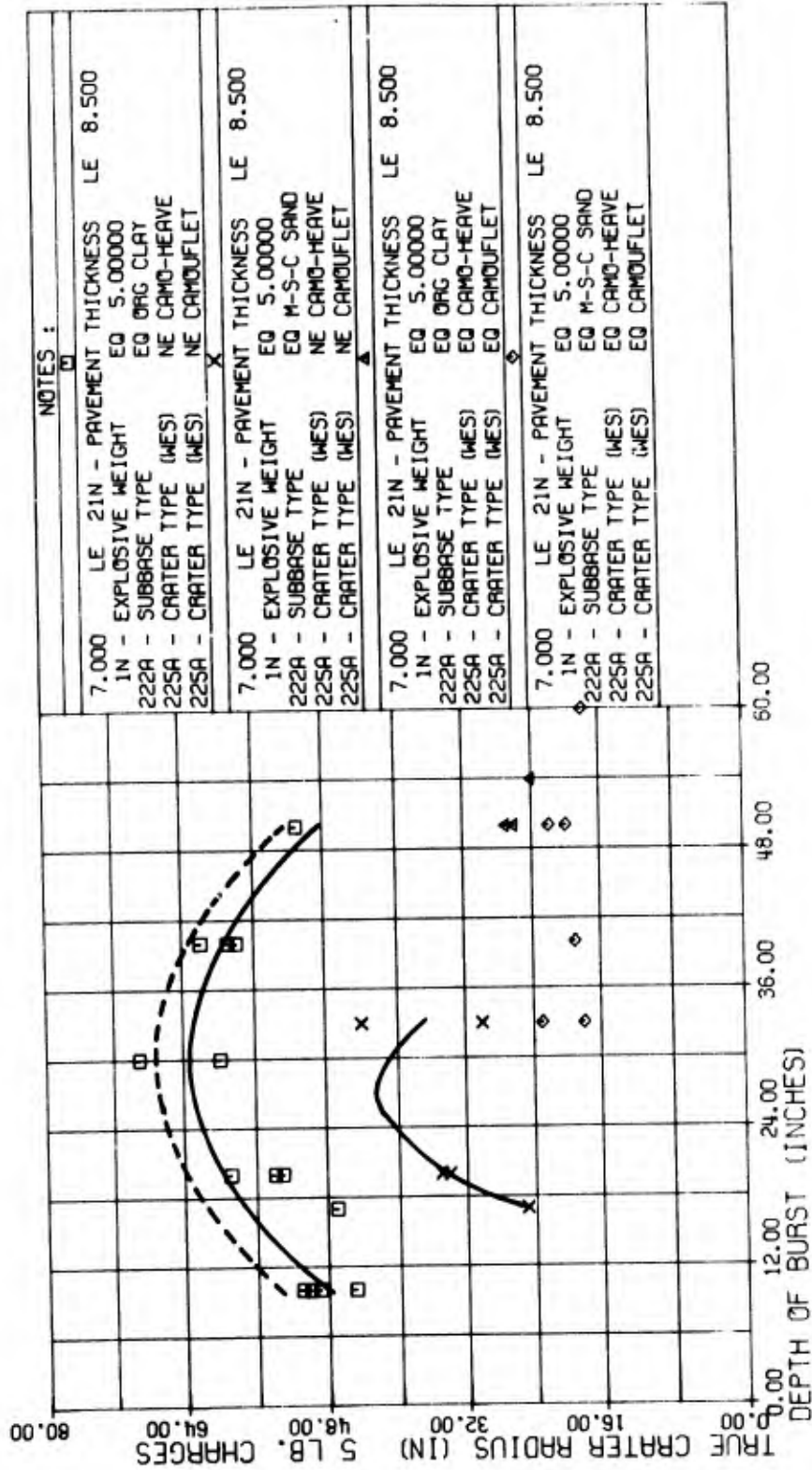
Versions of the data file/manipulation system have been implemented on both the Kirtland Air Force Base CDC 6600 computer and the contractor's IBM 370 computer. Conversion to other computer systems would require minimal reprogramming effort.

3. SIGNIFICANT PARAMETER IDENTIFICATION

The scope of data available from tests with good or fair estimated reliability significantly reduced the number of parameters available for use as inputs to damage prediction relationships. Input parameters were divided into two groups:

- a. Those which describe the weapon;
- b. Those which describe the target configuration.

TRUE CRATER RADIUS (IN) 5 LB. CHARGES VERSUS DEPTH OF BURST (INCHES)



NOTES :

7,000	LE 21N - PAVEMENT THICKNESS	LE 8.500
1N	EXPLOSIVE WEIGHT	EQ 5.00000
222A	SUBBASE TYPE	EQ ORG CLAY
225A	CRATER TYPE (MES)	NE CAMO-HEAVE
225A	CRATER TYPE (MES)	NE CAMOUFLET
7,000	LE 21N - PAVEMENT THICKNESS	LE 8.500
1N	EXPLOSIVE WEIGHT	EQ 5.00000
222A	SUBBASE TYPE	EQ M-S-C SAND
225A	CRATER TYPE (MES)	NE CAMO-HEAVE
225A	CRATER TYPE (MES)	NE CAMOUFLET
7,000	LE 21N - PAVEMENT THICKNESS	LE 8.500
1N	EXPLOSIVE WEIGHT	EQ 5.00000
222A	SUBBASE TYPE	EQ ORG CLAY
225A	CRATER TYPE (MES)	EQ CAMO-HEAVE
225A	CRATER TYPE (MES)	EQ CAMOUFLET
7,000	LE 21N - PAVEMENT THICKNESS	LE 8.500
1N	EXPLOSIVE WEIGHT	EQ 5.00000
222A	SUBBASE TYPE	EQ M-S-C SAND
225A	CRATER TYPE (MES)	EQ CAMO-HEAVE
225A	CRATER TYPE (MES)	EQ CAMOUFLET

Figure 12. Illustration of BDRPLOT Output Format

These were then further subdivided into groups, according to whether they varied independently over a significant range in the available information. Tables 7 and 8 are lists of parameters for weapons and targets respectively; their range of variation is also listed. Some parameters which varied widely - weapon length-over-diameter ratio (L/D), for instance - did not vary independently (i.e., most 5-pound charges had a L/D of 1.875, excluding only 2 out of 36, etc.). Another example is soil moisture content which has often been assumed to affect cratering phenomena. Moisture contents varied from 4 to 25 percent overall, but all clays had high (18-25 percent) moisture contents, and sands had the lower moisture contents.

Further reduction of the scope of data for which any statistical analysis could be performed was necessitated by the fact that the Hays and Fort Sumner tests made up over 85 percent of the data for which both weapon explosive weight and depth of burst varied. This was because the other group of high-reliability test data was taken at CERF where weapon weight and depth of burst were either 1.5 pounds and 30 inches or 15 pounds and 84 inches and held constant while other conditions were varied. This left the list of available parameters for statistical analysis shown in Table 9. Further survey of data showed that these parameters varied over a sufficient range and with enough distribution to perform a statistical analysis and determine damage prediction relationships. Figures 13 through 16 are bar charts which illustrate the distribution of the data listed in Table 9 versus numbers of test cases available. Annotation is included on the charts to show the scope of bomb data. Bars which have no annotation are all small charges.

Based on reasoning discussed above, the parameters listed in Table 9 were selected as those on which damage prediction relationships were based. Data from the CERF tests were then used to identify trends associated with other parameters listed in Tables 7 and 8. These trends were stated along with final damage prediction relationships, but since they were only reliable for the specific charge weights and depths of burst tested at CERF, they were not included in the actual relationships.

TABLE 7. WEAPON PARAMETERS

Weight	1.5 - 25 Pounds
Depth of Burst	10 - 110 Inches

TABLE 8. TARGET PARAMETERS

Pavement Thickness	6 - 18 Inches
Slab Area	100 - 900 Square Feet
Subbase Types	Sands - Clays
Pavement Types	PCC, ACC, CRCP, FRCP, Several Overlayments
Joint Types	Doweled, Keyed, Sawcut, Welded, Expansion, Contraction
Reinforcement	Bars, Mesh, Fiber, and None
Pavement Strength	4000 PSI - 10,000 PSI
Moisture Content	4 - 25 Percent

TABLE 9. HAYS AND FORT SUMNER
TEST PARAMETERS (115 TESTS)

Weapon:
Weight
Depth of Burst
Target:
Pavement Thickness
Soil Type

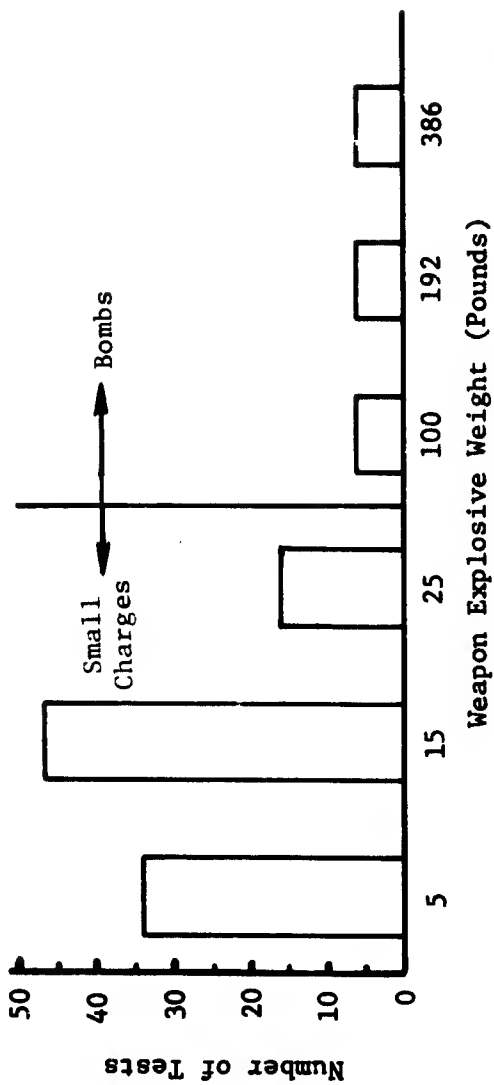


Figure 13. Weapon Weight Distribution for Hays and Fort Summer Tests

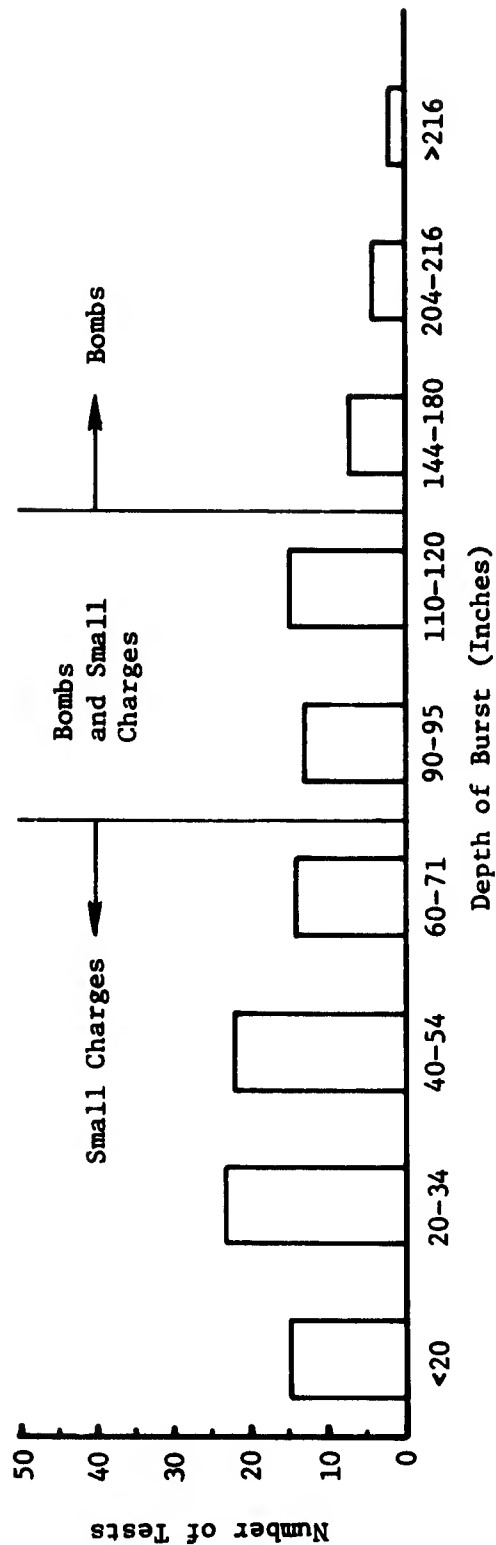


Figure 14. Depth of Burst Distribution for Hays and Fort Summer Tests

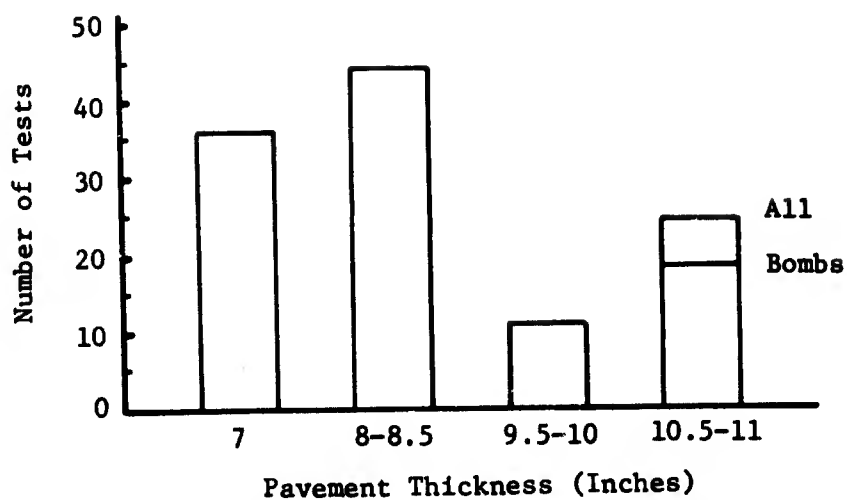


Figure 15. Pavement Thickness Distribution for Hays and Fort Sumner Tests

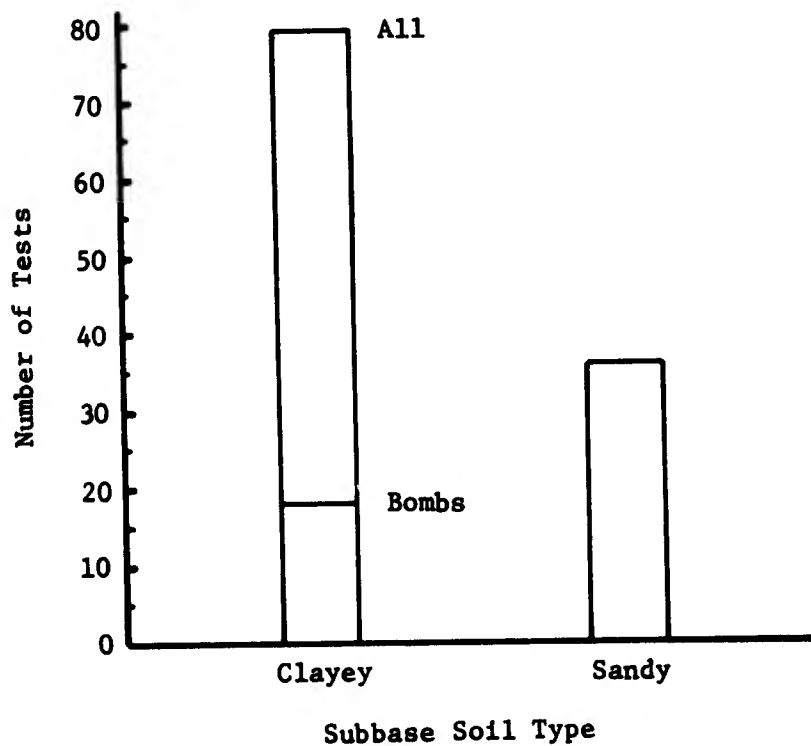


Figure 16. Soil Type Distribution for Hays and Fort Sumner Tests

SECTION IV
ANALYSIS AND CORRELATION OF DATA

1. ANALYTICAL METHODOLOGY

The physics of cratering and pavement disruption in paved runway systems is considerably more complex than cratering in ordinary in-situ geologic materials, due to a higher degree of layering and more complete confinement of explosive energy. Consequently, analysis of cratering data in layered pavement systems is complicated by a number of additional characteristic parameters defining thicknesses and properties of the layered materials. Empirical methods, scaling relationships, continuum mechanics computer codes, and static or quasi-static methods represent the four basic approaches to cratering analyses which have been applied to date (ref. 8).

The primary purpose of this effort is to derive bomb crater damage repair relationships from available experimental data in a form suited to field use. Thus, this analytical effort necessarily fits into the "empirical method" category. However, wherever possible, other methods are utilized to aid in the development of functional relationships and the explanation of anomalies and trends.

Plots of the unreduced (raw data) bomb damage data exhibit some trends, but do not readily lend themselves to development of general damage relationships. The development of functional relationships purely from statistical methods for multiple variables (multiple regression analysis) is a lengthy process and is limited by the necessity of assuming the order of the regressions. Any guidelines for possible functional forms which can be used to "preprocess" the data prior to regression analysis greatly simplify the mechanics of curve fitting.

Guidelines for possible empirical functional relationships among the multitude of parameters from previous efforts are virtually nonexistent for pavement cratering. However, several "scaling relationships" for buried explosions in naturally-occurring geologic materials have been suggested (ref. 19 - 21), using charge weight scaling where linear dimensions are scaled by some power of explosive charge weight, varying

from 1/4 to 1/3. These relationships assume that linear dimensions (radius, cube root of volume, square root of area) are related to the appropriate power of the equivalent explosive charge weight. These "scaling relationships" must be considered with caution, since none developed to date appears to apply in general to all data; however, they do yield clues as to possible functional trends to investigate.

Initial efforts to derive functional damage relationships involved a systematic scheme of elimination of dependence on input parameters by a series of related linear regressions. The procedure used to form functional relationships between input (weapon and target) parameters and damage parameters can be simply stated as follows:

- a. Generate a relationship of the form

$$D = f(d, w) \quad (3)$$

where D is a damage parameter

d is depth of burst

w is weapon explosive weight (TNT equivalent)

f is a functional form

- b. Incorporate Equation (3) in a relationship

$$D = g(f, s_1) \quad (4)$$

where s_1 is either subbase type or pavement thickness
and g is a function

- c. Incorporate Equation (4) in a relationship

$$D = h(g, s_2) \quad (5)$$

where s_2 is either subbase type or pavement thickness
(the one not used in Equation (4)) and h is
a function

The order of inclusion of soil type and pavement thickness in Equations (4) and (5) is determined by using as s_1 the one which initial study of the data shows to have the dominant effect on the particular damage parameter being considered.

Completion of these three steps results in an equation which relates a damage parameter to weapon weight, depth of burst, subbase type, and pavement thickness.

In each step of the process, the functions were evaluated as Gaussian least-squares polynomials. The functional relations derived by this method, however, proved unsatisfactory, due to excessive scatter of the experimental data points about the final plotted functional curve.

Further guidelines for the development of functional relations may be derived by dimensional analysis (ref. 21 and 22). Previous attempts to derive "scaling laws" based on similitude theory have appeared to fail, in that they do not fit all data. These apparent failures may be due to using an incomplete list of variables in the dimensional analysis (either overlooked by the analyst or simply not measured during experiments). However, a dimensional analysis of all the parameters considered important in the pavement cratering problem yields further possible functional forms, which can then be subjected to statistical evaluation in the form of regression analysis. The major parameters measured in the Hays and Fort Sumner test programs suggest the following functional form:

$$\frac{R}{d} = f\left(\frac{d}{W^{1/3}}, \frac{d}{W^{1/4}}, \frac{t}{d}, \text{subbase soil type}\right) \quad (6)$$

when subjected to dimensional analysis. The dependent variable, R , represents any of the damage parameters reduced to linear dimensions, such as $A^{1/2}$ (square root of area) or $V^{1/3}$ (cube root of volume), or crater radius. In the list of independent variables, d = depth of burst, W = explosive charge weight, and t = pavement thickness. Note that the subbase soil type has been included as an independent parameter to account for constitutive behavior effects. The soil type is treated parametrically in this analysis, rather than by quantitative constitutive properties such as density, compressive strength, elastic modulus, etc., since most of these parameters were either not measured, or were only measured at a few locations at the test site. In addition, it was felt that for field usable damage prediction, quantitative soil properties would not be available; therefore, a descriptive soil-type parameter should prove imminently more useful.

With the development of satisfactory groupings of the independent parameters (input properties being weapon and target data), the generation of the functional form through curve-fitting becomes greatly simplified.

By reducing the dependent and independent variable lists, as in Equation (6), such that the experimental data points exhibit definite trends and minimal deviation, more effort can be expended in deriving the final form of the function, "f", in order to obtain a "best fit" to the data.

The curve fits were accomplished using the technique of Gaussian least-squares polynomial approximation. The approximating polynomials derived from the least-squares fit are easier to manipulate than are many other types of polynomials, and the resulting curve fit exhibits lesser dependence on "maverick" data points (or "outliers") than do some other techniques. The "almost-equal error" property of Chebyshev polynomial approximation becomes difficult to apply to highly clustered data, and its heavier weighting of the ends of the region (ref. 23) puts undue weight on the shallow depth-of-burst data, which may not be physically justified.

The "goodness-of-fit" of a polynomial generated by the least-squares technique is measured through correlation coefficients, standard deviation, and the randomness of residual errors. An approximation to the standard deviation of the fitted polynomial error is obtained as the RMS (root-mean-square) residual (ref. 24). In addition, plots of the residuals (error at each data point, i.e., data values minus polynomial value) versus the corresponding value of the approximating polynomial are valuable indicators of the randomness of errors and also point out problems such as highly clustered data, "outliers" (bad data points), or incorrect functional form (ref. 25). A "good" polynomial fit exhibits purely random errors (residuals) and an RMS error small relative to the mean function value.

2. REDUCED PLOTS - FUNCTIONAL RELATIONSHIPS

The functional relationships for final field usage were derived from Hays, Kansas, and Fort Sumner, New Mexico, test site data because: (1) these data constitute over 50 percent of the data base; (2) a full set of all damage parameter values is available for all tests; and (3) the input parameters are limited to four (of significance), the values of which vary over a substantial range. Thus, each damage parameter is treated as a function of the four input parameters: (1) charge weight, W (equivalent TNT weight); (2) depth of burst, d; (3) pavement thickness, t; and (4) sub-base soil type.

Plots of the linearized damage parameters in the form:

$$\frac{R}{d} = f\left(\frac{d}{W^{1/3}}, \text{soil type}\right) \quad (7)$$

illustrate very good behavior and simplicity of form. The subbase soil type is treated parametrically by separating the data for the Hays test site (organic clay subbase) and the Fort Sumner test site (medium-silty-clayey sand subbase). A search failed to uncover any definite pavement thickness effects. However, this should in no way be construed to mean that pavement thickness is not a significant parameter in the cratering mechanism. In fact, analytical efforts and previous observations (ref. 8) indicate, for instance, that the lower cavity is smaller for thinner (8 inch versus 11 inch) pavement by approximately 7 percent for the same charge size. However, the pavement thickness variations exist only in some of the Hays data, and then are limited to a range of 8 to 11 inches in thickness. Additional tests conducted at CERF contain more pavement-type variations, but are for a single depth of burst and the most important damage measurements were not recorded in a manner consistent with the earlier Hays and Fort Sumner test data.

Both second-order polynomials and an exponential function exhibited a reasonable degree of fit to the test data. For example, Figures 17 and 18 show both functions and the available data points as a function of charge weight for the Hays data (organic clay subbase) and for the Fort Sumner data (M-S-C sand subbase), respectively, for a semipermanent repair earth replacement volume. Note the functional form of equation (7) in the plots, where the volume is plotted as the cube root and is divided by the depth of burst ($\frac{v^{1/3}}{DOB}$ versus $\frac{DOB}{W^{1/3}}$), and soil type is handled parametrically by presenting separate plots.

The RMS errors resulting from the second-order and the exponential functions are presented in Table 10. For the clay subbase, the error is slightly less with the second-order polynomial than with the exponential. However, when the residuals from each fit are plotted as a function of the polynomial value (Figures 19 - 22), a different result appears. Figures 19 and 21 illustrate that the errors resulting from the second-order

FUNC EARTH REPLACE VOL (SP) ($V \times 1/3 / DOB$) VERSUS REDUCED DEPTH OF BURST ($DOB / W \times 1/3$)

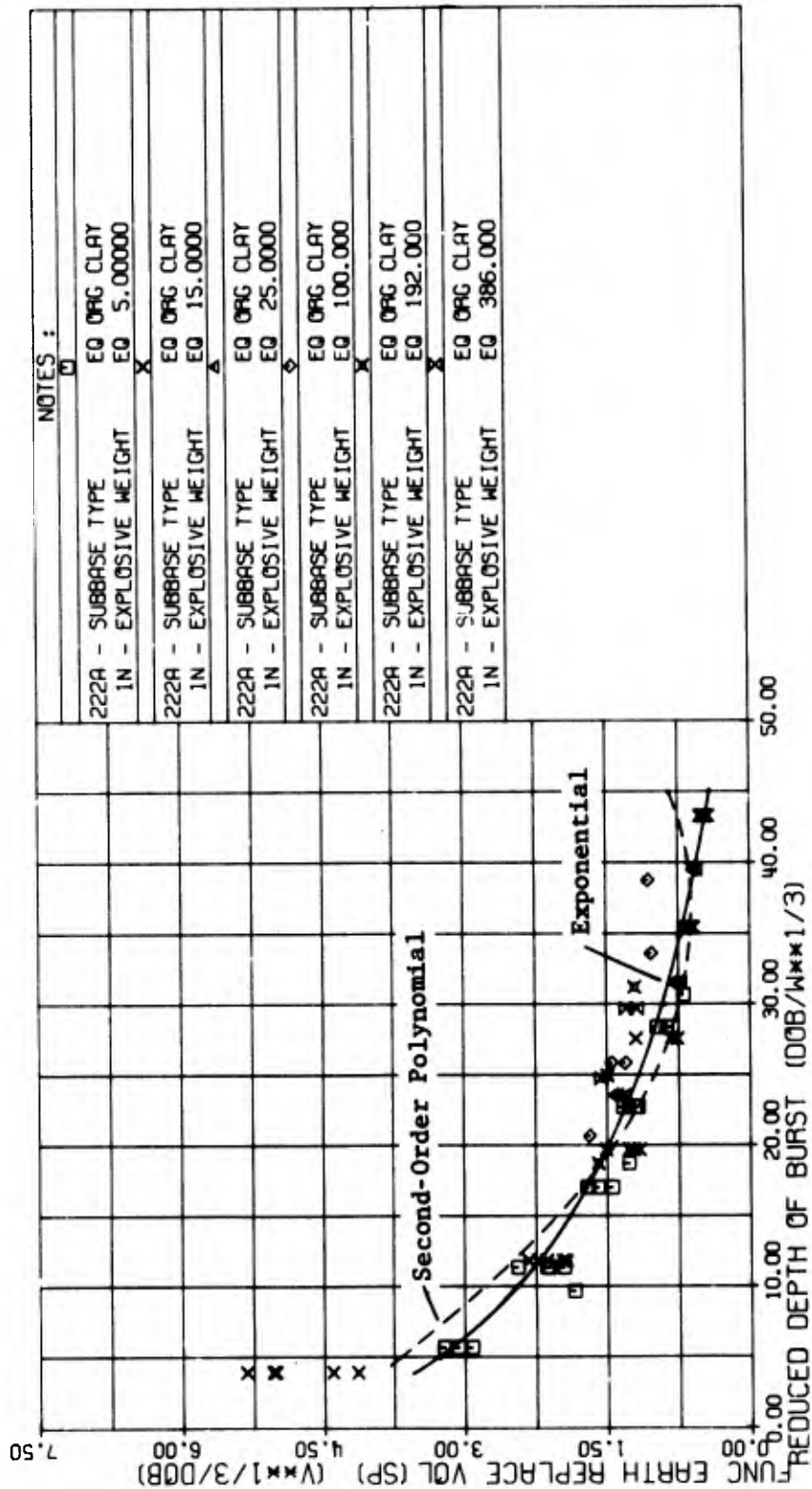


Figure 17. Comparison of Second-Order and Exponential Curve Fits to Reduced Earth Replacement Volume for Organic Clay Subbase

FUNC EARTH REPLACE VOL (SP) ($V \times 1/3 / DOB$) VERSUS REDUCED DEPTH OF BURST ($DOB / W \times 1/3$)

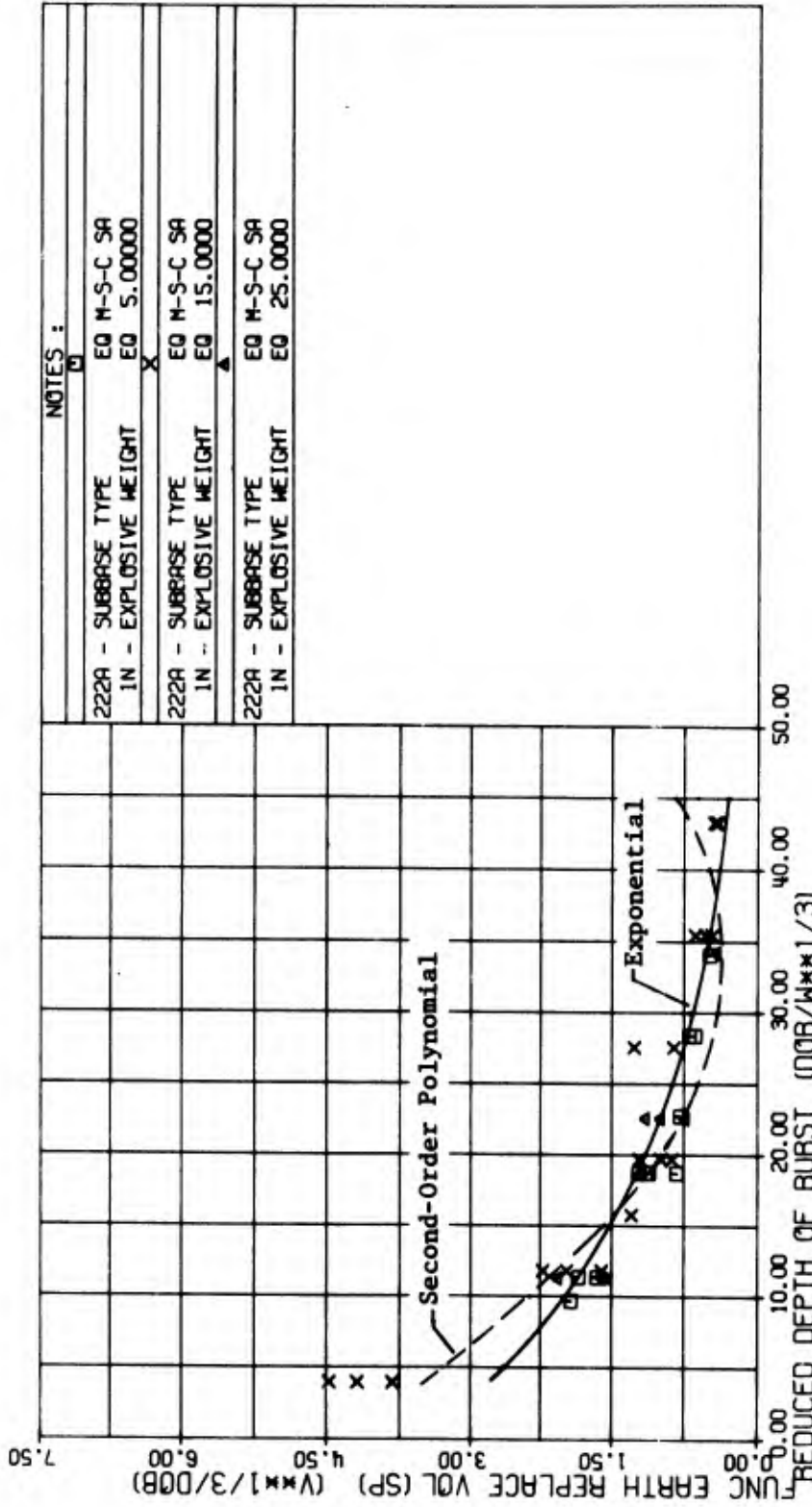


Figure 18. Comparison of Second-Order and Exponential Curve Fits to Reduced Earth Replacement Volume for Silty, Clayey Sand Subbase

TABLE 10. EARTH REPLACEMENT VOLUME, SEMIPERMANENT REPAIR; COMPARISON OF APPROXIMATING FUNCTIONS

Function Type	Function Coefficients			RMS Error	Adjusted RMS Error
	A	B	C		
<u>Organic Clay Subbase</u>					
Second Order	4.7329	-0.22554	0.003097	0.403	0.316
Exponential	1.4369	-0.051055	--	0.430	0.219
<u>Silty, Clayey Sand Subbase</u>					
Second Order	4.4403	-0.24311	0.003630	0.354	0.307
Exponential	1.2373	-0.053898	--	0.221	0.205

Function Form:
$$\frac{v^{1/3}}{d} = f\left(\frac{d}{W^{1/3}}\right)$$

Second Order Polynomial: $f(X) = A + B X + C X^2$

Exponential: $f(X) = e^{A + B X}$

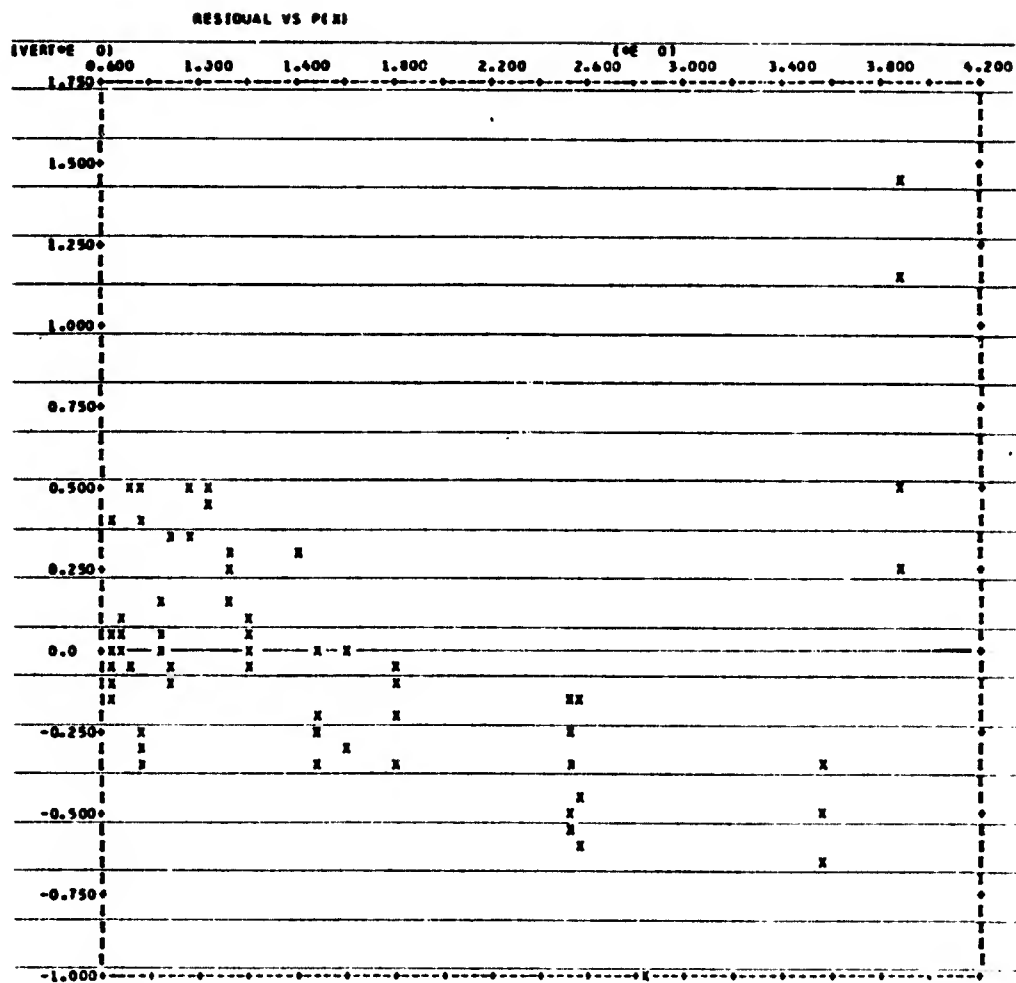


Figure 19. Residual Distribution for Second-Order Approximation, Semipermanent Earth Replacement Volume, Organic Clay Subbase

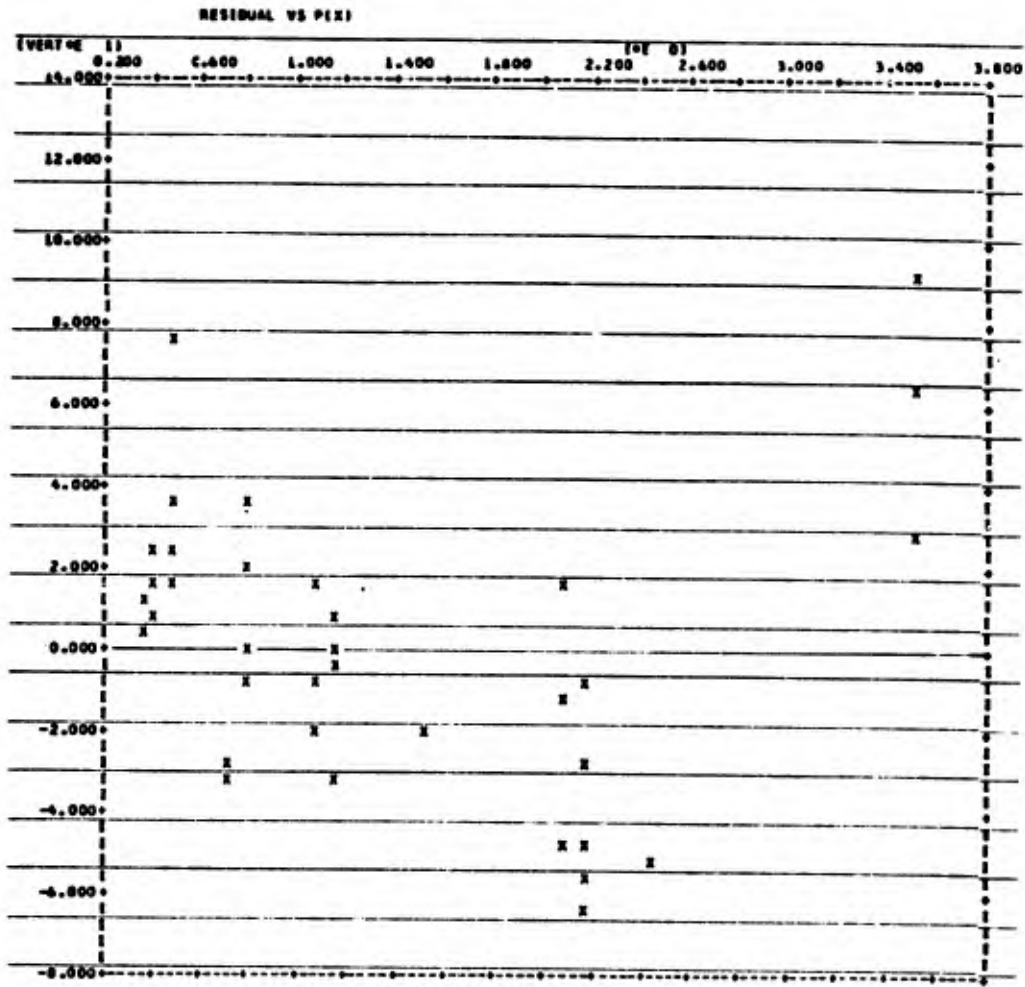


Figure 21. Residual Distribution for Second-Order Approximation, Semipermanent Earth Replacement Volume, Silty, Clayey Sand Subbase

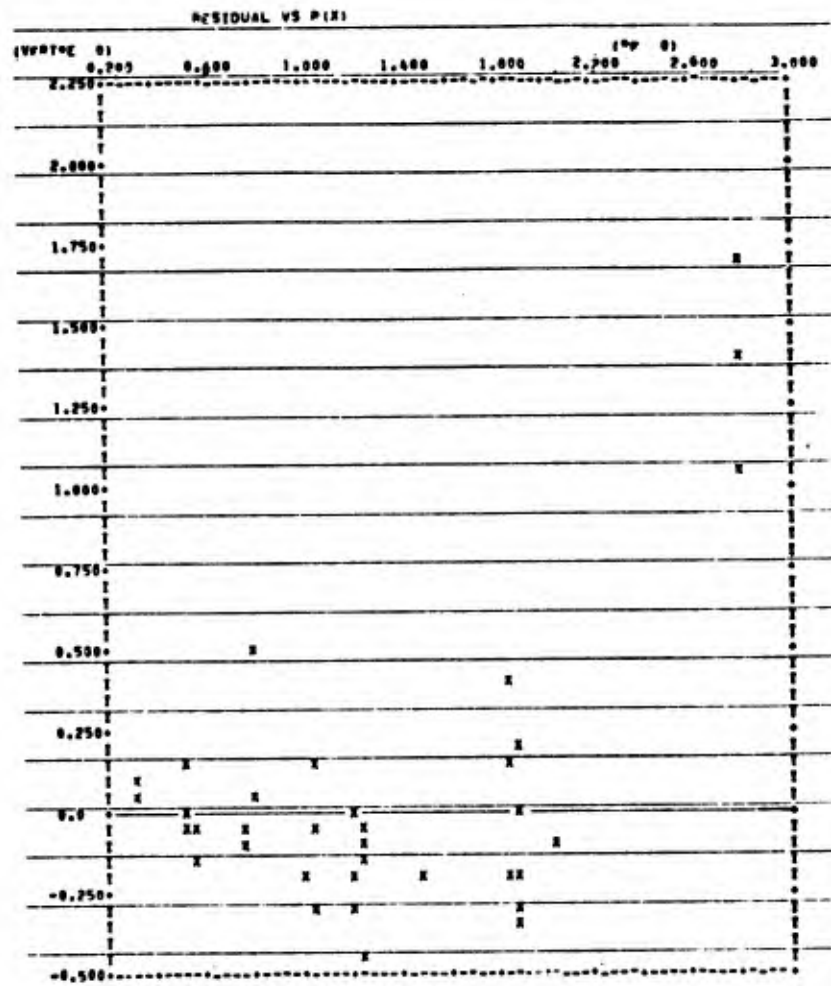


Figure 22. Residual Distribution for Exponential Approximation, Semipermanent Earth Replacement Volume, Silty, Clayey Sand Subbase

polynomial approximation, although providing a lower total RMS error than the exponential, are not evenly distributed about a mean of zero. The errors resulting from the exponential curve fit, on the other hand, illustrate a much better distribution about a mean of zero (Figures 20 and 22). In addition, both residual plots show the data points at high values of $P(X)$, the approximating function value, possess unduly large residuals. This leads one to suspect the validity of these data points. Upon closer inspection, these points were found to represent only the very shallow depths of burst - so shallow in fact, that in some of these cases the charge may not have been totally below the hole in the pavement. It is felt that this situation, with very shallow depths of burst, can be expected to exhibit slightly different behavior and for the observed experimental errors to be higher than for deeper burial depths. However, this was not considered sufficient justification for simply discarding the shallow burst data points, particularly since the total RMS errors were within acceptable bounds. The approximating polynomials were not altered, but the effect of removing these few apparently - deviant points was investigated by simply recalculating the RMS errors, ignoring the errors at these points. The resulting errors are then reduced to those shown in Table 10 under the heading "Adjusted RMS error". With this adjustment, the exponential function becomes a more attractive choice than the second-order polynomial. In addition, the second-order curve tends to reach a minimum and begin increasing again, with increasing values of reduced depth of burst ($\frac{DOB}{W^{1/3}}$). This would indicate the existence of a depth of burst (deeper than the optimum) corresponding to a minimum repair volume, beyond which volume would again begin to increase. This situation has not been observed in practice. Indeed, at depths of burst deeper than the optimum, the craters become smaller, approaching a constant value for very deep explosions. Thus, it seems the exponential function is a better representation of the data than the second-order polynomial. In fact, the same holds true for all the damage parameters relevant to repair. The resulting curve fits are presented in Figures 23 through 48 for both subbase types. The exponential coefficients and resultant RMS errors are shown for each damage plot in

RED EJECTA VOLUME (V^{1/3}/DOB) VERSUS REDUCED DEPTH OF BURST (DOB/W^{1/3})

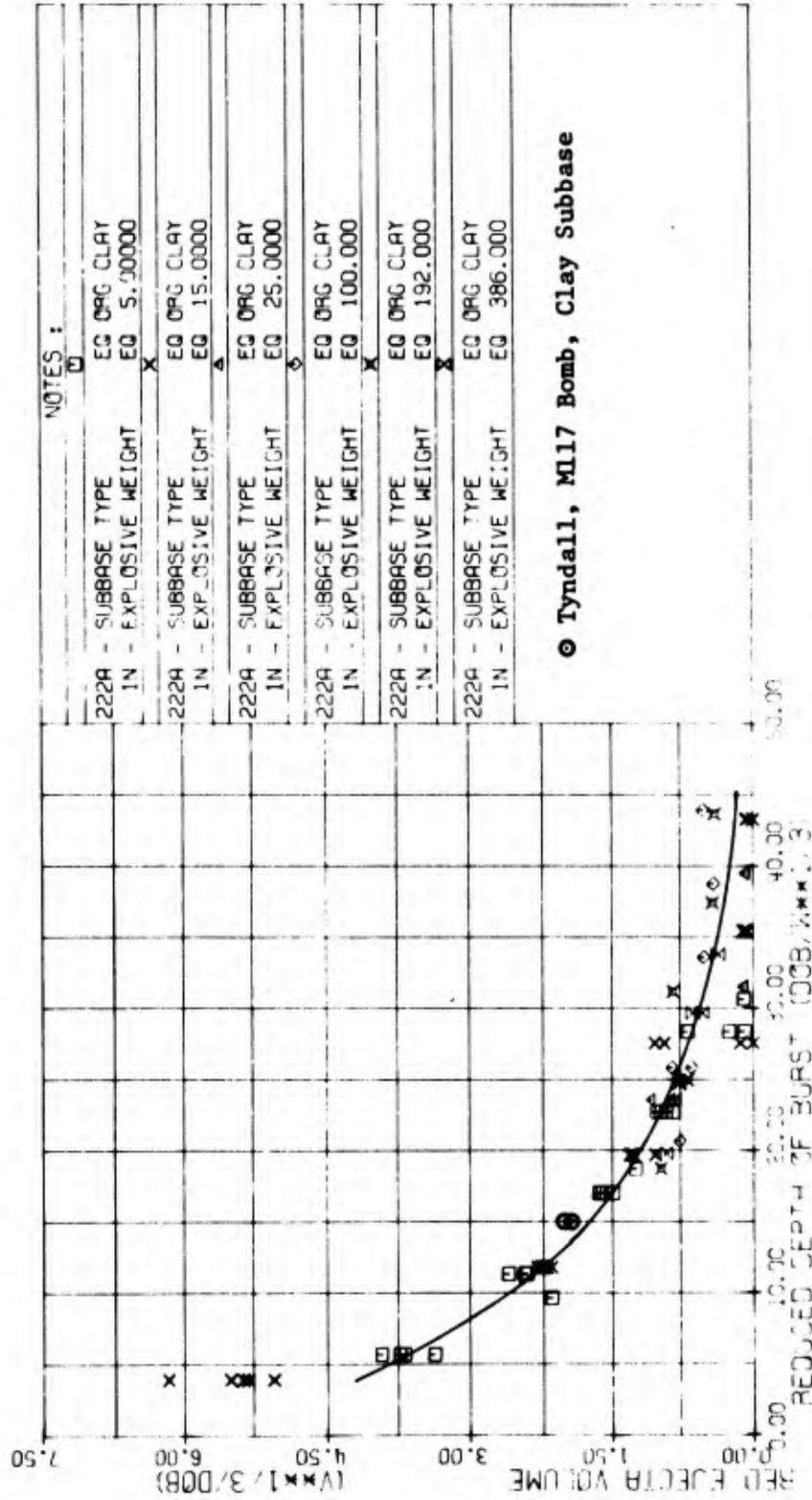


Figure 23. Reduced Ejecta Volume Versus Reduced Depth of Burst; Organic Clay Subbase

RED EJECTA VOLUME (V**1/3/DOB) VERSUS REDUCED DEPTH OF BURST (DOB/W**1/3)

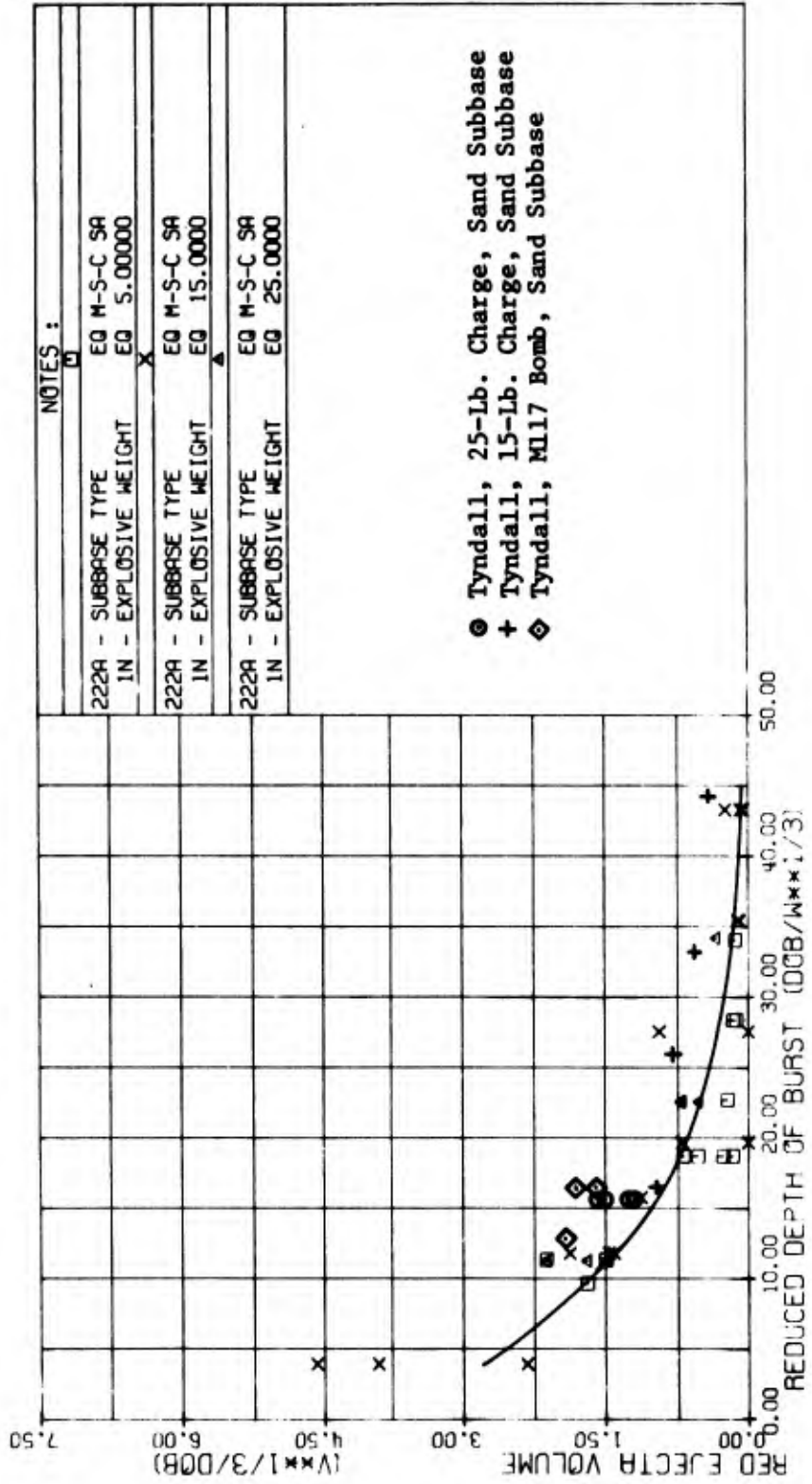


Figure 24. Reduced Ejecta Volume Versus Reduced Depth of Burst; Silty, Clayey Sand Subbase

FUNC EARTH REPLACE VOL (SP) ($V \times 1/3 / DOB$) VERSUS REDUCED DEPTH OF BURST ($DOB / W \times 1/3$)

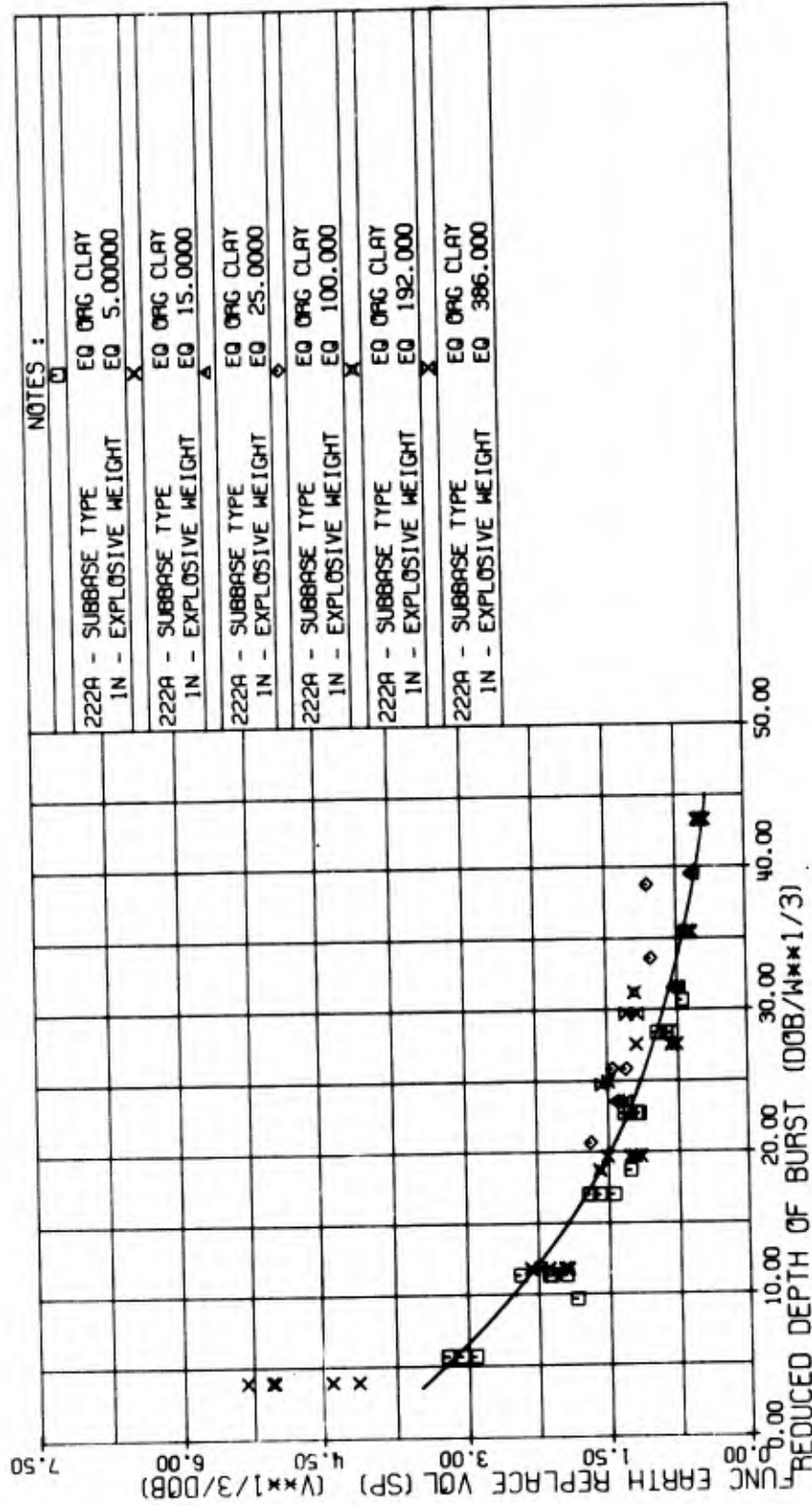


Figure 25. Reduced Earth Replacement Volume for Semi-permanent Repair Versus Depth of Burst;
Organic Clay Subbase

FUNC EARTH REPLACE VOL (SP) ($V \times 1/3 / DOB$) VERSUS REDUCED DEPTH OF BURST ($DOB / W \times 1/3$)

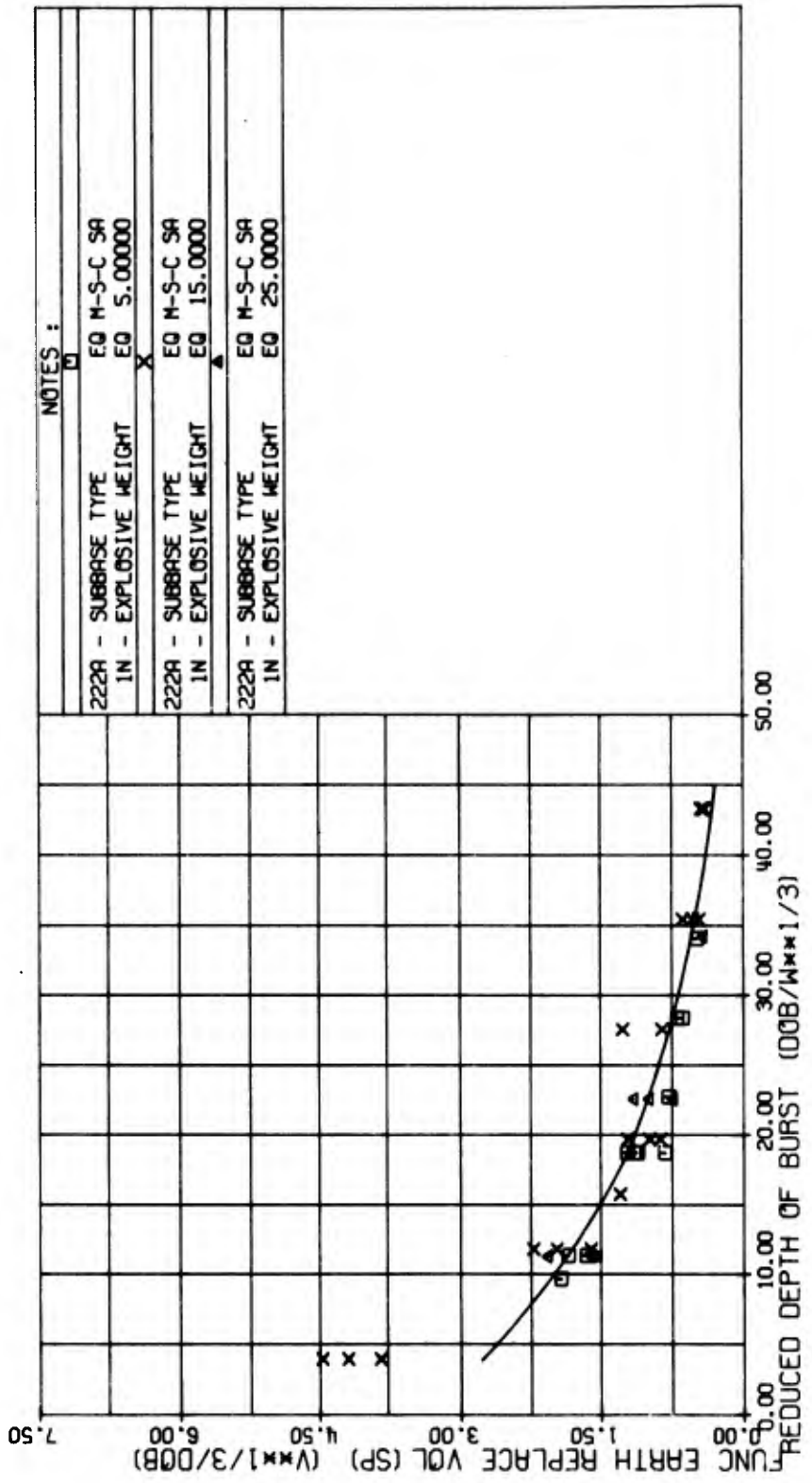


Figure 26. Reduced Earth Replacement Volume for Semipermanent Repair Versus Depth of Burst; Silty, Clayey Sand Subbase

FUNC VOL EARTH REMOVED (SP) (1/3/DOB) VERSUS REDUCED DEPTH OF BURST (DOB/W^{1/3})

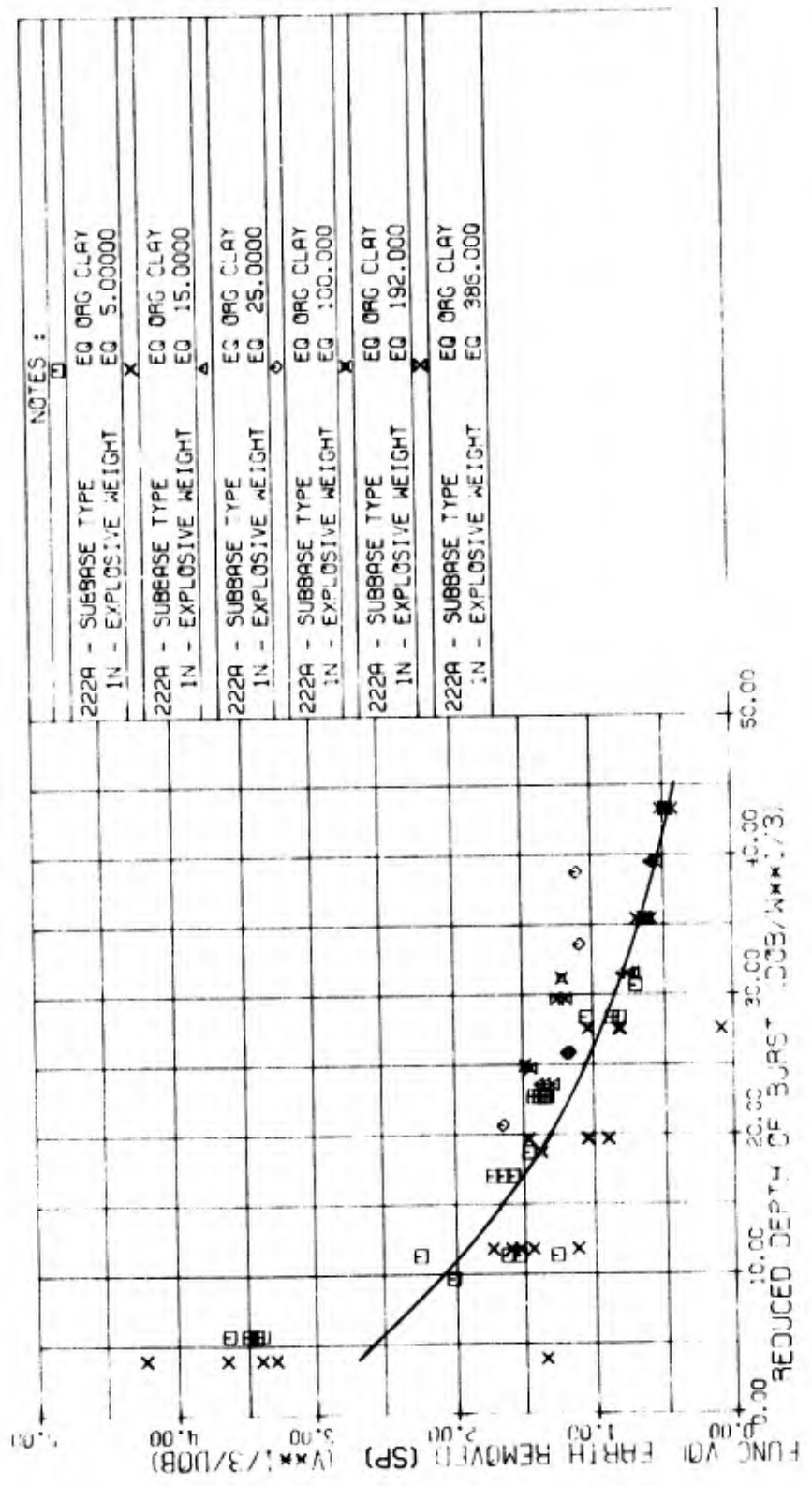


Figure 27. Reduced Earth Removal Volume for Semipermanent Repair Versus Depth of Burst; Organic Clay Subbase

FUNC VOL EARTH REMOVED (SP) (V**1/3/DOB) VERSUS REDUCED DEPTH OF BURST (DOB/W**1/3)

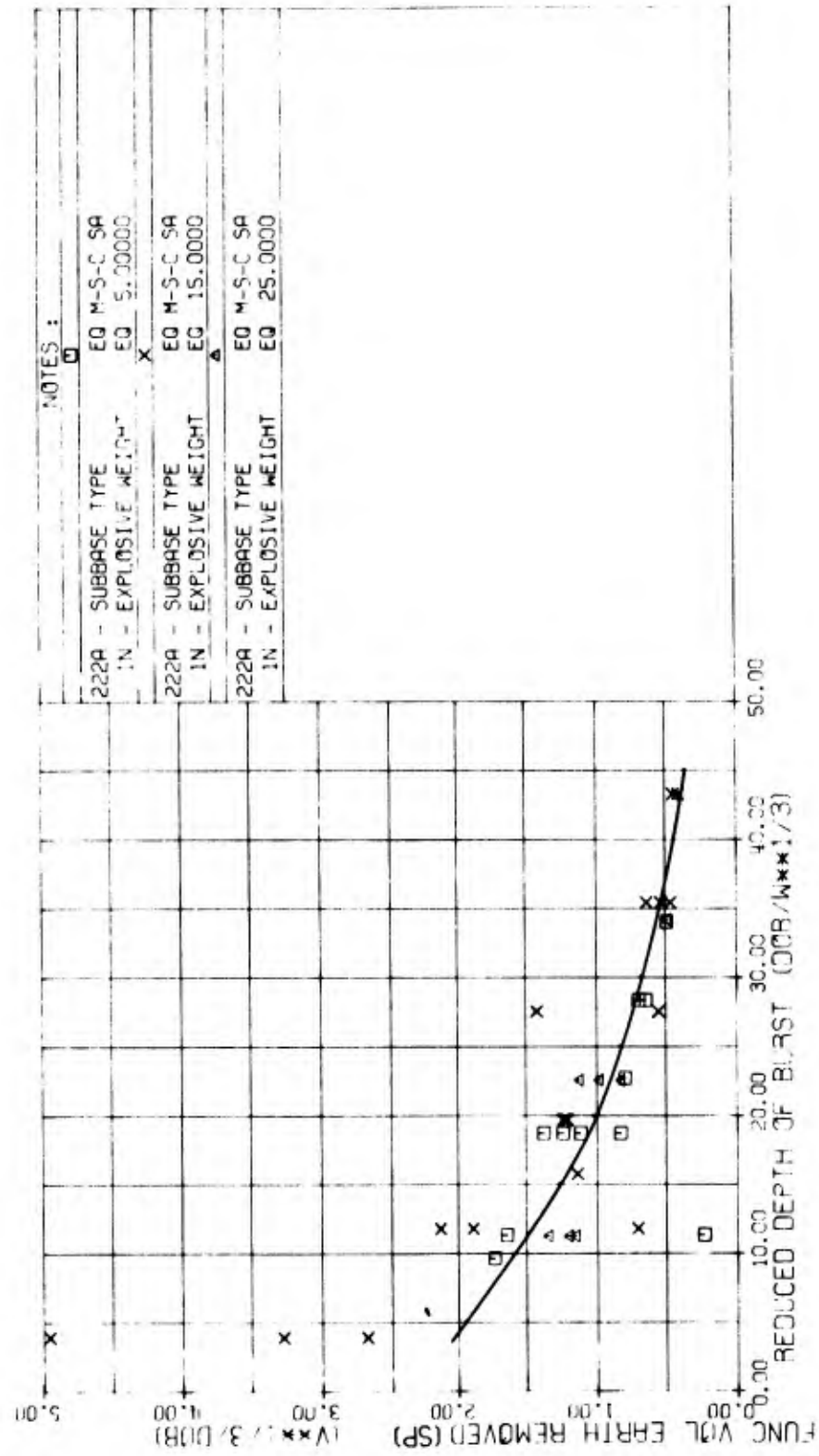


Figure 28. Reduced Earth Removal Volume for Semipermanent Repair Versus Depth of Burst; Silty, Clayey Sand Subbase

REDUCED VOL. EARTH REMOVED (E) (W*1/3, DOB) VERSUS REDUCED DEPTH OF BURST (DOB/W*1/3)

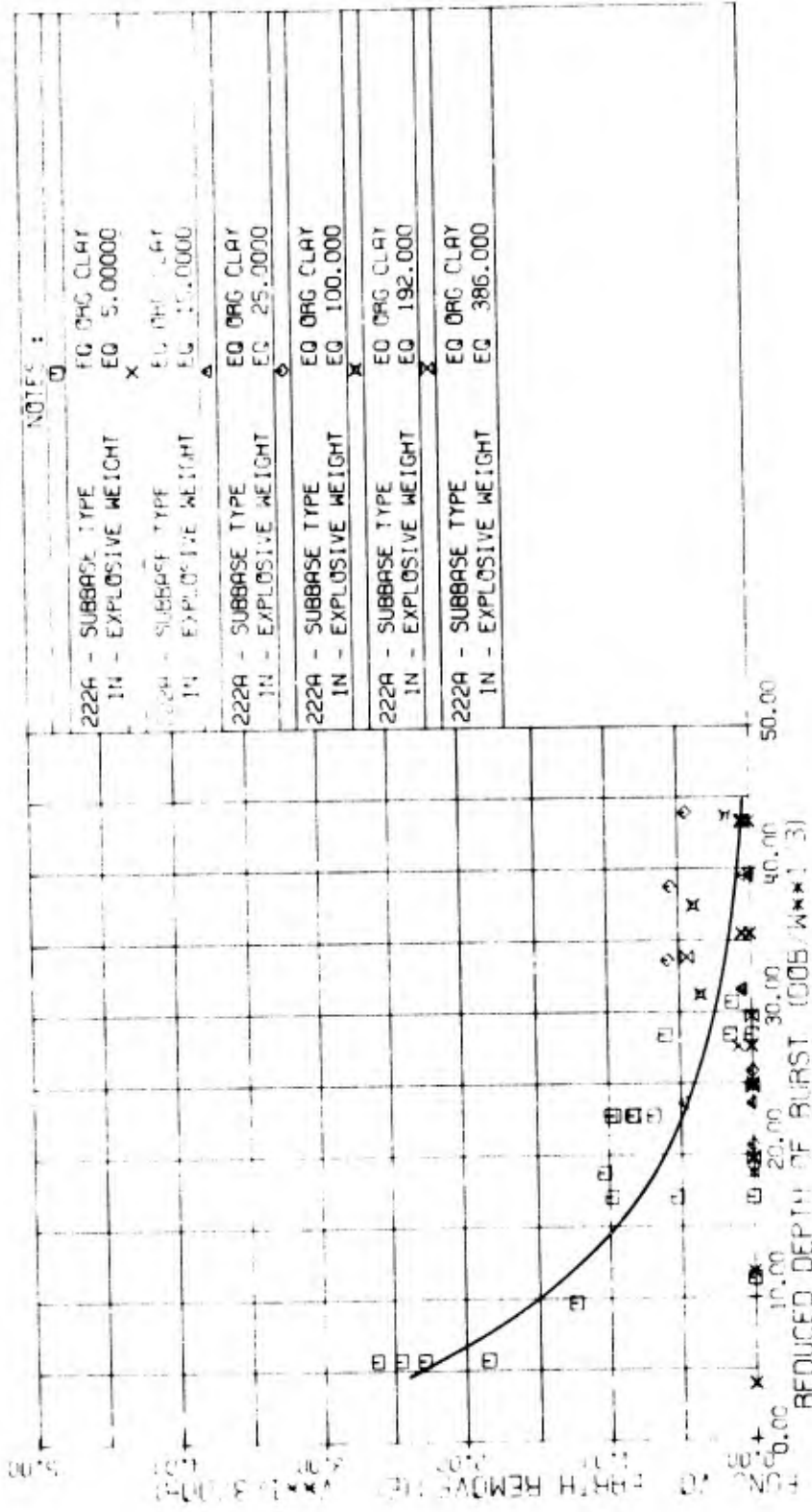


Figure 29. Reduced Earth Removal Volume for Expedient Repair Versus Depth of Burst; Organic Clay Subbase

FUNC VOL EARTH REMOVED (E) (V**1/3/DOB) VERSUS REDUCED DEPTH OF BURST (DOB/W**1/3)

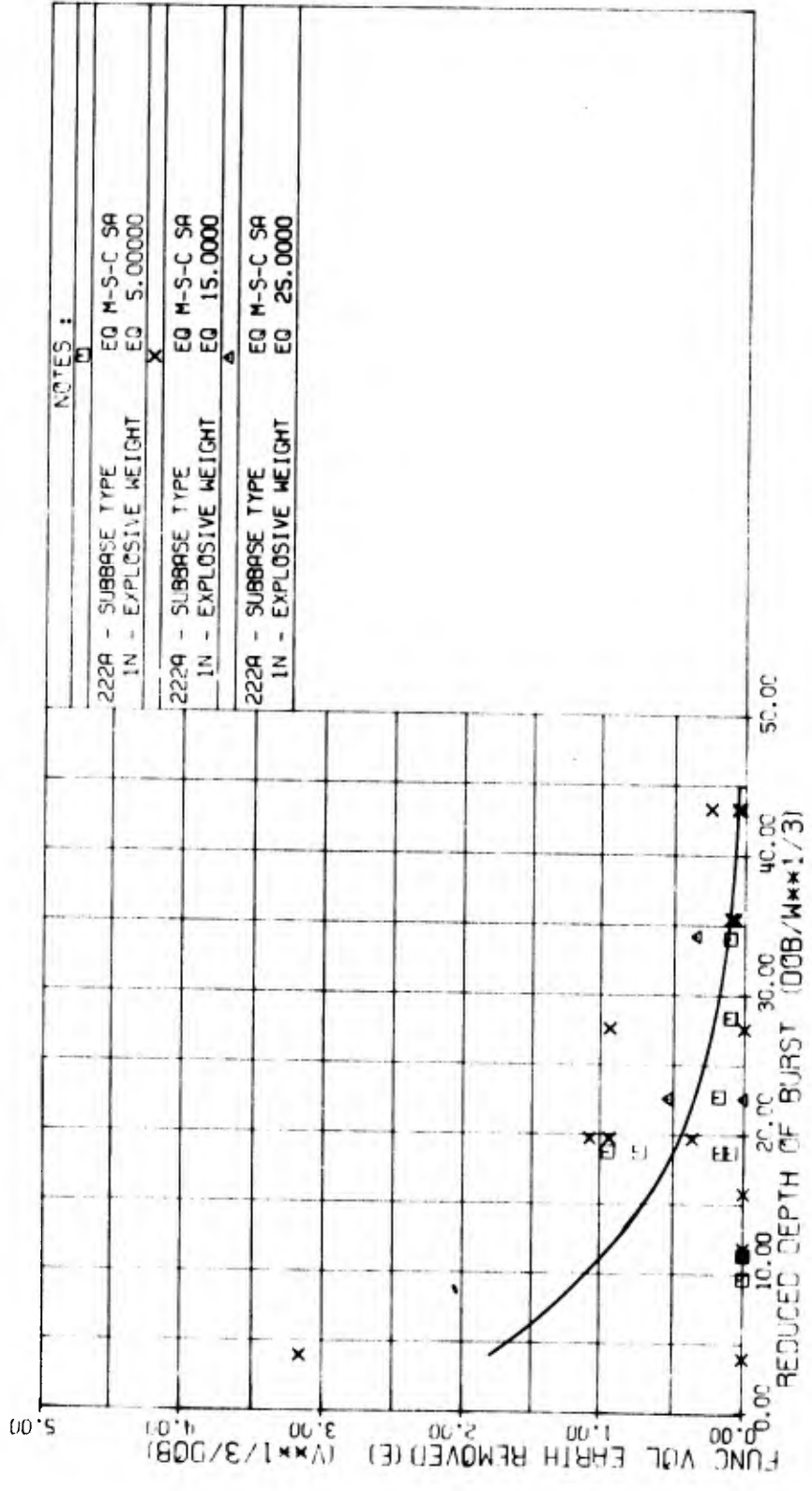


Figure 30. Reduced Earth Removal Volume for Expedient Repair Versus Depth of Burst; Silty, Clayey Sand Subbase

FUNC VOL EARTH REMOVED (P) ($V \times 1/3 / DOB$) VERSUS REDUCED DEPTH OF BURST ($DOB / W \times 1/3$)

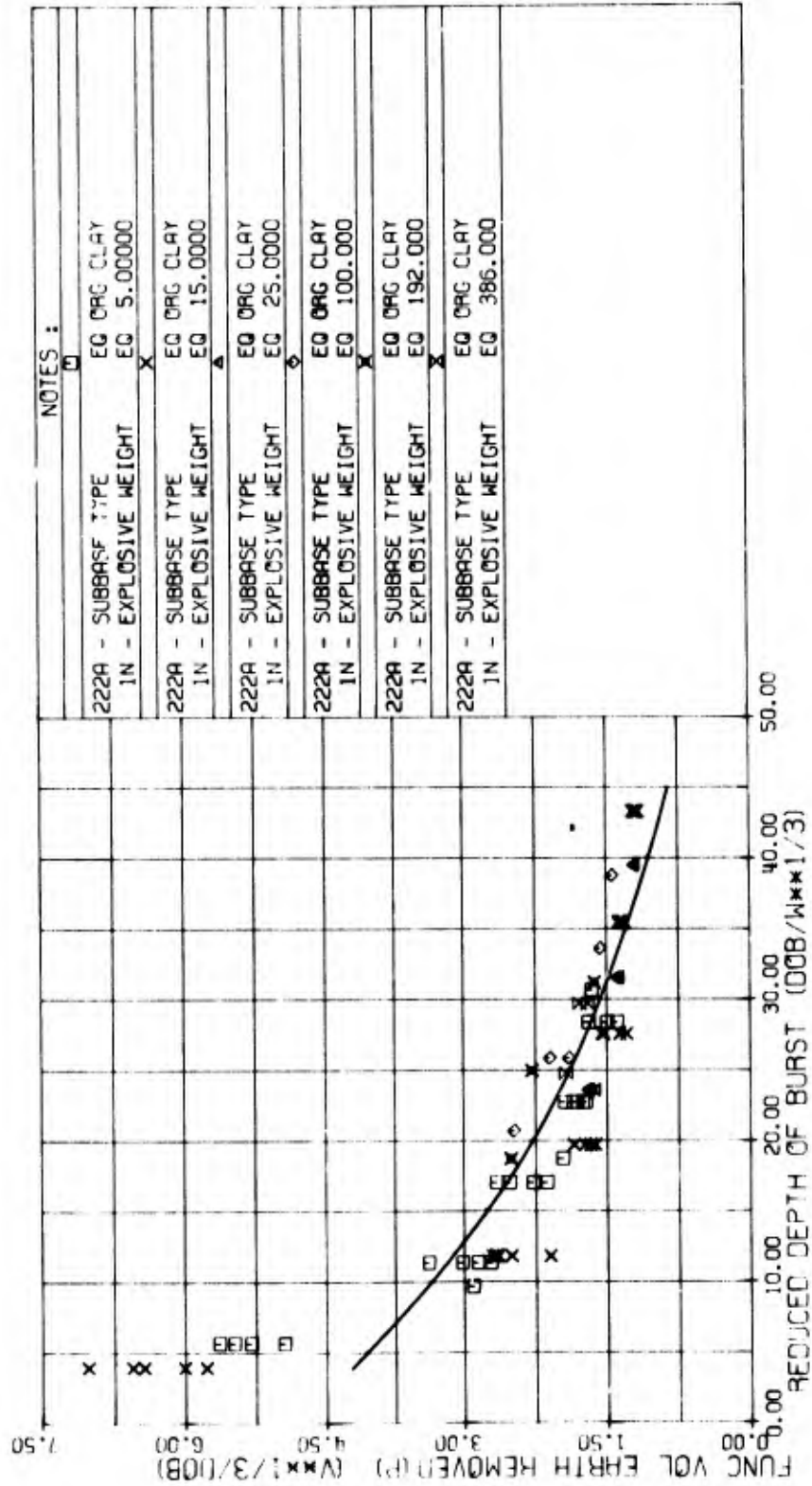


Figure 31. Reduced Earth Removal Volume for Permanent Repair Versus Depth of Burst; Organic Clay Subbase

FUNC VOL EARTH REMOVED (P) (W**1/3/DOB) VERSUS REDUCED DEPTH OF BURST (DOB/W**1/3)

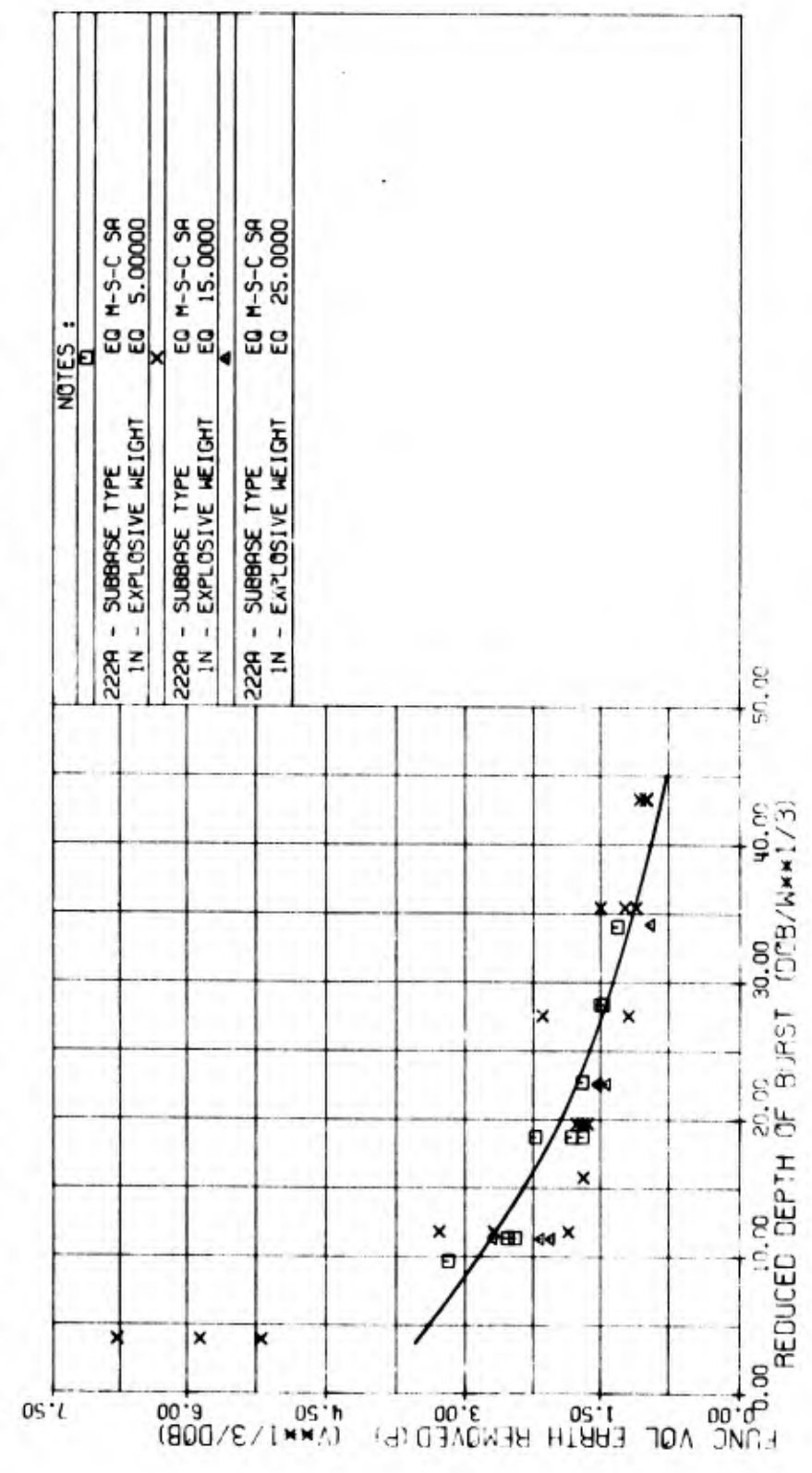


Figure 32. Reduced Earth Removal Volume for Permanent Repair Versus Depth of Burst; Silty, Clayey Sand Subbase

RED PAVEMENT REPAIR AREA (E) (A**1/2/DOB) VERSUS REDUCED DEPTH OF BURST (DOB/W**1/3)

RED PAVEMENT REPAIR AREA (E) (A**1/2/DOB) VERSUS REDUCED DEPTH OF BURST (DOB/W**1/3)

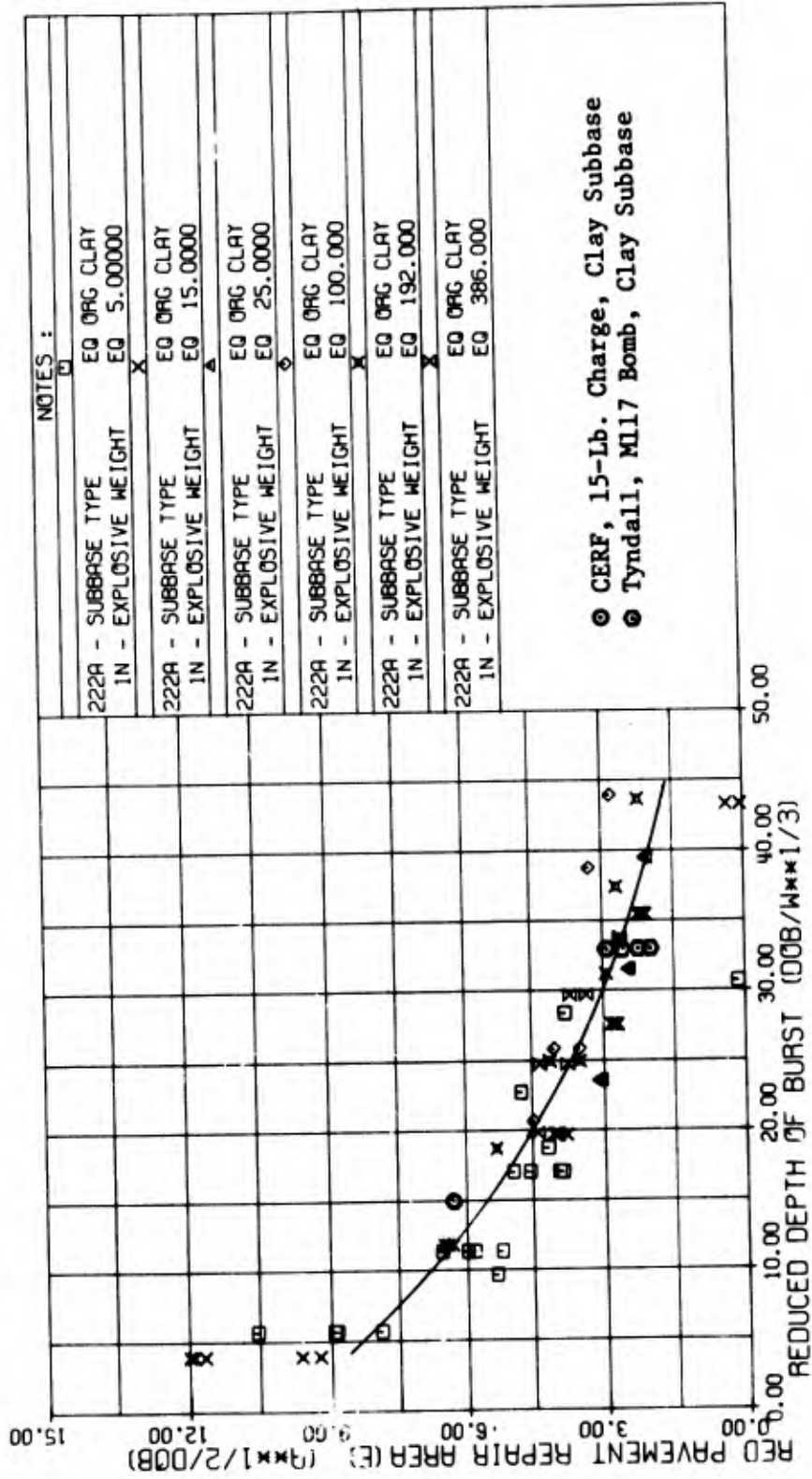


Figure 33. Reduced Pavement Repair Area for Expedient Repair Versus Depth of Burst; Organic Clay Subbase

RED PAVEMENT REPAIR AREA (E) (A^{1/2}/DOB) VERSUS REDUCED DEPTH OF BURST (DOB/W^{1/3})

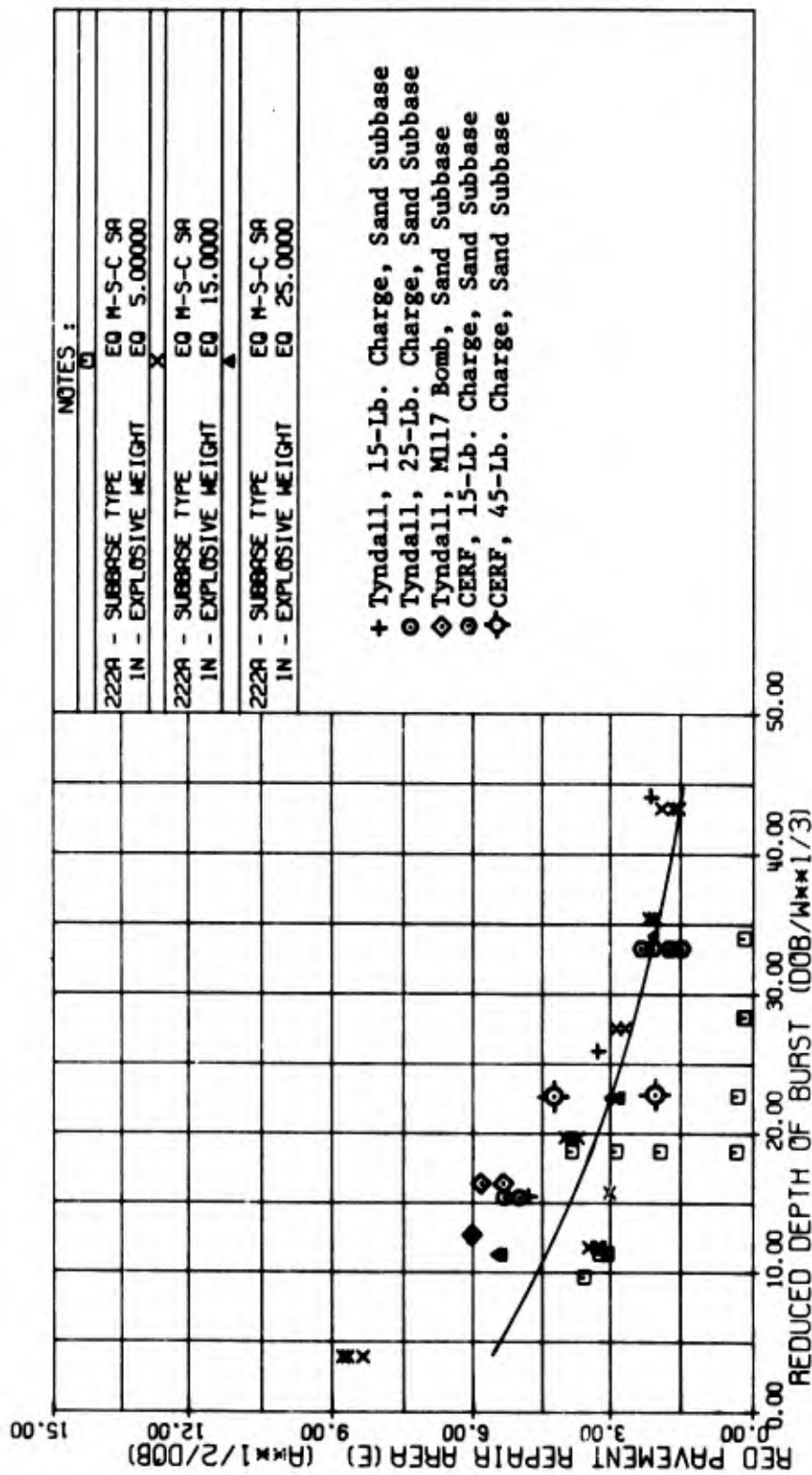


Figure 34. Reduced Pavement Repair Area for Expedient Repair Versus Depth of Burst; Silty, Clayey Sand Subbase

RED PAVEMENT REPAIR AREA (SP) ($A \times 1/2 / DOB$) VERSUS REDUCED DEPTH OF BURST ($DOB / W \times 1/3$)

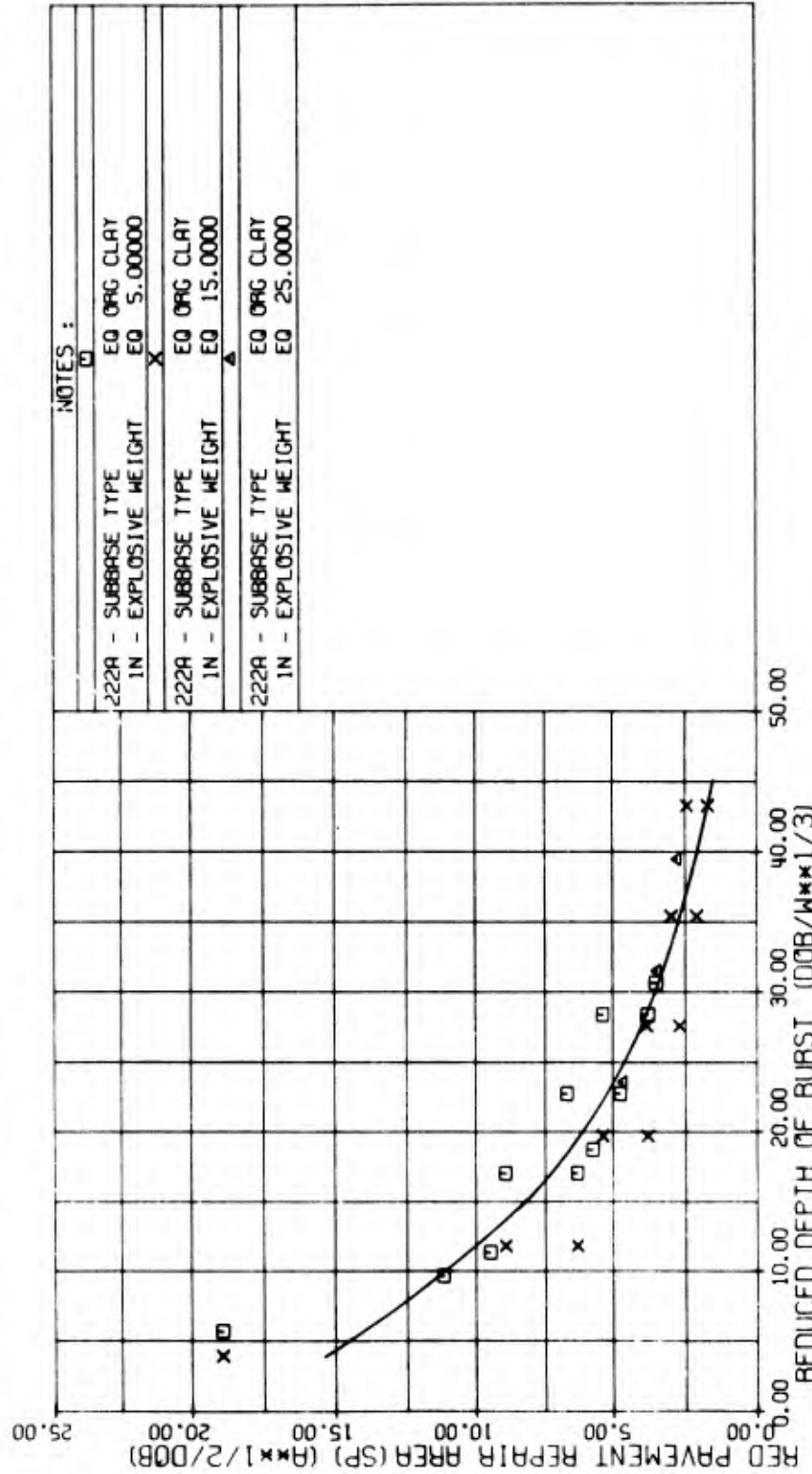


Figure 35. Reduced Pavement Repair Area for Semipermanent Repair Versus Depth of Burst;
Organic Clay Subbase

RED PAVEMENT REPAIR AREA (SP) ($A \times 1/2 / DOB$) VERSUS REDUCED DEPTH OF BURST ($DOB / W \times 1/3$)

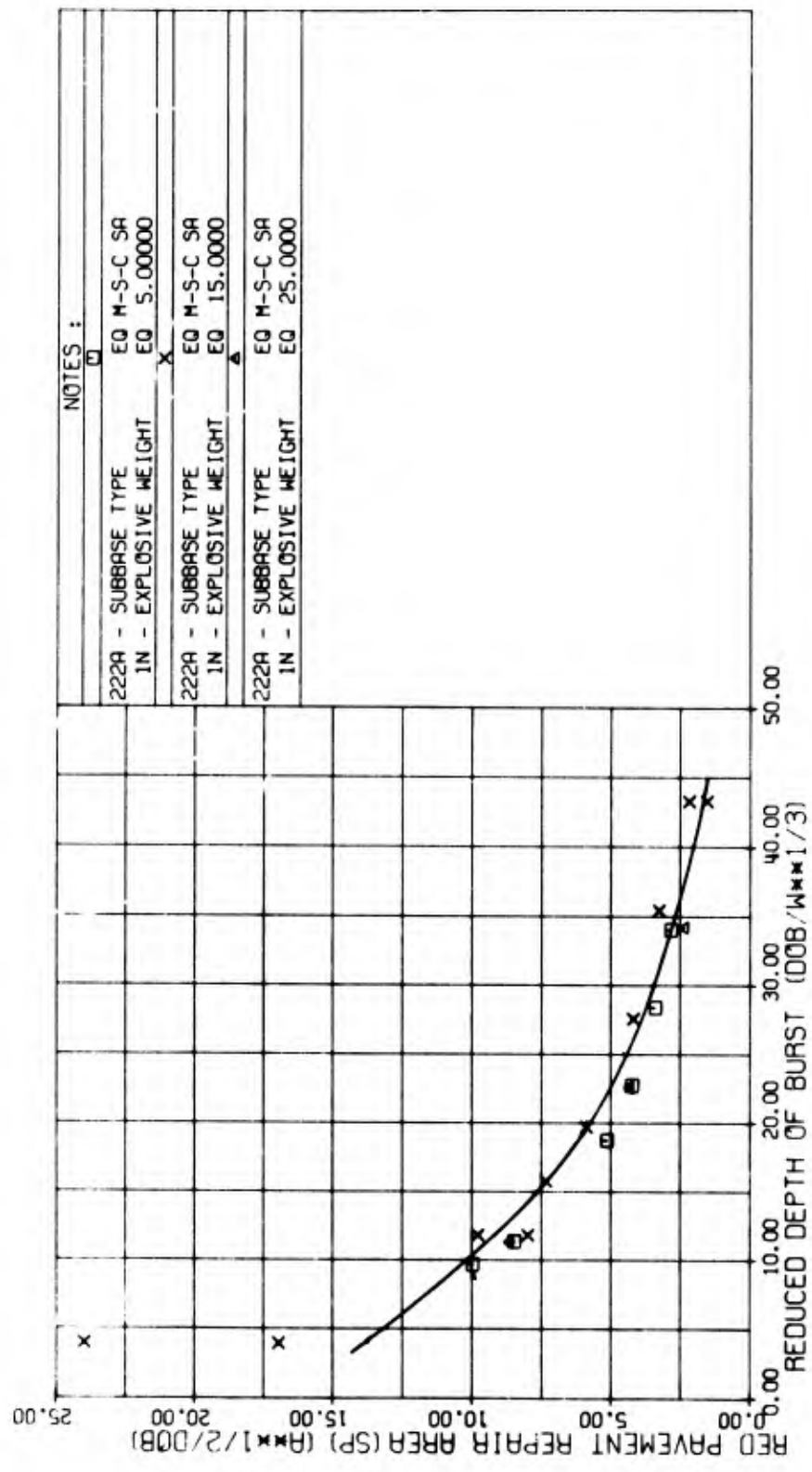


Figure 36. Reduced Pavement Repair Area for Semipermanent Repair Versus Depth of Burst; Silty, Clayey Sand Subbase

RED PAVEMENT REPAIR AREA (P) (A**1/2/DOB) VERSUS REDUCED DEPTH OF BURST (DOB/W**1/3)

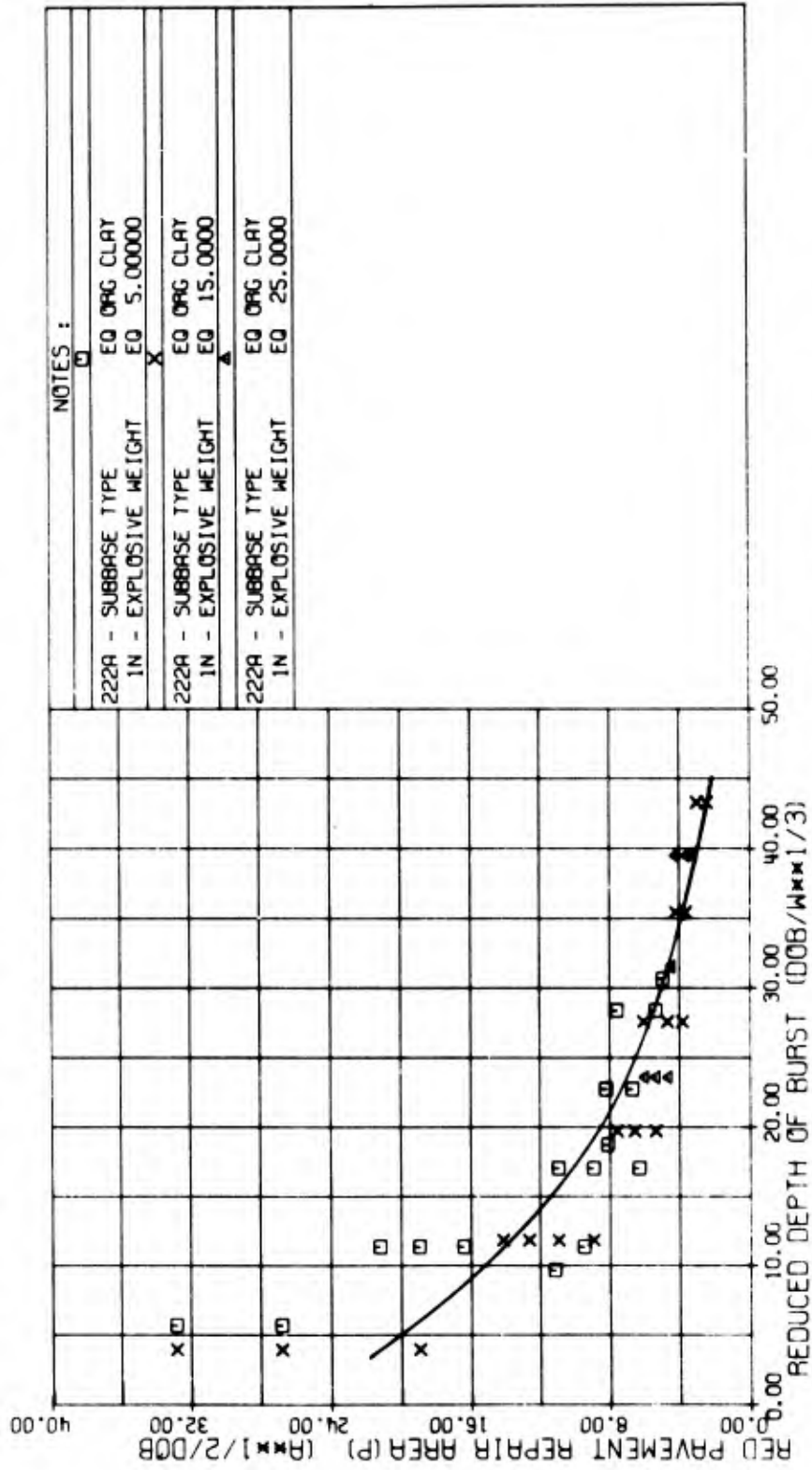


Figure 37. Reduced Pavement Repair Area for Permanent Repair Versus Depth of Burst;
Organic Clay Subbase

RED PAVEMENT REPAIR AREA (P) ($A \times 1/2/DOB$) VERSUS REDUCED DEPTH OF BURST ($DOB/W^{1/3}$)

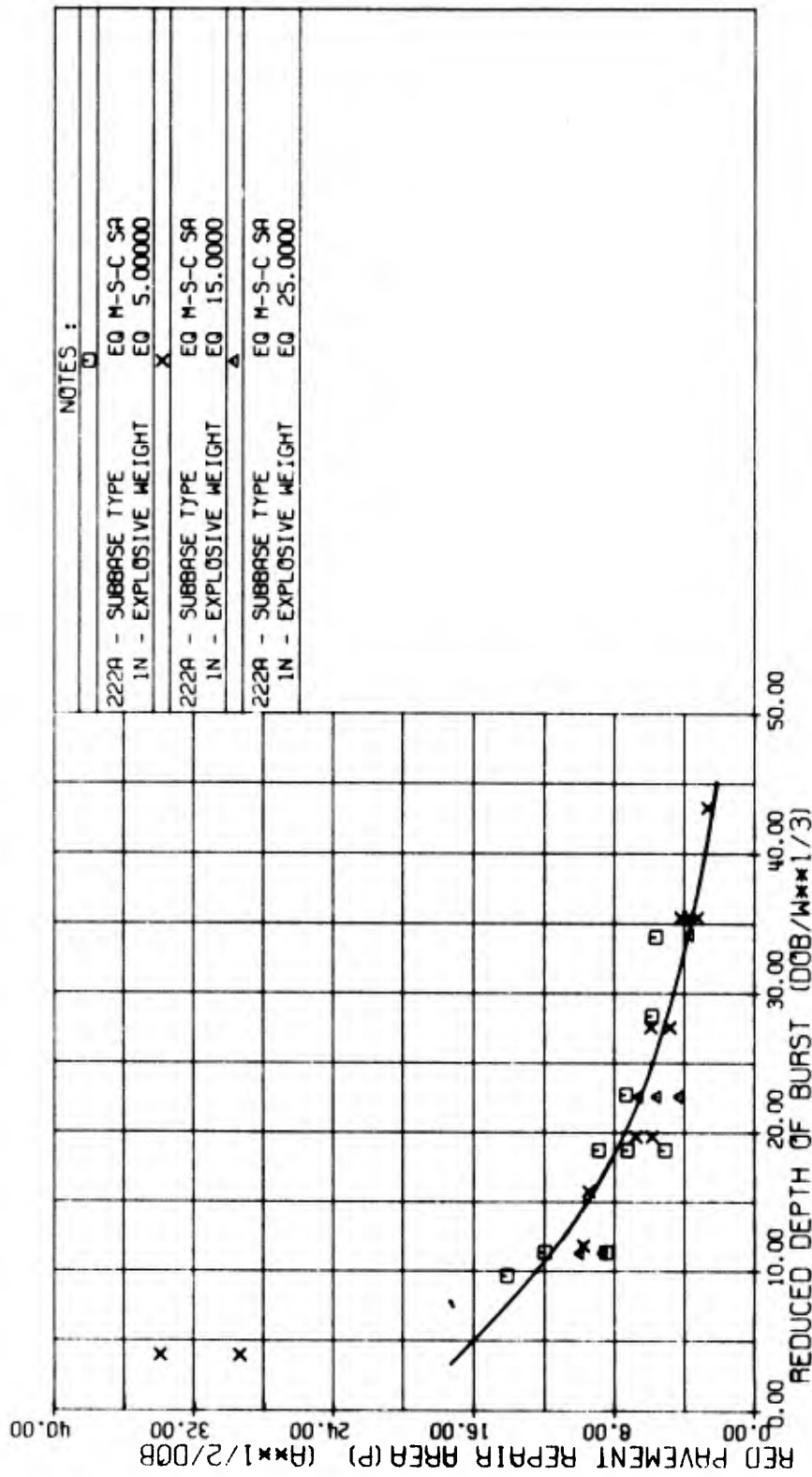
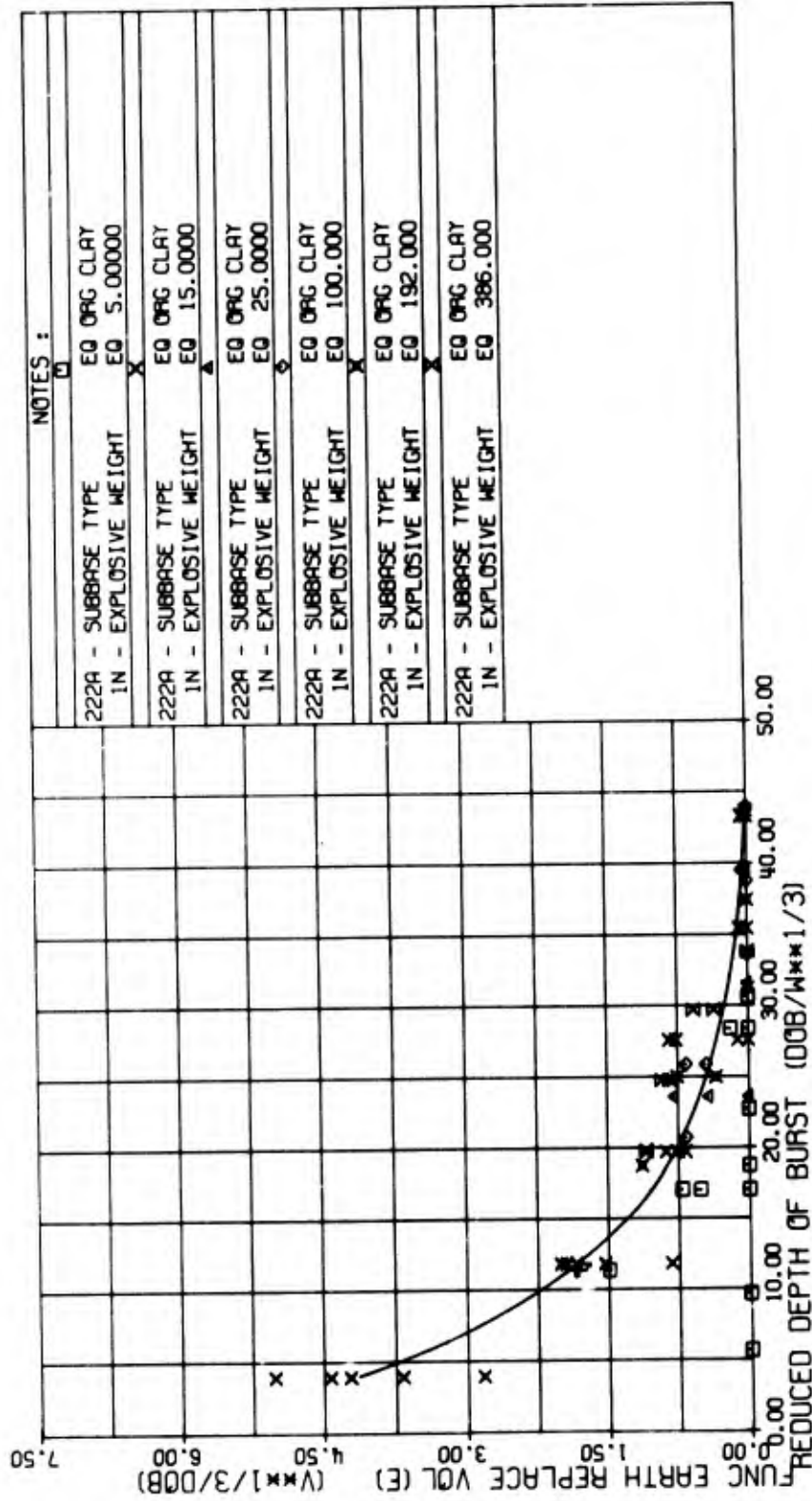


Figure 38. Reduced Pavement Repair Area for Permanent Repair Versus Depth of Burst;
Silty, Clayey Sand Subbase

FUNC EARTH REPLACE VOL (E) (V**1/3/DOB) VERSUS REDUCED DEPTH OF BURST (DOB/W**1/3)



NOTES :

222A - SUBBASE TYPE	EQ ORG CLAY
IN - EXPLOSIVE WEIGHT	EQ 5.00000
222A - SUBBASE TYPE	EQ ORG CLAY
IN - EXPLOSIVE WEIGHT	EQ 15.00000
222A - SUBBASE TYPE	EQ ORG CLAY
IN - EXPLOSIVE WEIGHT	EQ 25.00000
222A - SUBBASE TYPE	EQ ORG CLAY
IN - EXPLOSIVE WEIGHT	EQ 100.00000
222A - SUBBASE TYPE	EQ ORG CLAY
IN - EXPLOSIVE WEIGHT	EQ 192.00000
222A - SUBBASE TYPE	EQ ORG CLAY
IN - EXPLOSIVE WEIGHT	EQ 386.00000

Figure 39. Reduced Earth Replacement Volume for Expedient Repair Versus Depth of Burst;
Organic Clay Subbase

FUNC EARTH REPLACE VOL (E) (V**1/3/DOB) VERSUS REDUCED DEPTH OF BURST (DOB/W**1/3)

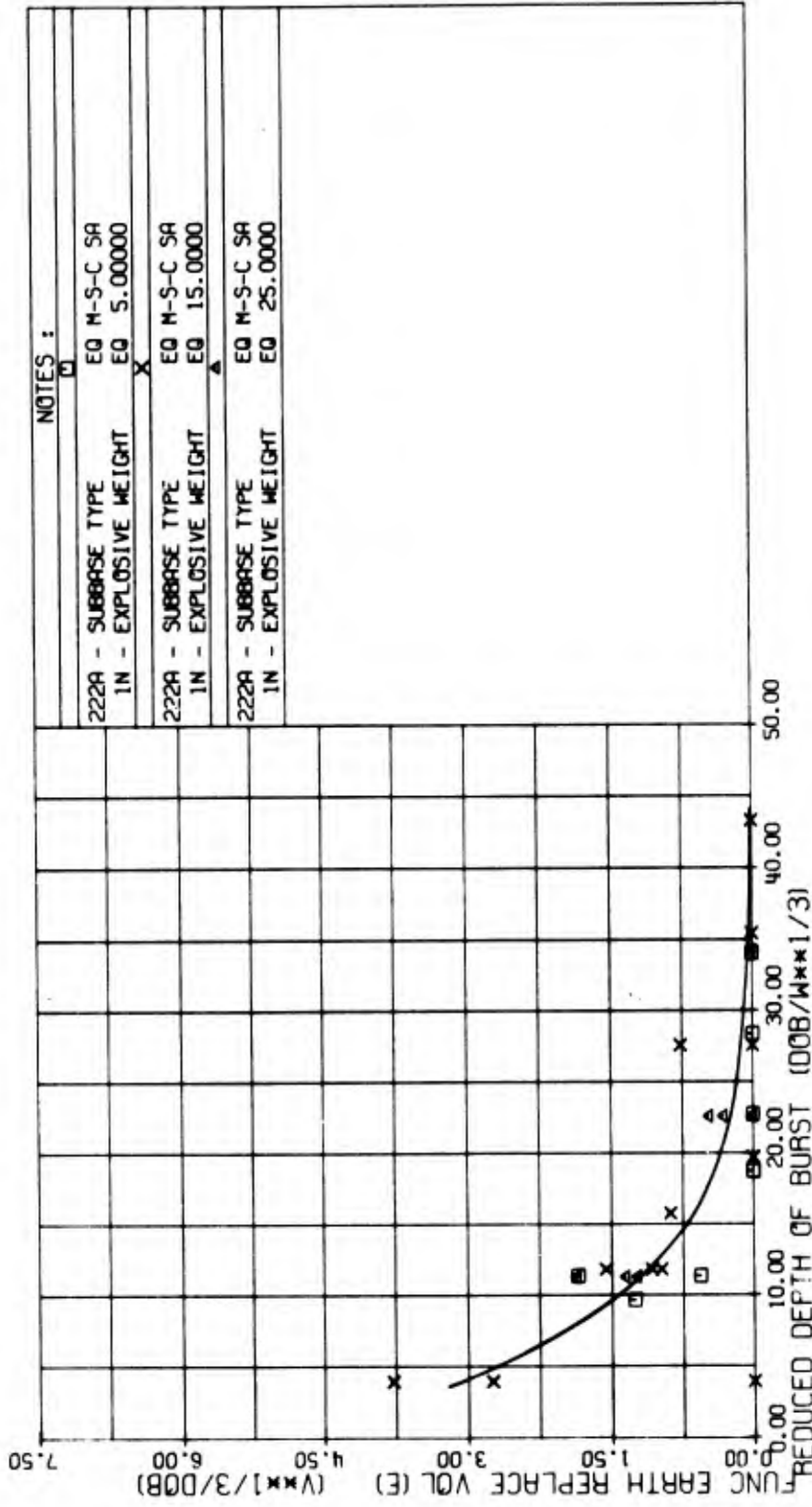


Figure 40. Reduced Earth Replacement Volume for Expedient Repair Versus Depth of Burst; Silty, Clayey Sand Subbase

FUNC EARTH REPLACE VOL (P) (V**1/3/DOB) VERSUS REDUCED DEPTH OF BURST (DOB/W**1/3)

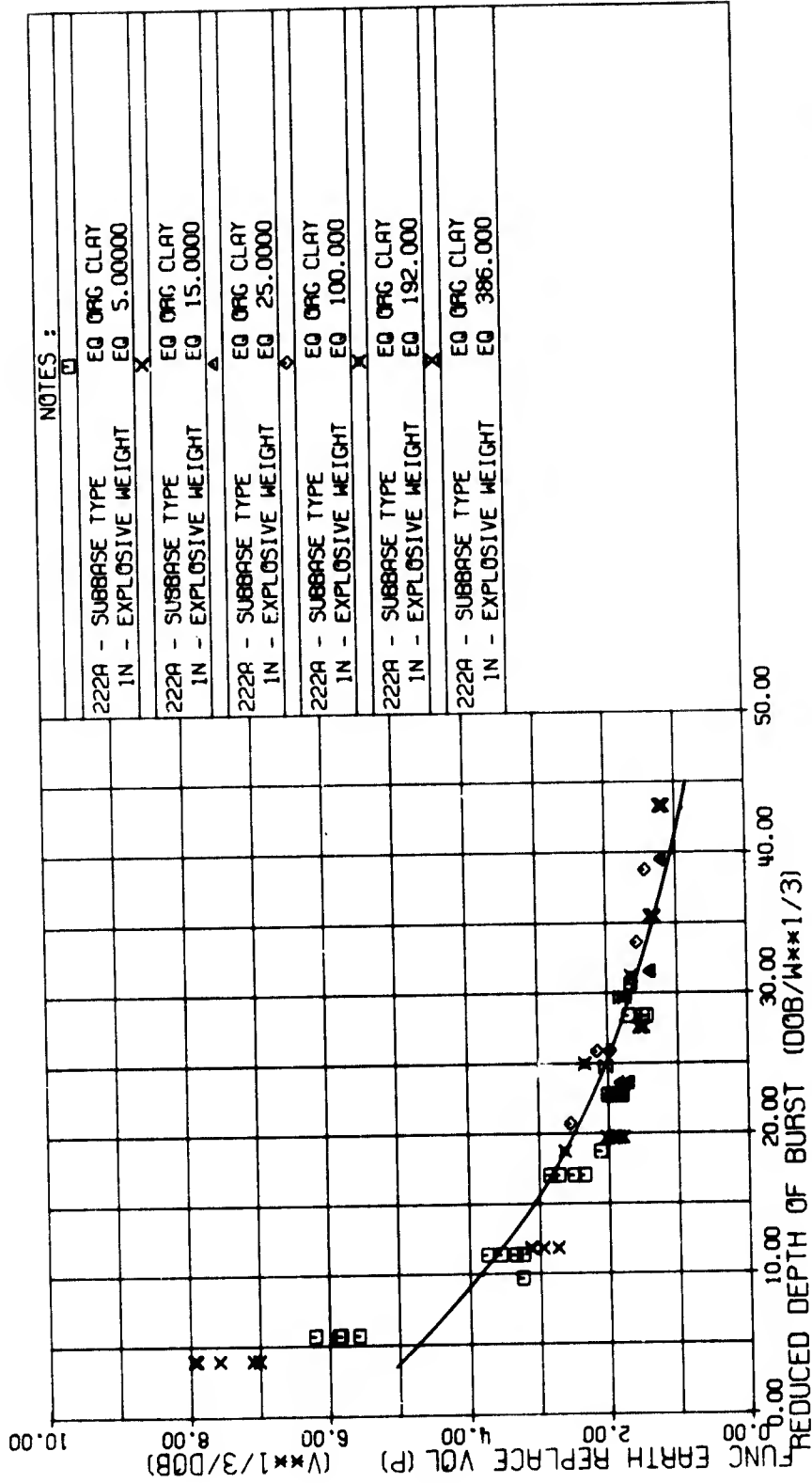
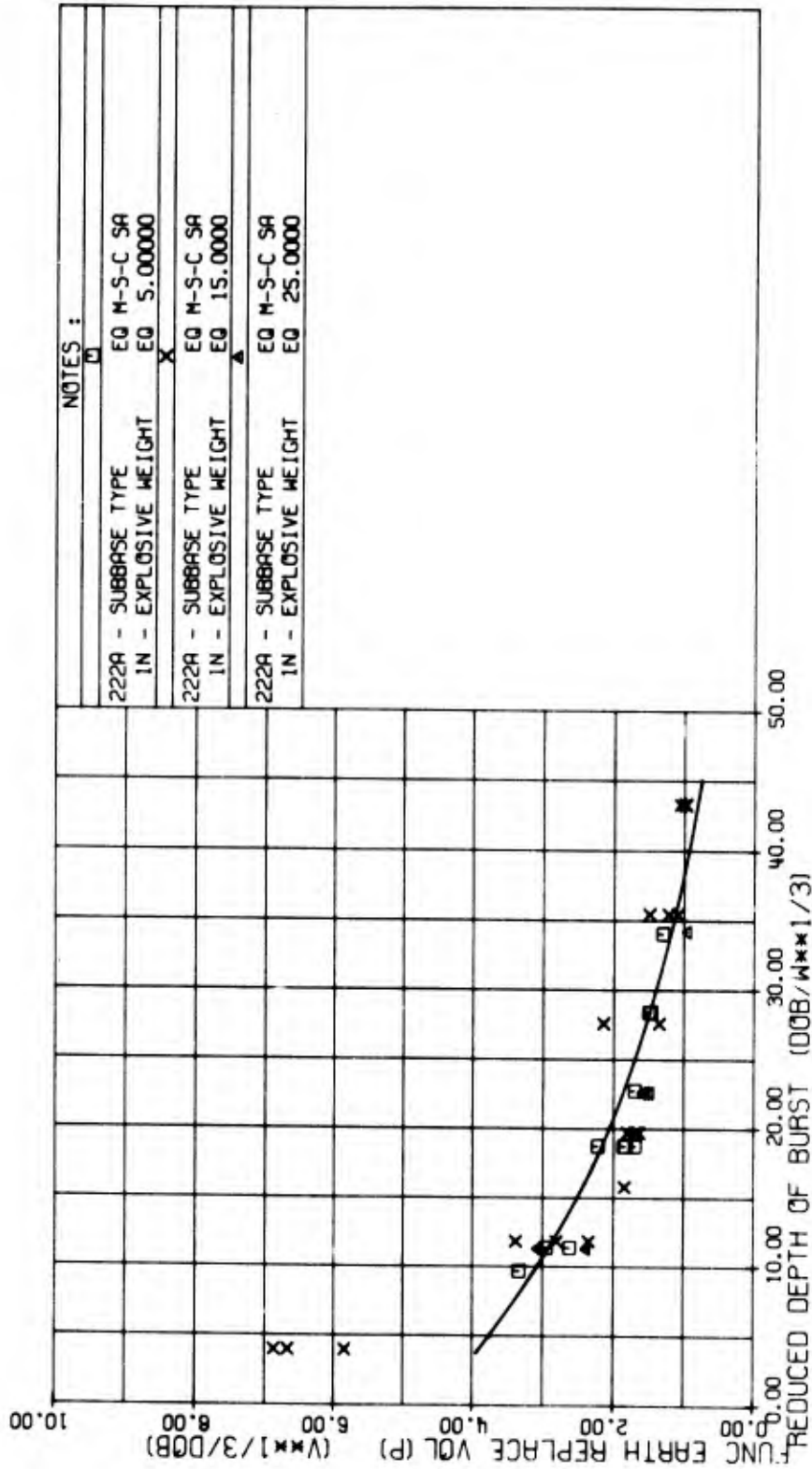


Figure 41. Reduced Earth Replacement Volume for Permanent Repair Versus Depth of Burst;
Organic Clay Subbase

FUNC EARTH REPLACE VOL (P) (V**1/3/DOB) VERSUS REDUCED DEPTH OF BURST (DOB/W**1/3)



NOTES :

222A - SUBBASE TYPE	EQ M-S-C SA
IN - EXPLOSIVE WEIGHT	EQ 5.00000
222A - SUBBASE TYPE	EQ M-S-C SA
IN - EXPLOSIVE WEIGHT	EQ 15.00000
222A - SUBBASE TYPE	EQ M-S-C SA
IN - EXPLOSIVE WEIGHT	EQ 25.00000

Figure 42. Reduced Earth Replacement Volume for Permanent Repair Versus Depth of Burst; Silty, Clayey Sand Subbase

RED PAVE REMOVAL AREA (E) (A**1/2/DOB) VERSUS REDUCED DEPTH OF BURST (DOB/W**1/3)

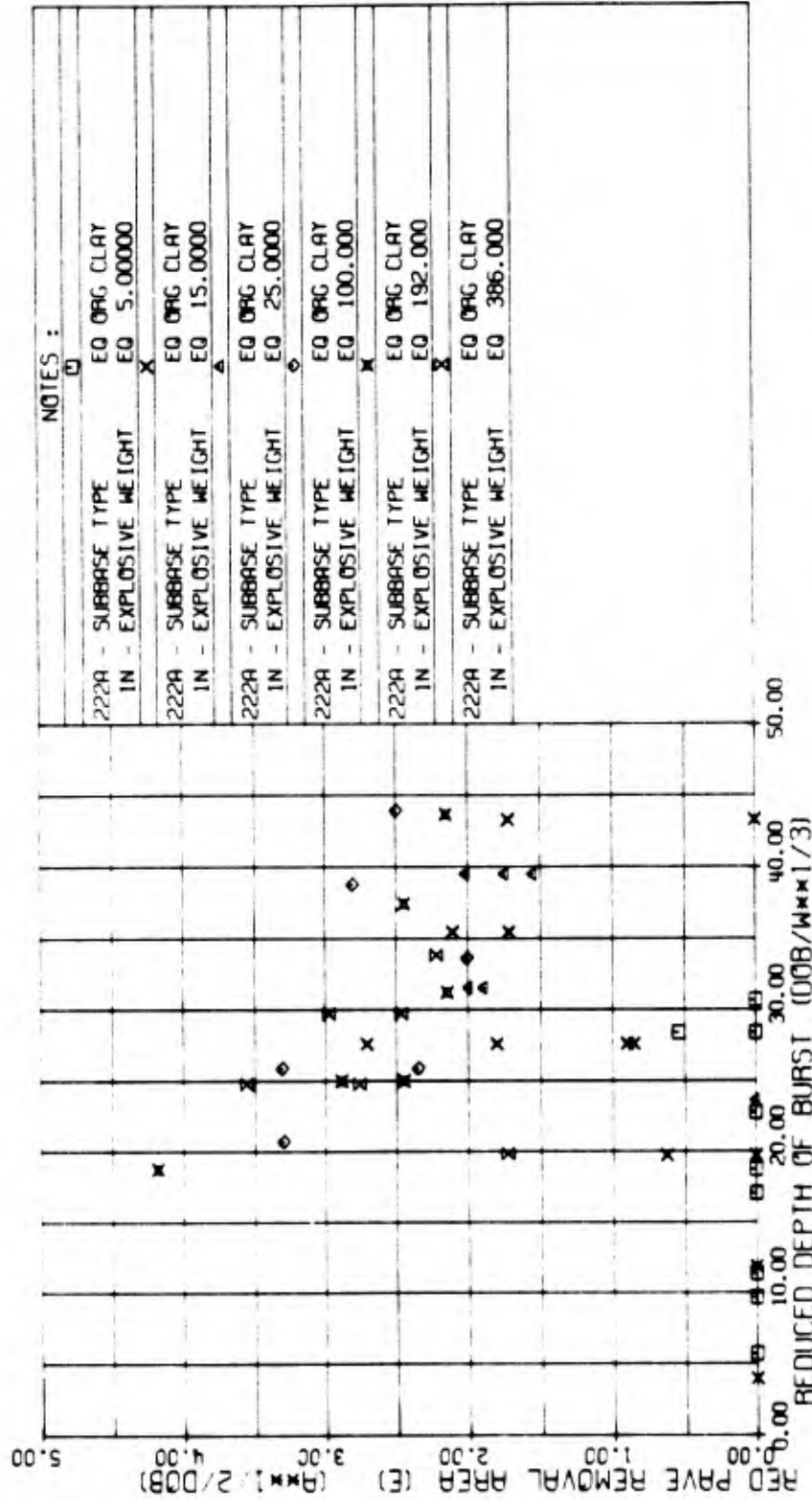


Figure 43. Reduced Pavement Removal Area for Expedient Repair Versus Depth of Burst;
Organic Clay Subbase

RED PAVE REMOVAL AREA (E) ($A \times 1/2 / DOB$) VERSUS REDUCED DEPTH OF BURST ($DOB / W \times 1/3$)

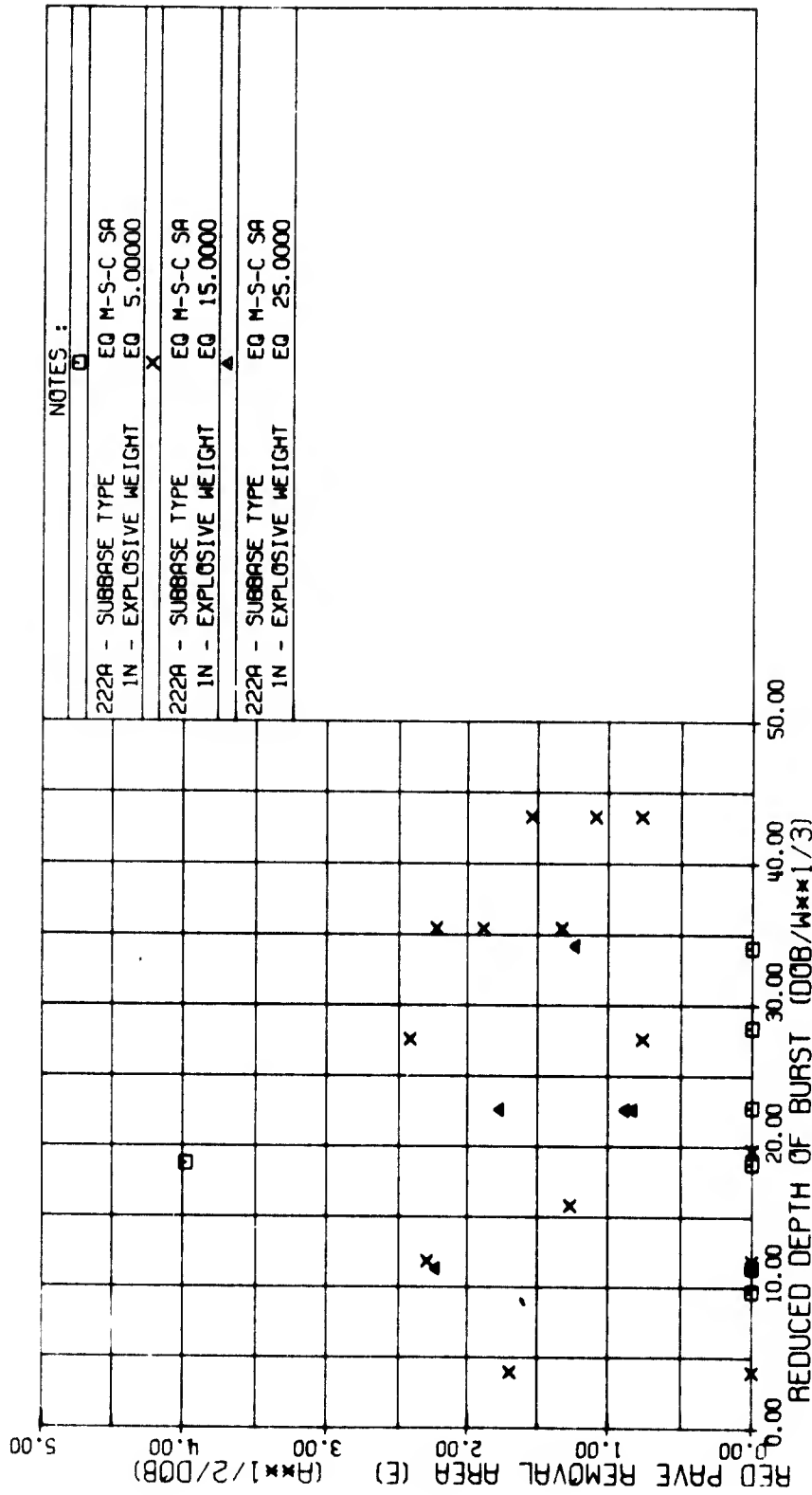


Figure 44. Reduced Pavement Removal Area for Expedient Repair Versus Depth of Burst; Silty, Clayey Sand Subbase

RED PAVE REMOVAL AREA (SP) ($A \times 1/2 / DOB$) VERSUS REDUCED DEPTH OF BURST ($DOB / W \times 1/3$)

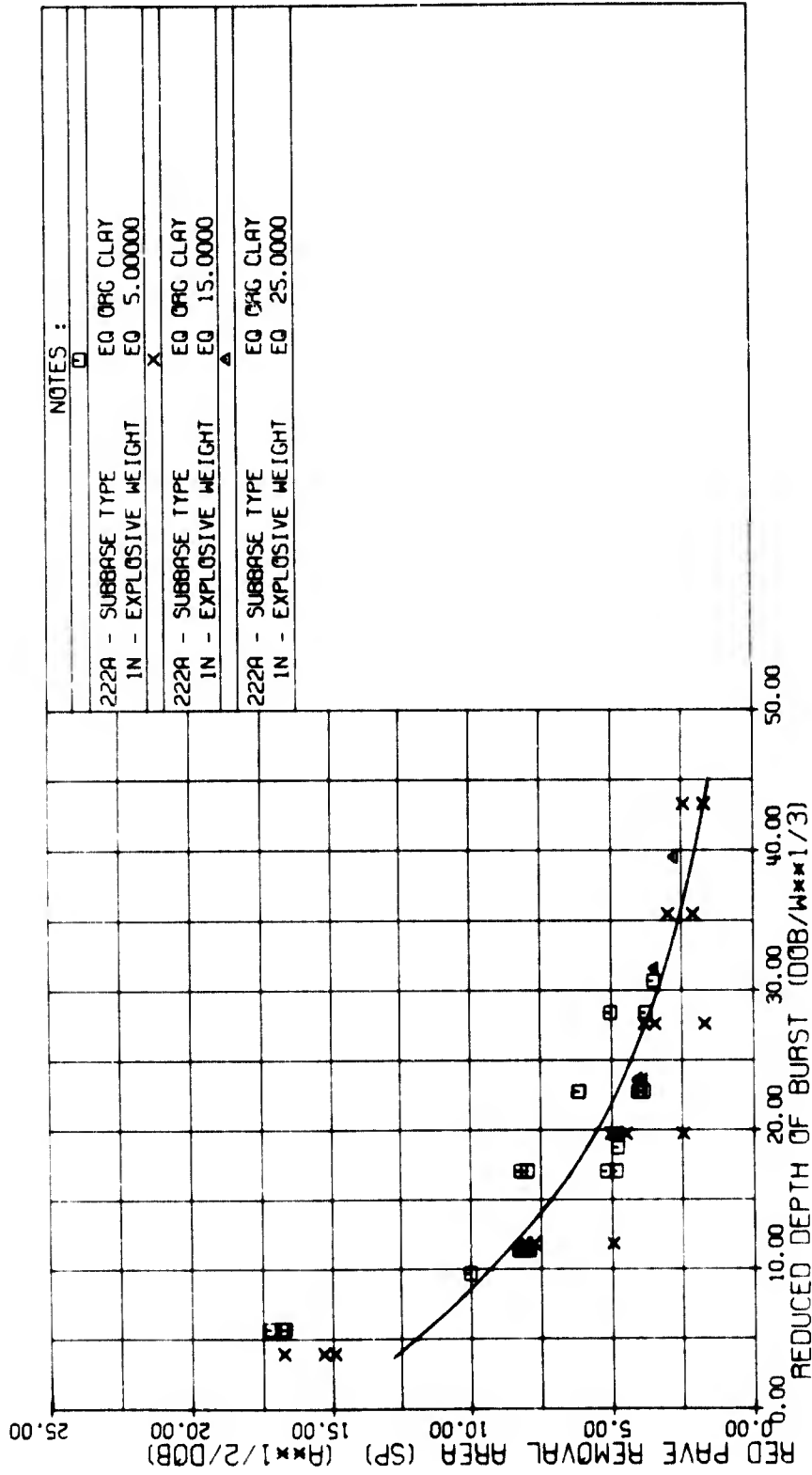
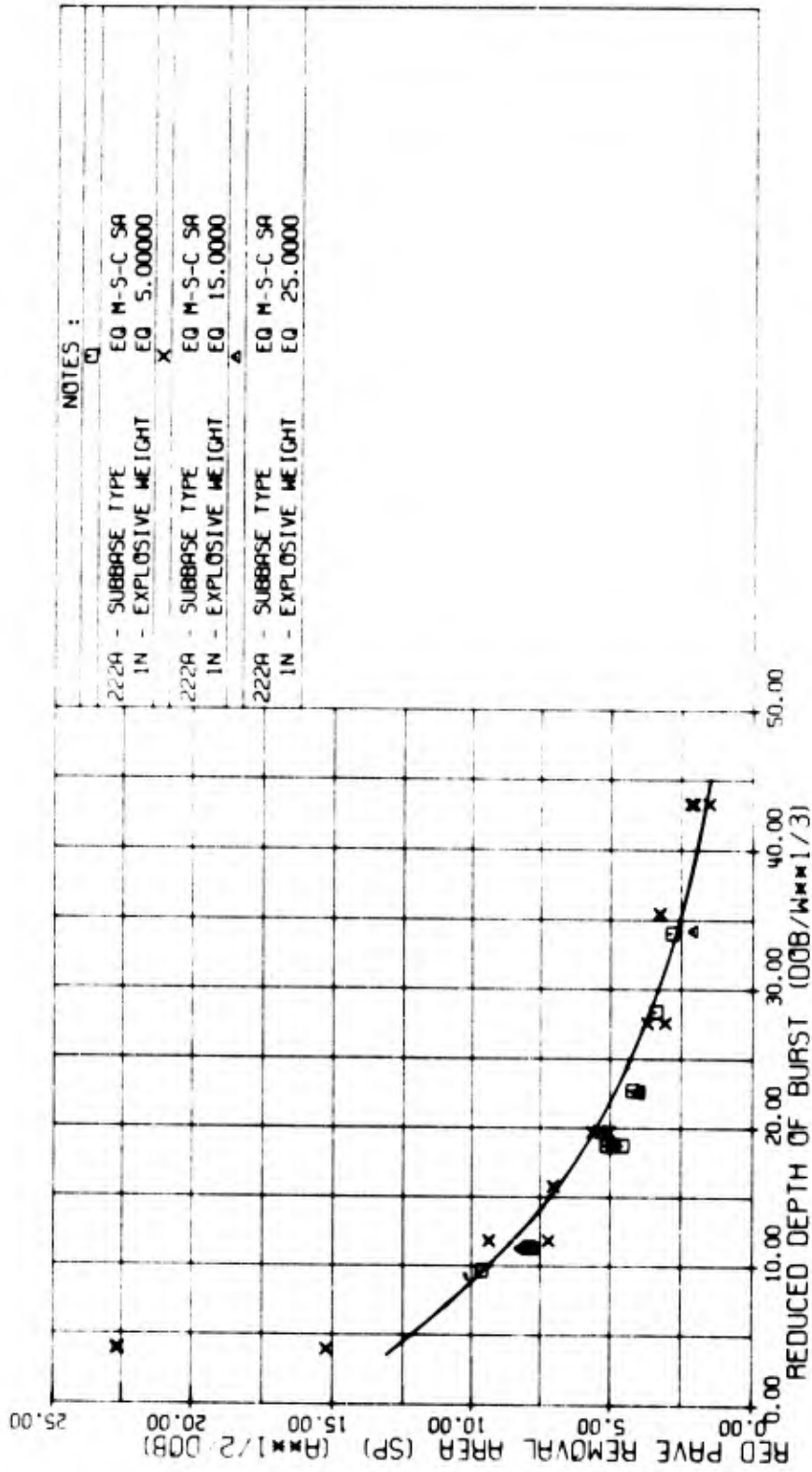


Figure 45. Reduced Pavement Removal Area for Semipermanent Repair Versus Depth of Burst;
Organic Clay Subbase

RED PAVE REMOVAL AREA (SP) ($A \times 1/2 / DOB$) VERSUS REDUCED DEPTH OF BURST ($DOB / W \times 1/3$)



NOTES :

222A - SUBBASE TYPE EQ M-S-C SA
 IN - EXPLOSIVE WEIGHT EQ 5.00000 X

222A - SUBBASE TYPE EQ M-S-C SA
 IN - EXPLOSIVE WEIGHT EQ 15.00000 A

222A - SUBBASE TYPE EQ M-S-C SA
 IN - EXPLOSIVE WEIGHT EQ 25.00000

Figure 46. Reduced Pavement Removal Area for Semipermanent Repair Versus Depth of Burst; Silty, Clayey Sand Subbase

RED PAVE REMOVAL AREA (P) (A**1/2/DOB) VERSUS REDUCED DEPTH OF BURST (DOB/W**1/3)

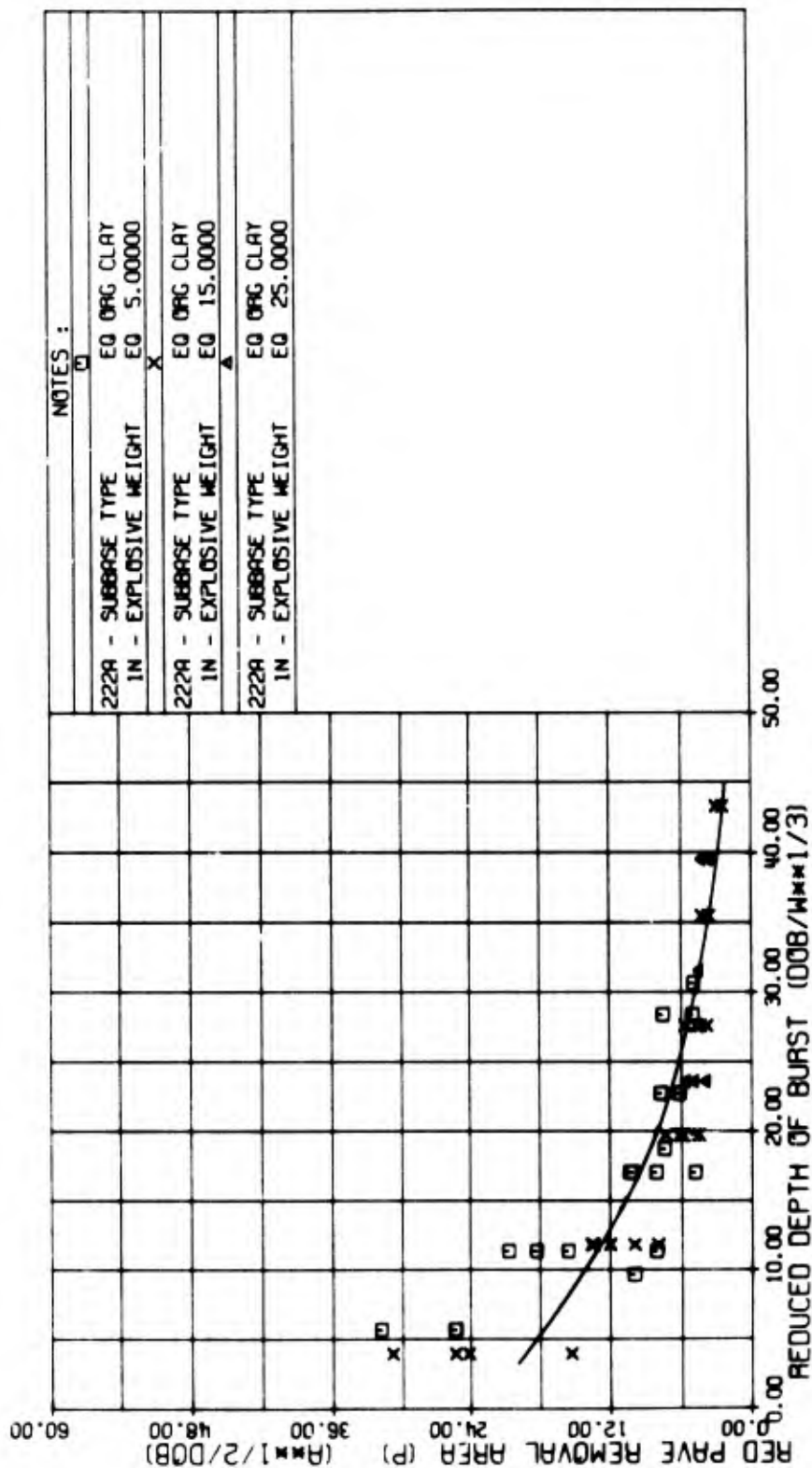
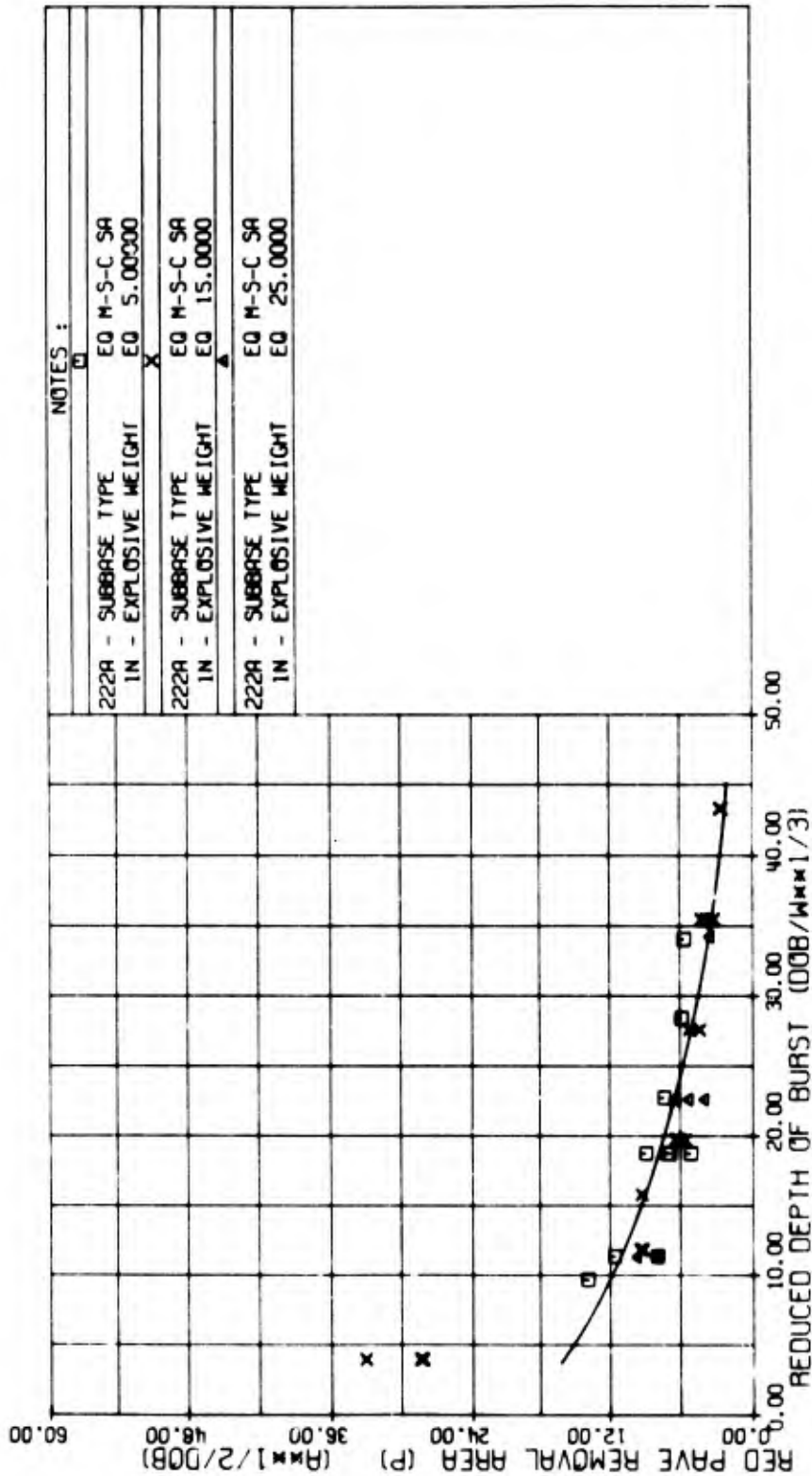


Figure 47. Reduced Pavement Removal Area for Permanent Repair Versus Depth of Burst;
Organic Clay Subbase

RED PAVE REMOVAL AREA (P) (A**1/2/DOB) VERSUS REDUCED DEPTH OF BURST (DOB/W**1/3)



NOTES :

222A - SUBBASE TYPE	EQ M-S-C SA
IN - EXPLOSIVE WEIGHT	EQ 5.00000
222A - SUBBASE TYPE	EQ M-S-C SA
IN - EXPLOSIVE WEIGHT	EQ 15.00000
222A - SUBBASE TYPE	EQ M-S-C SA
IN - EXPLOSIVE WEIGHT	EQ 25.00000

Figure 48. Reduced Pavement Removal Area for Permanent Repair Versus Depth of Burst; Silty, Clayey Sand Subbase

Table 11. These curve fits represent the complete range of experimental data available, including the very shallow depths of burst. However, the area of pavement requiring removal to effect an expedient repair exhibits excessive scatter (Figures 43 and 44), in both subbase types, and no function or new grouping of parameters could be found which would reduce this variation to an acceptable level. It is felt that this extreme scatter is inherent in the definition of this damage parameter which represents the area of pavement requiring replacement, minus the area of the pavement ejected (surface crater area). For an expedient repair criterion, these areas are generally very similar (particularly for the smaller explosive charges), and the random experimental errors and observation and measurement errors tend to accumulate to a magnitude nearly equivalent to that of the desired damage quantity. This situation precludes the development of any meaningful curve fit; therefore it was concluded that no valid relationship could be developed for the expedient repair pavement removal area.

The definition of earth removal and replacement volumes for an expedient repair leads to the conclusion that if one is nonzero, the other must be zero. If, for instance, the earth volume requiring removal for expedient repair is positive, this implies that the level of fall-back is above the pavement base level and must be excavated to this level before the pavement is repaired. In this case, no additional fill is required, as the crater is filled to the desired level with fall-back. On the other hand, if the volume of earth requiring replacement is positive, then, by definition the volume of earth to be removed is zero. These situations are apparent in Figures 29, 30, 39 and 40 where they constitute what appears to be two "branches" of data.

Initial efforts aimed at correlating these two events with depth of burst or explosive charge weight were thwarted by an apparently large amount of scatter, particularly in the smaller charge-size regime. However, it was noted that the data for bombs (charge weights 100 pounds and above) exhibited a well-defined break at a reduced depth of burst, $d/W^{1/3}$, of 30 inches/pound^{1/3}, with shallower bursts requiring some earth volume replacement and deeper bursts requiring some removal and thus no replacement. In addition, it was established that this same relationship could be extended to the 15- and 25-pound charges with a reliability of 0.75. However, for 5-pound

TABLE 11. BOMB DAMAGE REPAIR PREDICTION RELATIONSHIPS,
EXPONENTIAL FUNCTION APPROXIMATION

Damage Parameter	Subbase Type	Function Coefficients		RMS Error
		B	C	
Ejecta Volume	C	1.7254	-0.07763	0.44092
	S	1.4085	-0.092278	0.48115
Earth Replacement Volume (SP)*	C	1.4369	-0.051055	0.43005
	S	1.2373	-0.053898	0.44963
Earth Removal Volume (SP)	C	1.1737	-0.044316	0.45447
	S	0.88343	-0.042548	0.63069
Earth Removal Volume (E)	C	1.2758	-0.087070	0.26138
	S	0.97580	-0.088293	0.40606
Earth Removal Volume (P)	C	1.5983	-0.038239	0.73008
	S	1.4144	-0.036709	0.23204
Pavement Repair Area (E)	C	2.3214	-0.040342	0.91603
	S	1.8618	-0.033114	1.1579
Pavement Repair Area (SP)	C	2.9557	-0.055873	1.9195
	S	2.8473	-0.053472	2.5114
Pavement Repair Area (P)	C	3.2887	-0.056100	3.6289
	S	3.0170	-0.049400	4.3474
Earth Replacement Volume (E)	C	1.8535	-0.10629	0.37859
	S	1.6839	-0.13618	0.32699
Earth Replacement Volume (P)	C	1.7741	-0.043025	0.80555
	S	1.5237	-0.039740	0.81089
Pavement Removal Area (E)	C	————	Excessive Scatter No Fit Possible	————
	S			
Pavement Removal Area (SP)	C	2.7384	-0.050839	1.9655
	S	2.7602	-0.052276	2.4446
Pavement Removal Area (P)	C	3.1772	-0.053506	3.8102
	S	2.9559	-0.048377	4.3508

TABLE 11. BOMB DAMAGE REPAIR PREDICTION RELATIONSHIPS,
EXPONENTIAL FUNCTION APPROXIMATION (CONCLUDED)

$$\text{Volume Functions: } \frac{V^{1/3}}{d} = e^{B + C(d/W^{1/3})}$$

$$\text{Area Functions: } \frac{A^{1/2}}{d} = e^{B + C(d/W^{1/3})}$$

d = depth of burst, inches

W = equivalent explosive weight, pounds (TNT)

V = volume, cubic inches

A = Area, square inches

Subbase Type:

C = organic clay

S = medium silty, clayey sand

* () Refers to type of repair:

(E) = expedient repair

(SP) = semipermanent repair

(P) = permanent repair

charges, the transition appears to have decreased to $d/W^{1/3} = 17$ (with a prediction reliability of 0.73).

Although only Hays and Fort Sumner data were used to develop the prediction relationships, wherever possible other test results were checked for agreement with the derived relationships. For example, Figures 23, 24, 33, and 34 illustrate the relationship of data from test series at Tyndall Air Force Base, Florida, and the University of New Mexico, CERF, to the derived relationships. These data points generally show good correlation with the derived relations; however, the craters produced in Tyndall Air Force Base sand subbase were apparently slightly larger than those in the Fort Sumner silty, clayey sand subbase. This may have been due, in part, to the proximity of the ground water table to the surface (11 - 12 feet) at Tyndall Air Force Base.

The residuals (already used to check goodness-of-fit for normal random distribution) were also plotted as a function of pavement thickness and nondimensional pavement thickness, t/d , where t = pavement thickness and d = depth of burst. Only the Hays test site exhibited variations in pavement thickness, so investigations were necessarily limited to the organic clay subbase. (As before, no test data, other than from the Hays and Fort Sumner tests, contained sufficient damage parameter measurements and depth of burst variation to be included in the regression analyses.) Again, using the semipermanent earth replacement volume, for example, the residuals from the exponential curve fit are shown in Figure 49 as a function of pavement thickness and as a function of nondimensional pavement thickness. Also shown as dotted lines on each plot are the envelopes of plus and minus one standard deviation ($\pm 1\sigma$). The data do indicate a possibility of being correct for 8.0- and 8.5-inch pavement, but underpredicting for the 10.0-inch pavement and overpredicting for 11.0-inch pavement. In addition, when considering the nondimensional pavement thickness, one observes a "hint" of a trend, showing slight underprediction at t/d values below about 0.1 and slight overprediction for t/d values above about 0.2. However, the data become sparse above $t/d = 0.3$, and a complete gap exists for t/d between 0.5 and 0.8. Since the "possible trend" is confined totally within the $\pm 1\sigma$ envelope on the residual plot, any generalization which might be made, quantifying a trend in the dependence of pavement thickness, would have a very low confidence level attached to it. Therefore it is concluded that thickness-induced variations in the damage parameters cannot be quantified with the experimental data presently available. Extrapolation of these results outside the pavement thickness region included in the present data file should be done with caution.

In Figure 17, the data points corresponding to the bomb craters (100-, 192- and 386-pound charges) all lie slightly above the smaller charge data (5-, 15-, and 25-pound charges). This difference is small (well within one standard deviation) and was ignored when the curve fits were generated because: (1) the reliability of the bomb-generated craters was judged to be less than for the smaller charges, (2) the data

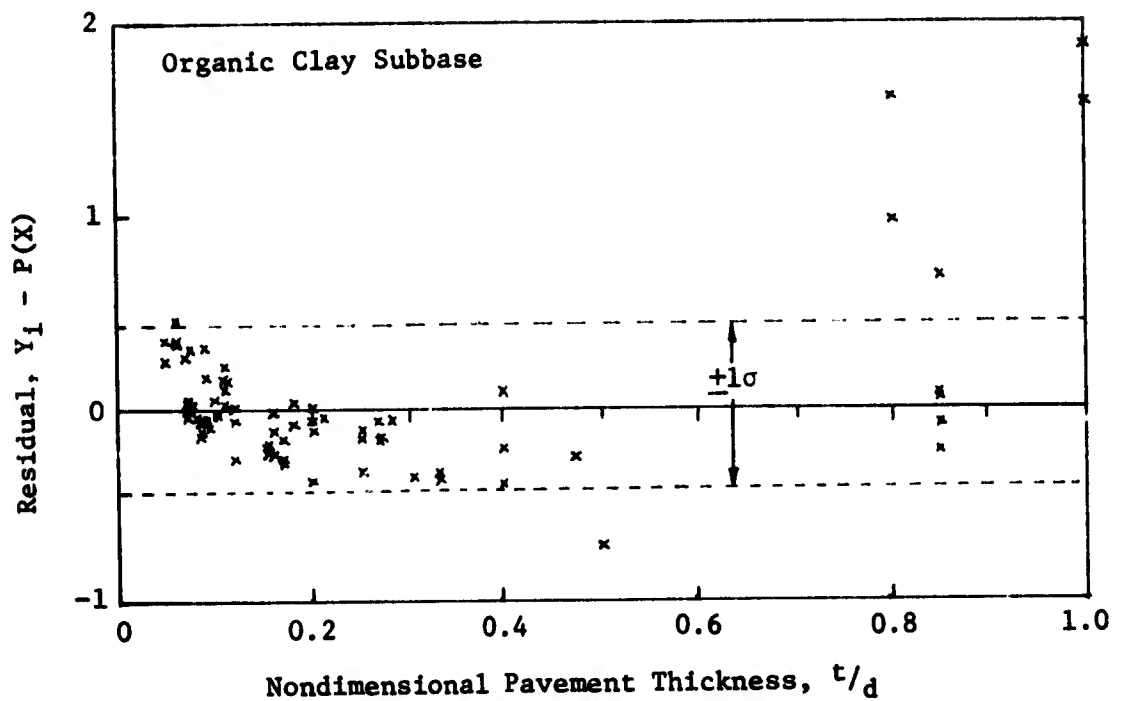
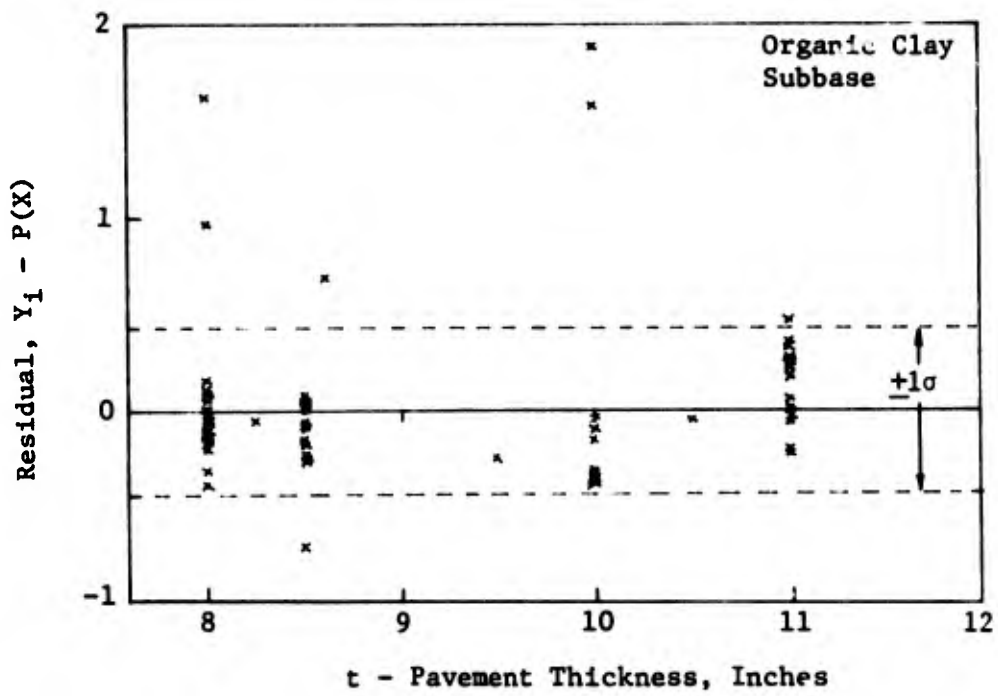


Figure 49. Semipermanent Earth Replacement Volume Function; Exponential Approximation Residuals as a Function of Pavement Thickness

were not available for the silty, clayey sand subbase, and (3) the magnitude of the possible trend does not justify the additional complication which would be introduced by considering further charge-weight dependence. However, to verify the wisdom of neglecting this possible effect, the semipermanent earth replacement volume in organic clay subbase was investigated, using further charge-weight scaling in the following forms:

(1) Cube-root scaling, $\frac{v^{1/3}}{dW^{1/3}} = f\left(\frac{d}{W^{1/3}}\right)$

(2) 7/24 - power scaling, $\frac{v^{1/3}}{dW^{7/24}} = f\left(\frac{d}{W^{7/24}}\right)$

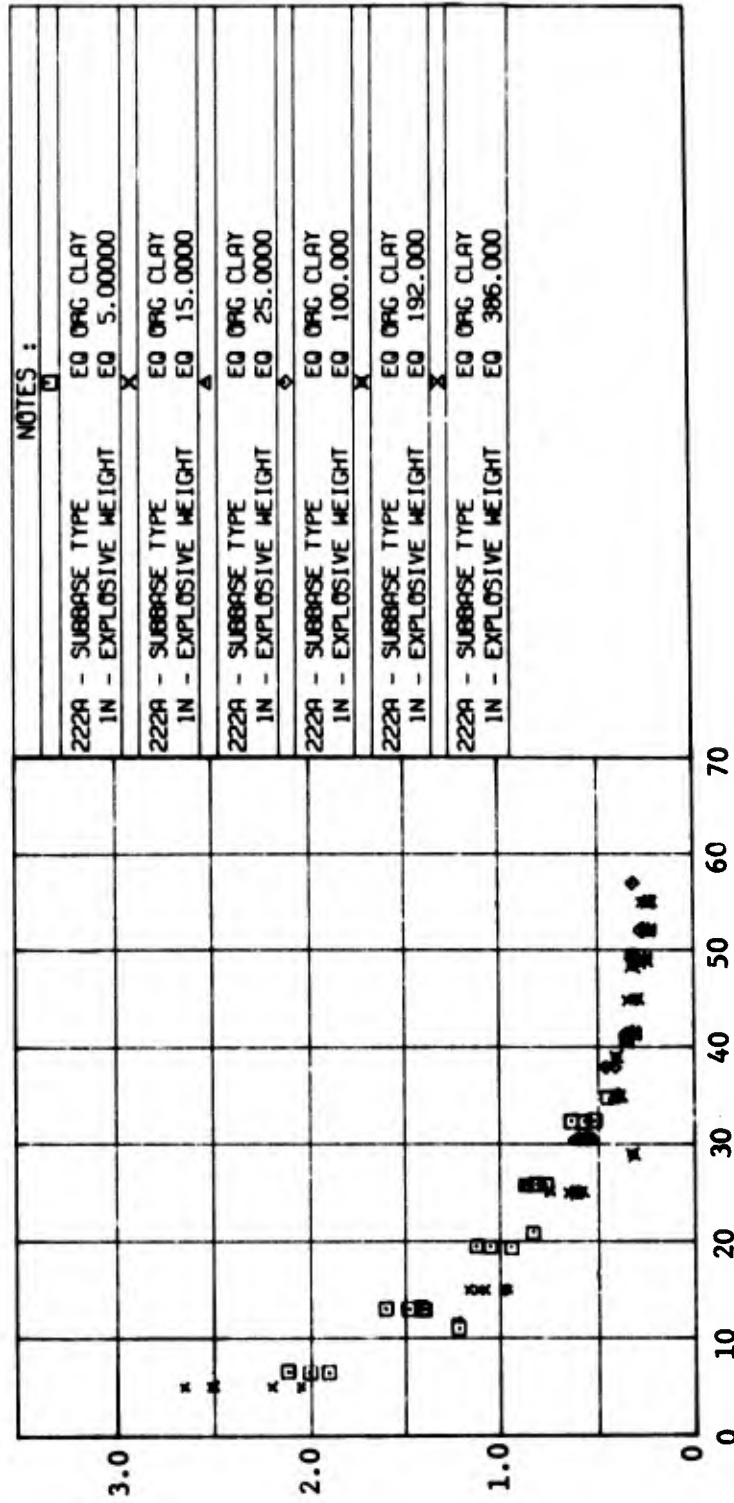
(3) 1/4 - power scaling, $\frac{v^{1/3}}{dW^{1/4}} = f\left(\frac{d}{W^{1/4}}\right)$.

The first two methods led to overcompensation, where the volumes for large charges were overpredicted by an approximating function. Fourth-root scaling yielded a slightly more consistent set of data, as shown in Figure 50. All charge-weight dependence appears to have been removed from this functional plot. However, the curve fit generated for this case indicates less than a 5 percent improvement in the data scatter; thus, as earlier believed, any further reduction of the functional relationships in this form is not justified at this time.

Other pavement system parameters which may affect the level of damage sustained by a paved runway system include joint type, type of paving material, presence of reinforcing rod or mesh, and preparation of base materials. Unfortunately, the existing data on these parameters are too limited in scope and volume to enable prediction of effects and generation of damage prediction relationships. However, based on observations made of test results and comparison with damage prediction data for other parameters, several trends can be identified:

- a. Unreinforced pavements appear to fail at an earlier time than reinforced systems when subjected to detonations of penetrating weapons. Most of the explosive energy is expended in imparting kinetic energy to pavement segments, soil, and other debris. Reinforced pavements tend to mound up and exhibit larger camouflets rather than be blown away

Reduced Earth Replacement Volume (SP), $\frac{V_{1/3}}{V_{1/4}}$



Reduced Depth of Burst, $DOB/W^{1/4}$

Figure 50. Fourth-Root Reduced Semipermanent Earth Replacement Volume

when subjected to explosive effects. However, the required repair time of reinforced systems is greater since the reinforcing bars have to be cut away before broken pavement segments can be removed.

- b. Joints and slab sizes have a pronounced effect on the extent of damage, although the effect is difficult to quantify because of limited data availability. Particularly, for the smaller munitions, the number of slabs damaged is a function of slab size, since the effect of joints is basically to alter the transmission of shear, moment, and tension. For large weapons, the effect is not so pronounced.
- c. Flexible pavement overlays tend to help confine explosive gases, and the amount of damaged pavement is greater than in rigid pavements of similar overall thickness.
- d. Clay subgrades tend to produce much greater upheaval than sand subgrades in the same pavements. However, this may be at least in part a function of the normally higher moisture content of clay as well as constitutive effects.

3. FUZING RELIABILITY AND PENETRATION CAPABILITY

An additional consideration in developing pavement damage prediction relationships is an evaluation of the ability of a weapon to penetrate the pavement and detonate in a location which maximizes damage. Experience has shown that some weapons will break up upon target impact and thus have no penetration capability. In these cases as well as in the case of impact fuzing, detonation may occur on the pavement surface and produce mostly scabbing effects rather than cratering. Some form of delay fuzing is therefore needed to allow a weapon to detonate beneath the pavement and maximize damage. Further, for general purpose weapons, ricochet becomes a problem at obliquity angles above 30 to 40 degrees.

While a detailed analysis of foreign weapons and fuzes is beyond the scope of this effort, some general observations and calculations yield much insight into the penetration problem and its impact on weapon delivery properties. Many procedures have been developed for predicting

projectile penetration, but perhaps the most useful is the one developed by the Sandia Corporation (ref. 26). This method is based on empirical techniques rather than attempts to solve drag equations and on an assumed relationship of parameters affecting penetration. These parameters are nose shape, projectile area and weight, impact velocity, and characteristics of the medium being penetrated. The final form of the developed equation is:

$$D = 0.53 SN (W/A)^{1/2} \ln (1 + 2V^2 10^{-5}) \quad V < 200 \text{ Ft/S}$$

$$D = 0.0031 SN (W/A)^{1/2} (V-100) \quad V \geq 200 \text{ Ft/S} \quad (8)$$

where

- D = depth of penetration (ft)
- V = velocity (ft/sec)
- S = penetration medium constant
- W = vehicle weight (lb)
- A = cross-sectional (frontal) area (in²)
- N = nose-performance constant

Example values of S and N are listed in Table 12.

TABLE 12. EXAMPLE SOIL AND NOSE CONSTANTS

Soil	S	Nose Shape	N
Silty Sand	5.0	Flat Nose	0.56
Eglin Sand	6.5	6.0 CRH* Tangent Ogive	1.00
Sandstone	1.3	Cone, 1/d = 2	1.08
Soft/Wet Clay	40-50	Biconic, 1/d = 3	1.31

* CRH - Caliber Radius Head

To better illustrate the effects of fuzing reliability, it is instructive to first consider a weapon's penetrating capability. For example, a weapon in the 250 pound class will typically have a W/A of about 2.6, and with 6.0 CRH nose configuration, N = 1.0. Under average conditions, S for soil is assumed 5.0, and S for concrete is 0.57*. For an impact velocity of 1000 ft/sec at zero degrees obliquity, and a pavement thickness of 12 inches, penetration data were computed according to the Sandia procedure. The predicted penetration into concrete is given by

* Values of S for concrete varying from 0.28 - 1.0 can be found in the literature. The value used is an average number.

$$D = 0.0031 (0.57) (1.0) (2.6)^{1/2} (900) \\ = 2.56 \text{ ft.}$$

The velocity of the projectile upon exiting the actual 12 inch-thick pavement is therefore $V_2 = V_1 \sqrt{1 - \frac{D_1}{D}}$ (9)

where

V_2 = exit velocity

V_1 = impact velocity

D_1 = thickness of actual medium

D = hypothetical depth penetrated

Thus

$$V_2 = 1000 \sqrt{1 - \frac{1}{2.56}} \\ = 781 \text{ ft/sec}$$

Therefore, the projectile, assuming no breakup and that the flight path is a straight line, enters the subsoil beneath the pavement at the velocity V_2 .

The time of travel through the pavement is given by:

$$t = \frac{2D}{V_1 + V_2} \quad (10) \\ = \frac{2(1)}{1000 + 781} \\ = 0.00112 \text{ sec.}$$

By reapplying Equation (8) and using the new velocity and soil constant, the total depth of penetration in the soil is

$$D = 0.0031 (5.0) (1.0) (2.6)^{1/2} (681) \\ = 17.0 \text{ ft.}$$

Using average values, the time required for the vehicle to come to rest in soil is $t = 0.0435$ second. Thus, the total time from impact to rest is about 45 milliseconds.

Thus, penetrating projectiles will be at near-optimal depths of burst within a few milliseconds after impacting pavements. By applying the above procedure in other cases, the effects of other impact angles, different material properties, and various penetrator configurations can be evaluated. Even small errors in fuze delay time or low fuzing

reliability will greatly affect the depth of burst and thus the damage inflicted upon a pavement system. Standard delay fuze items have values of time delay from 0.1 to 60 seconds. In the above example, any of these values would result in the weapon coming to rest prior to detonation. Integrating fuzes which can detect the pavement and soil and cause detonation of the round at an optimal point have been investigated, but are not known to be in use. Similarly, if a fuze delay train fails, the round may detonate upon target impact. In either case (no delay or excessive delay) the round will not detonate at an optimal location to cause pavement damage. The effects of depth of burst variation can be determined by reference to curves presented in this report. Reference 13 contains a more detailed discussion of pavement penetration prediction calculations.

SECTION V
DAMAGE PREDICTION RELATIONSHIPS

1. DERIVATION AND USE OF NOMOGRAPHS

The functional relationships developed in the previous section were developed as the best representations of the significant damage repair parameters in terms of weapon and target parameters. These relationships were developed in the form

$$\frac{R}{d} = f\left(\frac{d}{W^{1/3}}, \text{soil type}\right), \text{ where}$$

R = linearized damage parameter, $(V^{1/3}, A^{1/2})$

V = volume damage parameter, cubic inches

A = area damage parameter, square inches

d = depth of burst, inches

W = charge weight, TNT equivalent pounds.

These relationships may prove unwieldy for field use; therefore, they have been converted into the following nomographs for easy reference. In addition, the scales on the nomographs have been converted to field-convenient units (depth of burst in inches, charge weight in pounds of TNT, volume in cubic yards, and area in square feet).

A typical example of the use of the bomb damage repair nomographs is shown in Figure 51, which illustrates the use of the nomograph to find the earth replacement volume for a semipermanent repair, given a 15-pound TNT charge at a 90-inch depth of burst in a clay subbase. Aligning the depth of burst (square at 90 inches) and the charge weight (triangle at 15 pounds) on the lower Z-chart, yields the corresponding value of reduced depth of burst $(d/W^{1/3})$ as the intercept on the graph horizontal axis (36.5). Proceeding vertically to the clay subbase curve provides the value of the reduced volume $(V^{1/3}/d)$ as 0.65. Proceeding from this ordinate value (at the right-hand side of the grid) through the diagonal depth-of-burst scale to the right yields the resultant value of volume as 4.3 cubic yards.

The nomographs may also be used only for determining the values of functional ordinates and abscissas, while the parameters are reduced

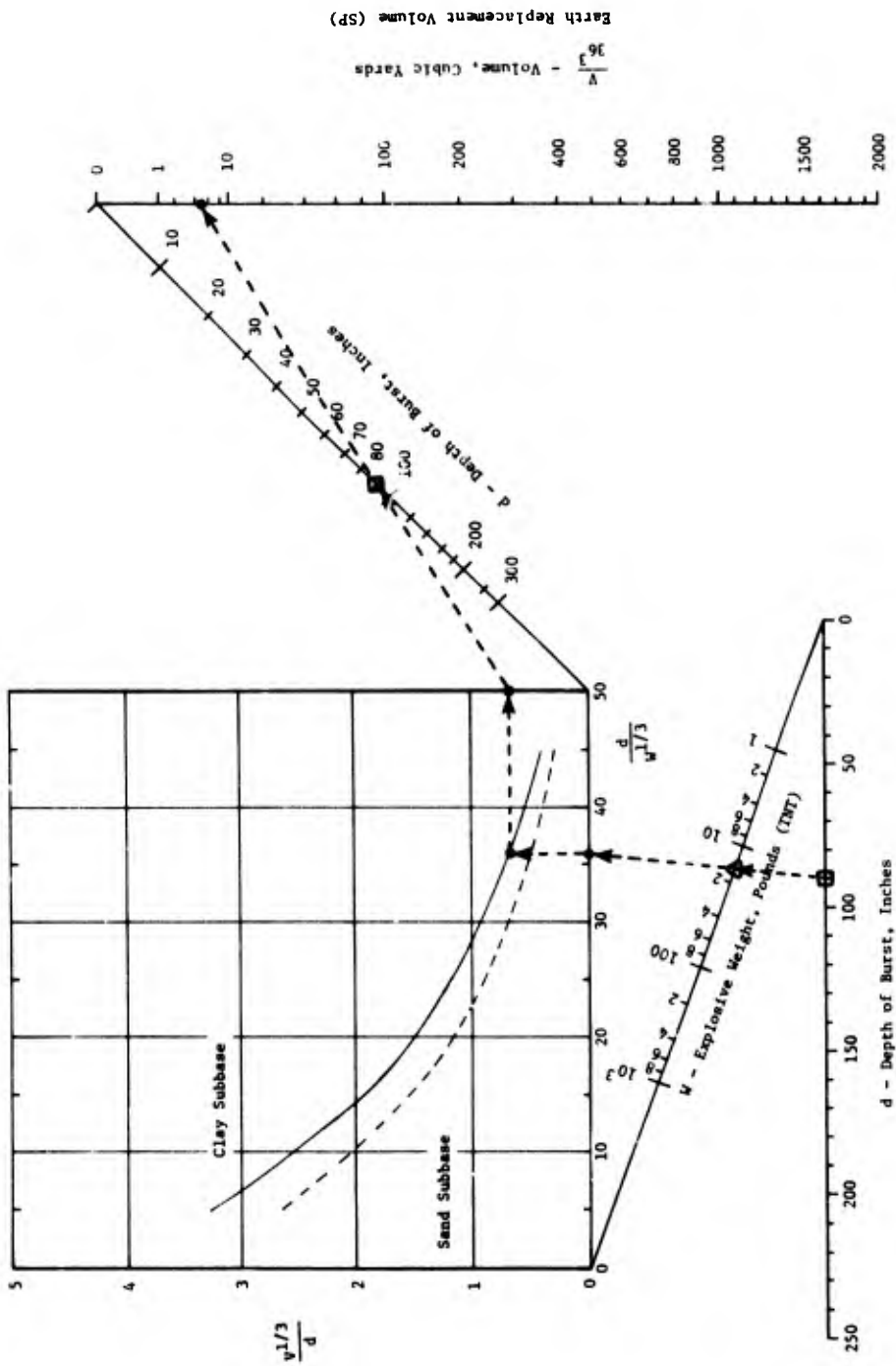


Figure 51. Bomb Damage Repair Nomograph; Instructional Example

through slide rule or pocket calculator computations. If the nomographs are used in this manner, the resultant damage parameters will be in consistent units (volume in cubic inches, area in square inches).

Due to the definition of expedient repair, either the earth replacement volume or the earth removal volume will be zero, but not both. The ranges of depth of burst and weapon explosive weight corresponding to the regions of replacement (no removal) and removal (no replacement) are indicated on the nomographs in Figures 53 and 56.

2. DAMAGE PREDICTION NOMOGRAPHS

The nomographs developed for making airfield pavement damage predictions are presented in Figures 52 through 63. As noted earlier, all prediction relationships which involve explosive weight are based on equivalent weight of TNT. Table 13 supplies conversion factors for several common explosives. Prior to use of any prediction relationship or nomograph, the actual explosive weight should be multiplied by the proper factor to obtain equivalent TNT weight.

TABLE 13. EQUIVALENT WEIGHT OF TNT FOR SELECTED EXPLOSIVES

Explosive	Equivalent TNT* (lb/lb)
TNT	1.00
Composition B	1.10
Composition C4	1.09
Tritonal	1.15
Composition H-6	1.13
Octol 75/25	1.25
Cyclotol 75/25	1.26
Cyclotol 60/40	1.16
* Based on air blast impulses	

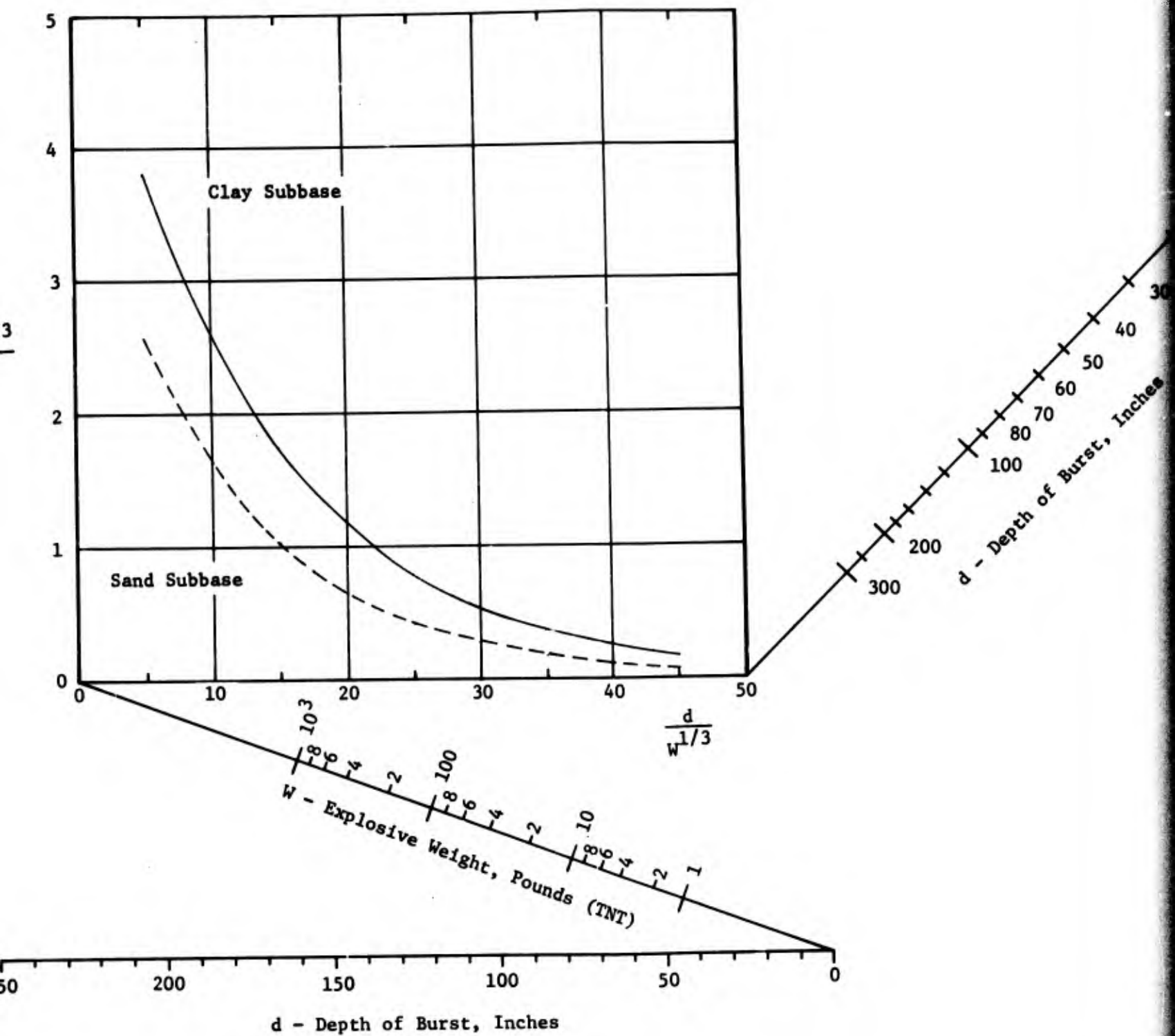


Figure 52. Bomb Damage

(The rever

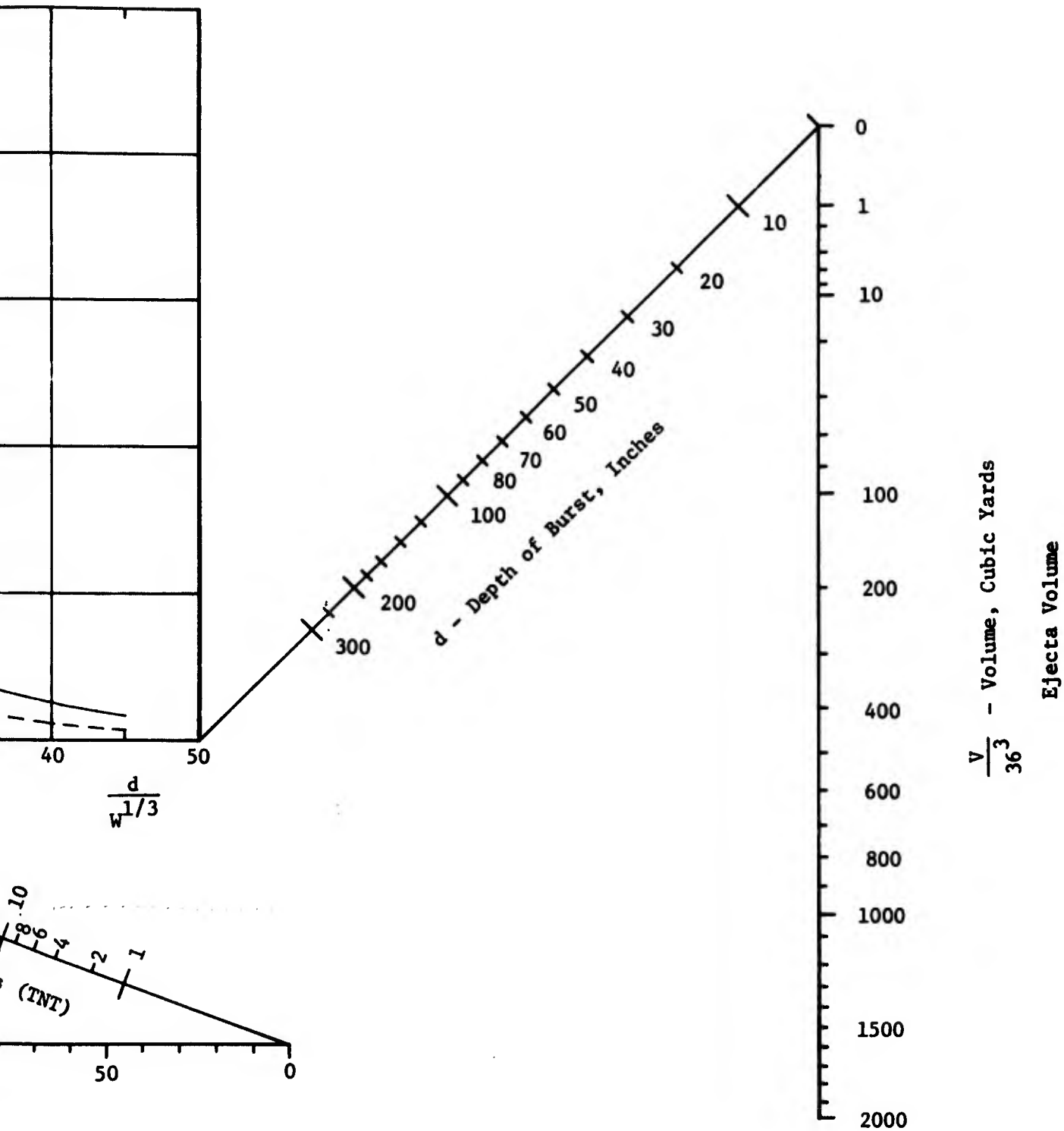


Figure 52. Bomb Damage Repair Nomograph; Ejecta Volume.

b Preceding page blank

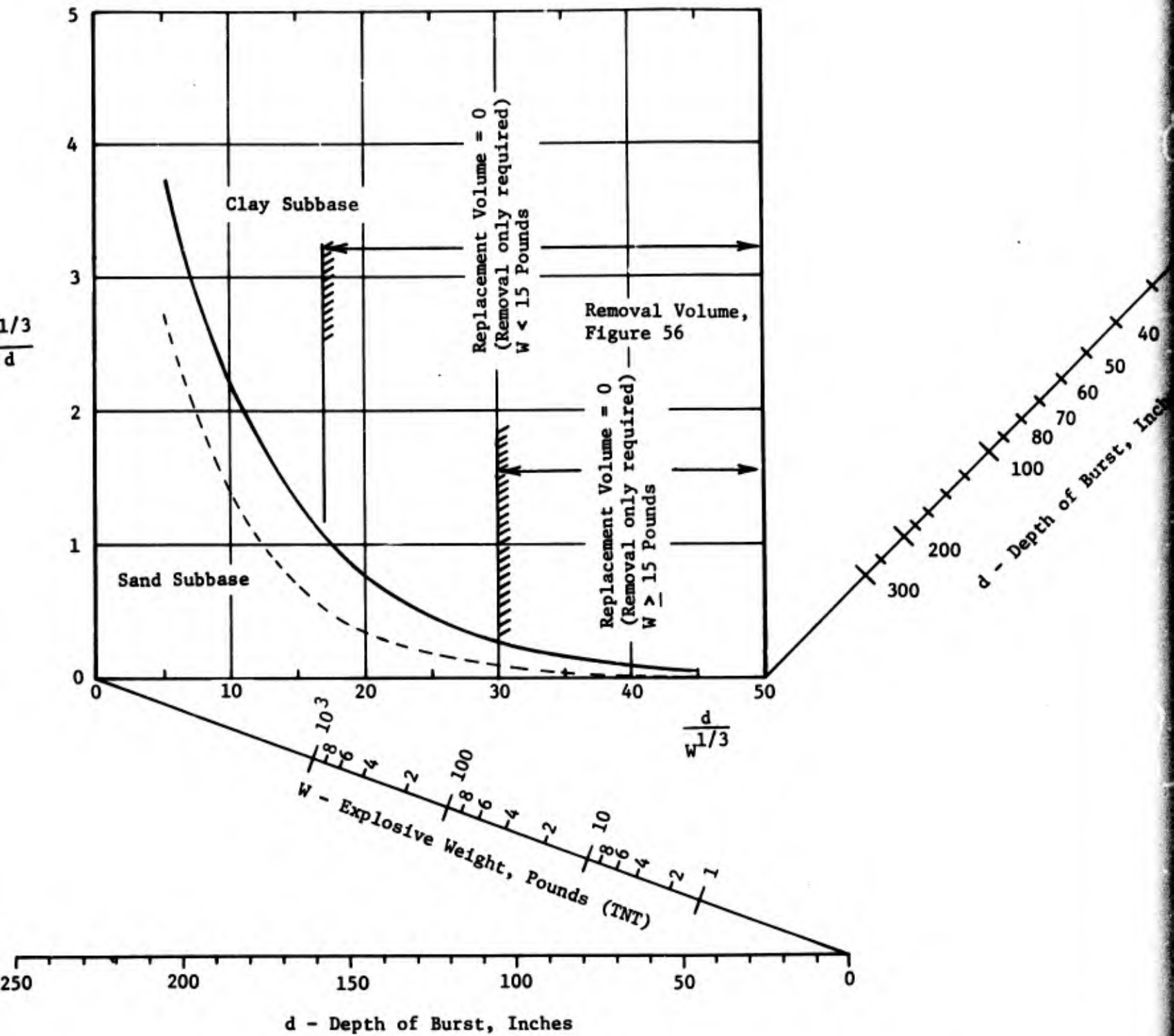


Figure 53. Bomb Damage Repair
Expe

(The reverse

a

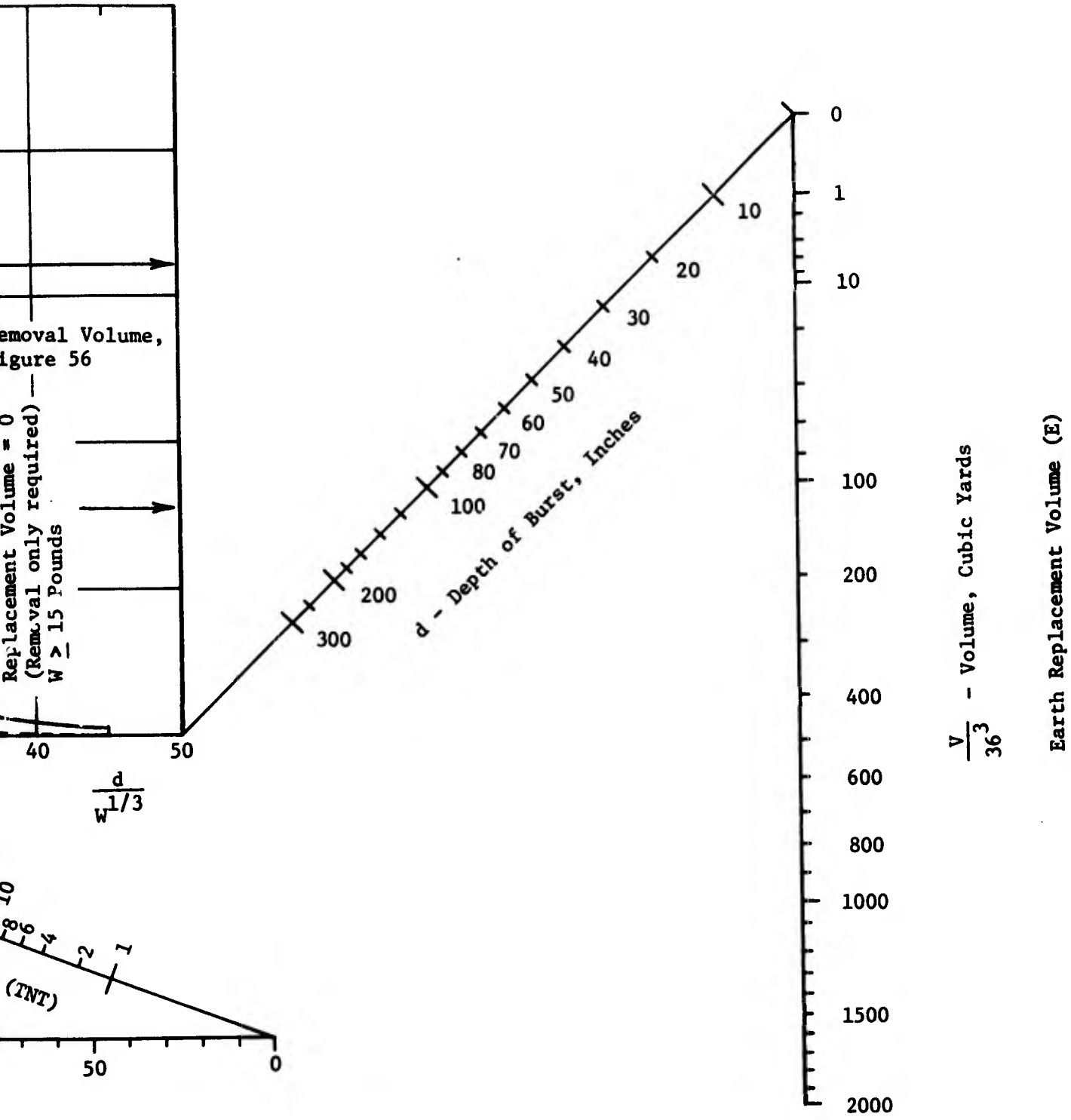
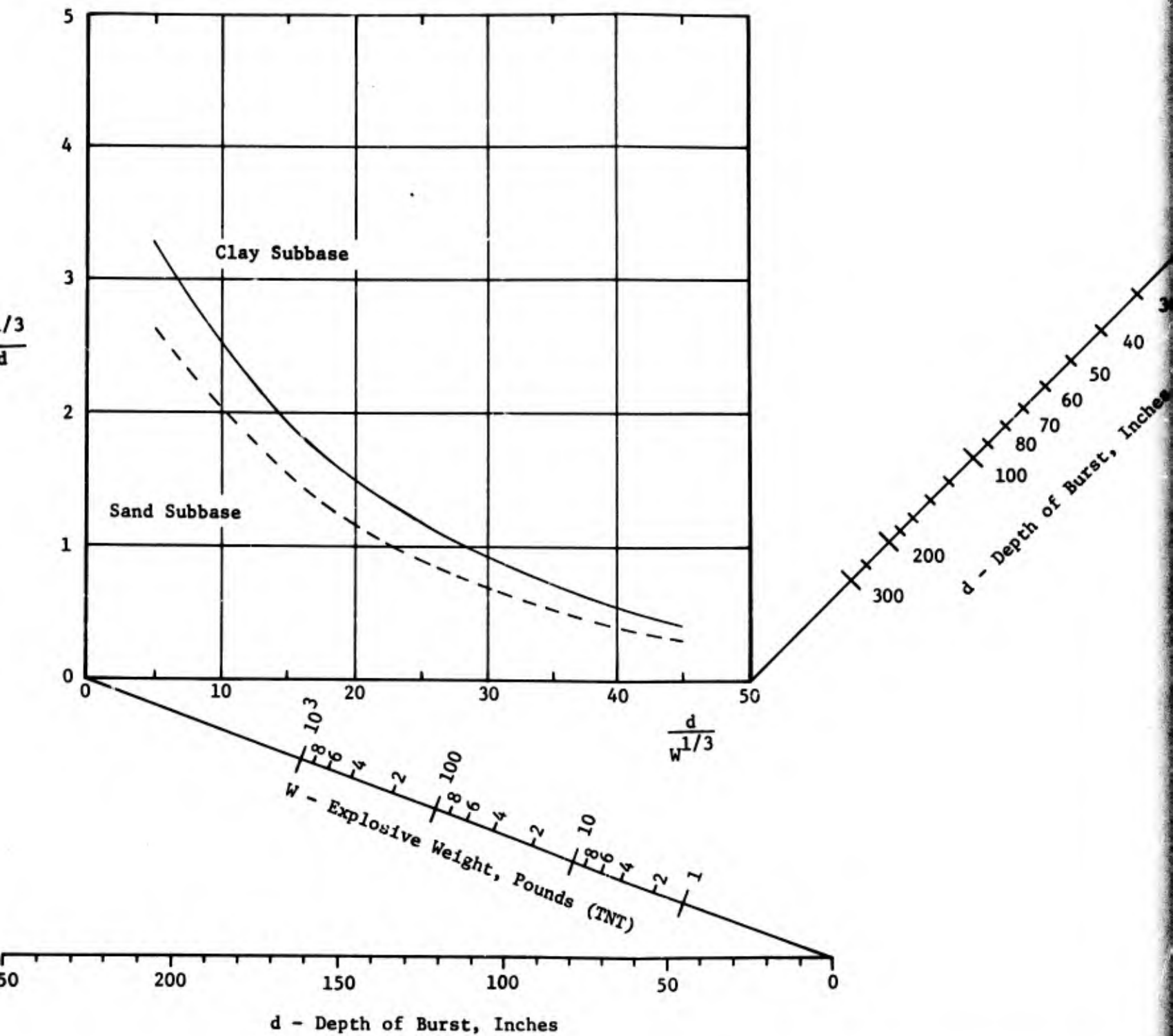


Figure 53. Bomb Damage Repair Nomograph; Earth Replacement Volume, Expedient Repair

Preceding page blank



a

Figure 54. Bomb Damage Repair Method
Semipermanent

(The reverse of)

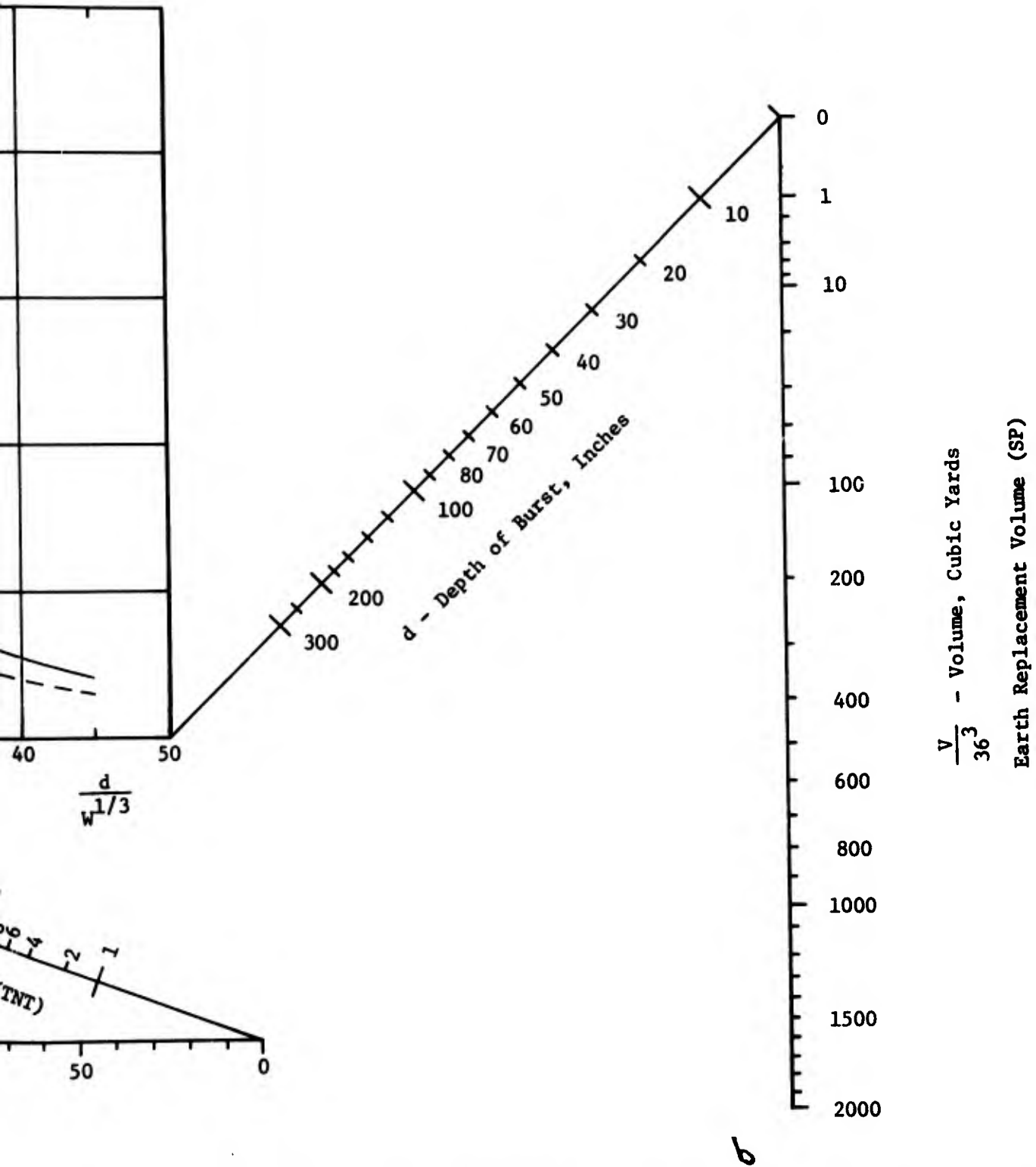


Figure 54. Bomb Damage Repair Nomograph; Earth Replacement Volume, Semipermanent Repair

Preceding page blank

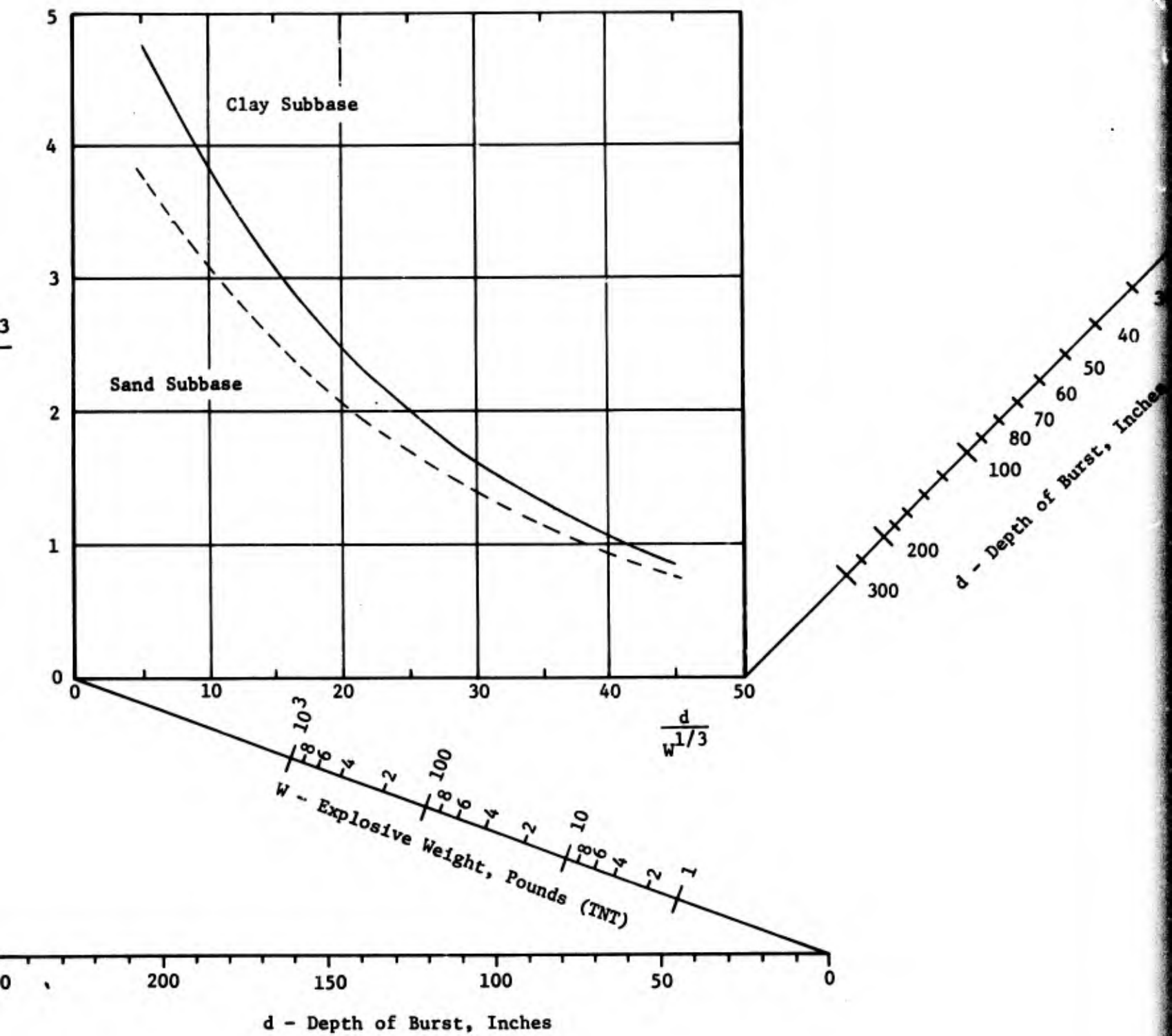


Figure 55. Bomb Damage Repair Percent

(The reverse side)

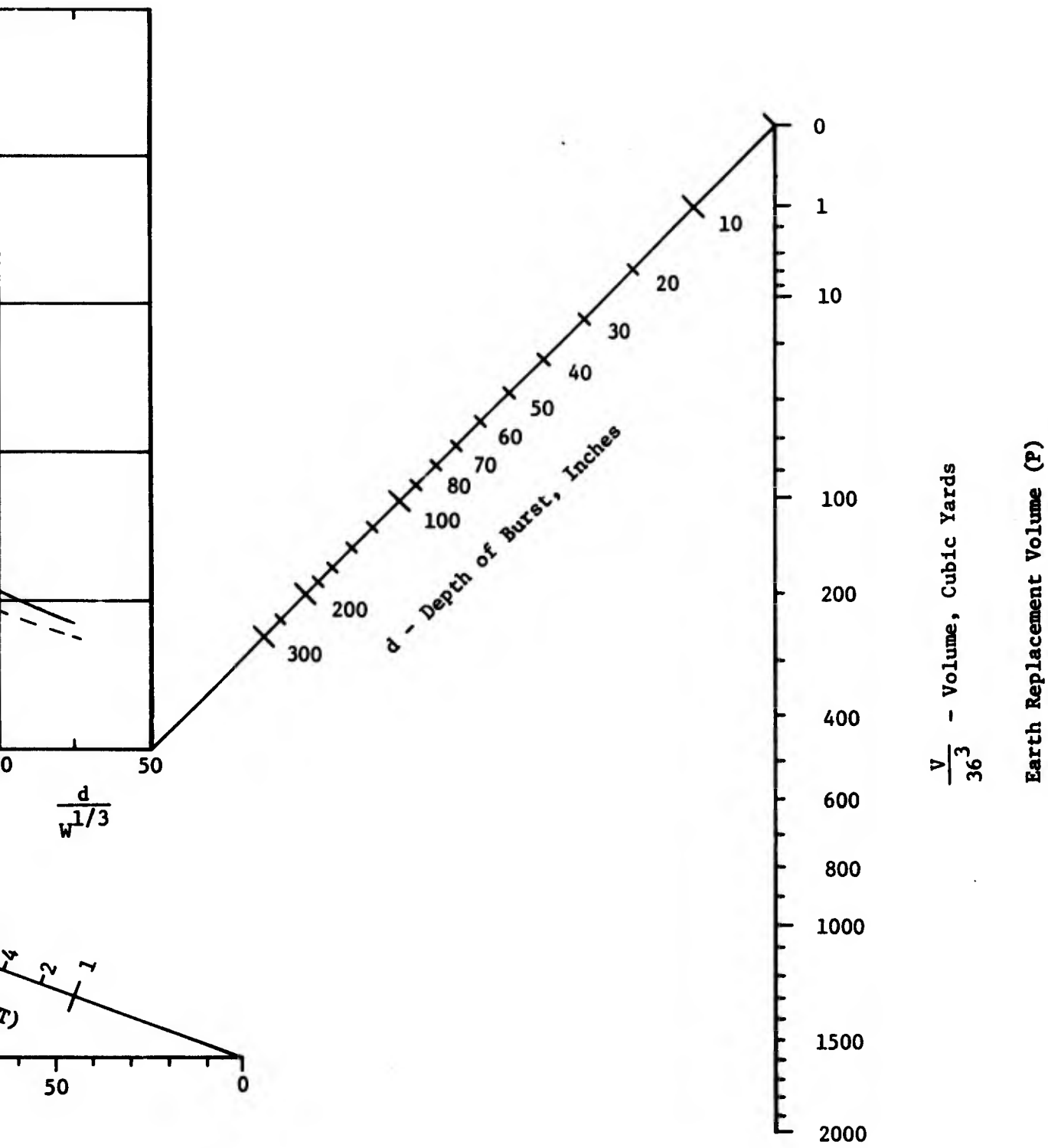


Figure 55. Bomb Damage Repair Nomograph; Earth Replacement Volume, Permanent Repair

b

Preceding page blank

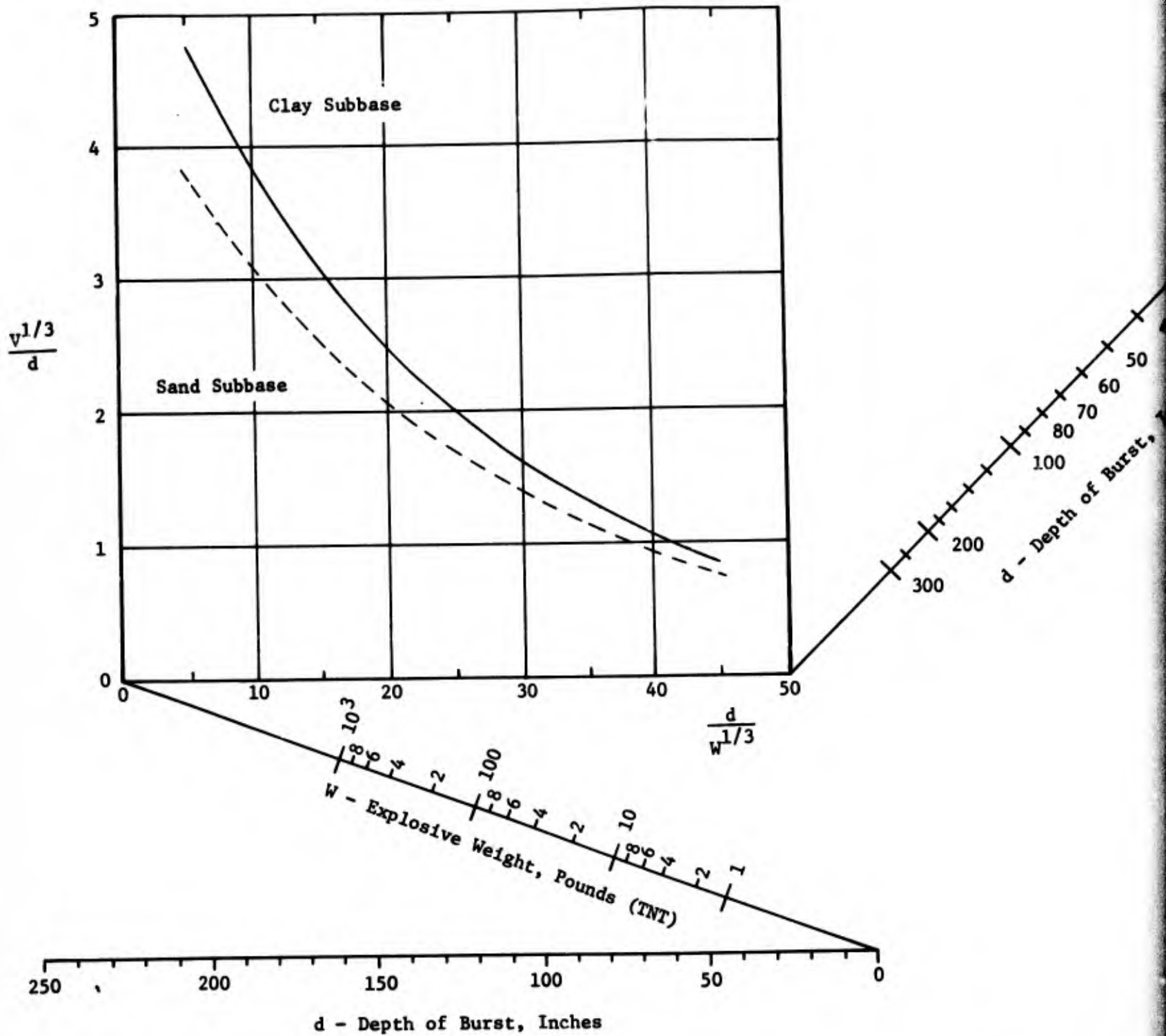


Figure 55. Bomb Damage

(The rev

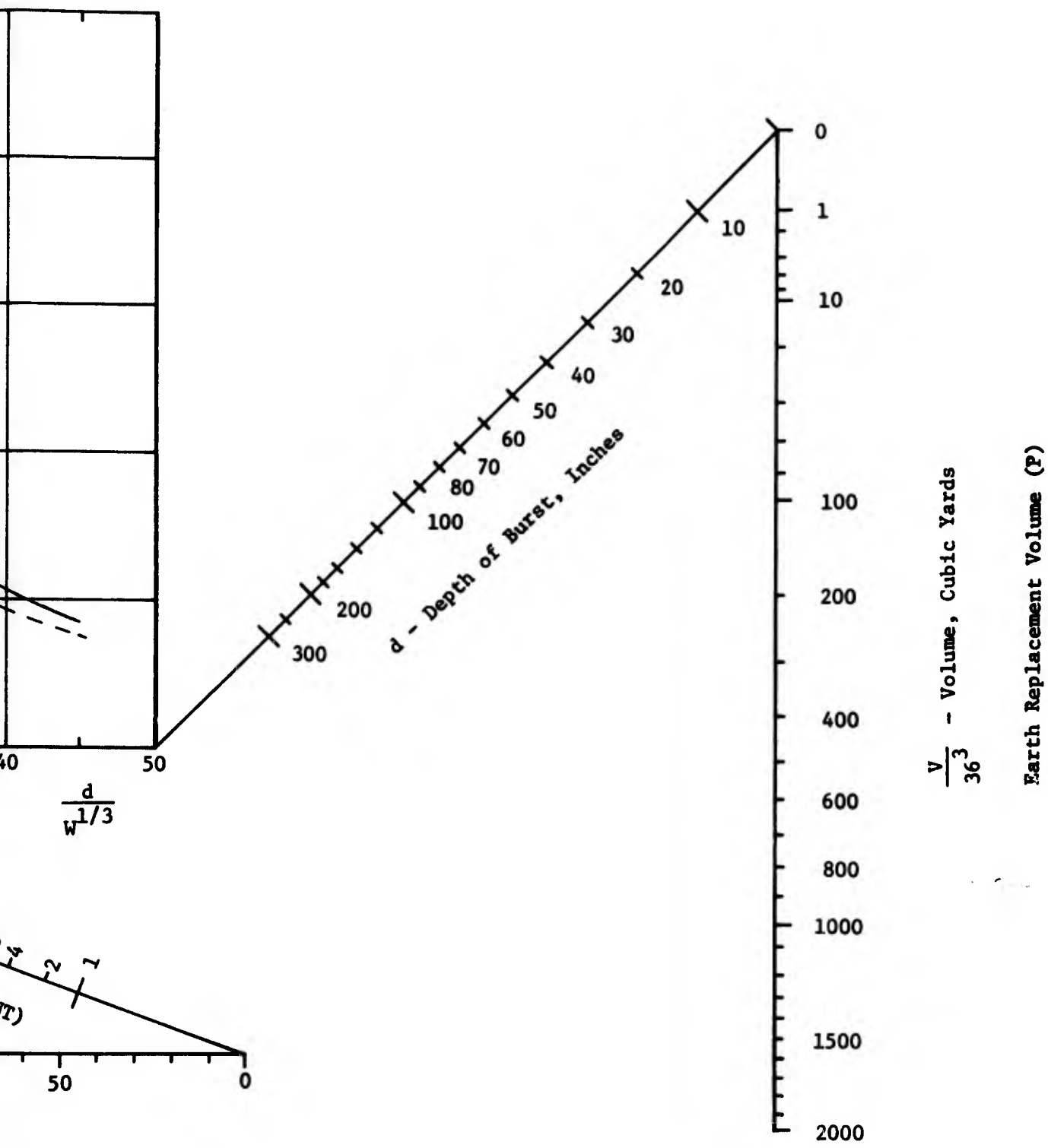


Figure 55. Bomb Damage Repair Nomograph; Earth Replacement Volume, Permanent Repair

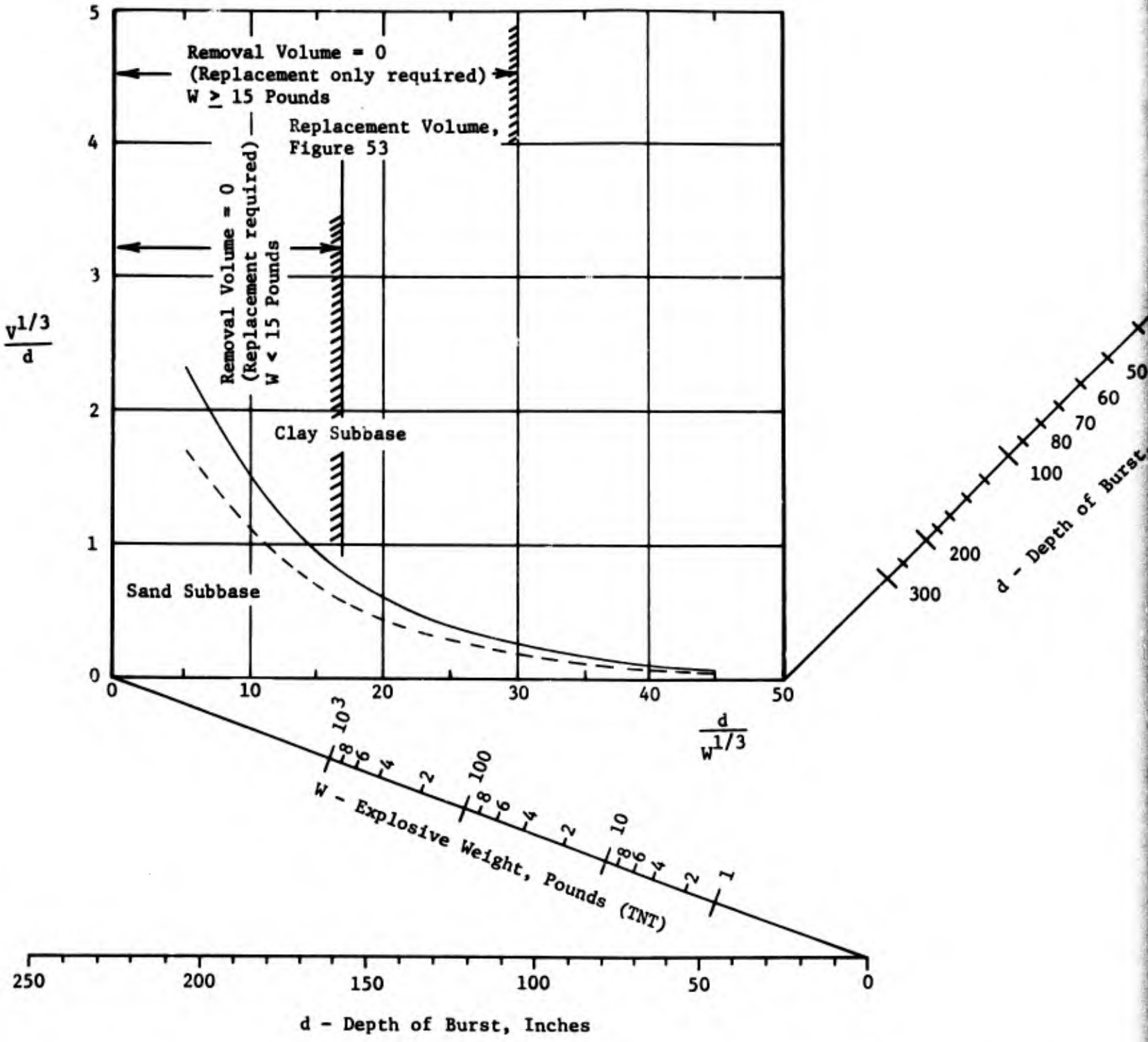


Figure 56. Bomb Damage

(The r

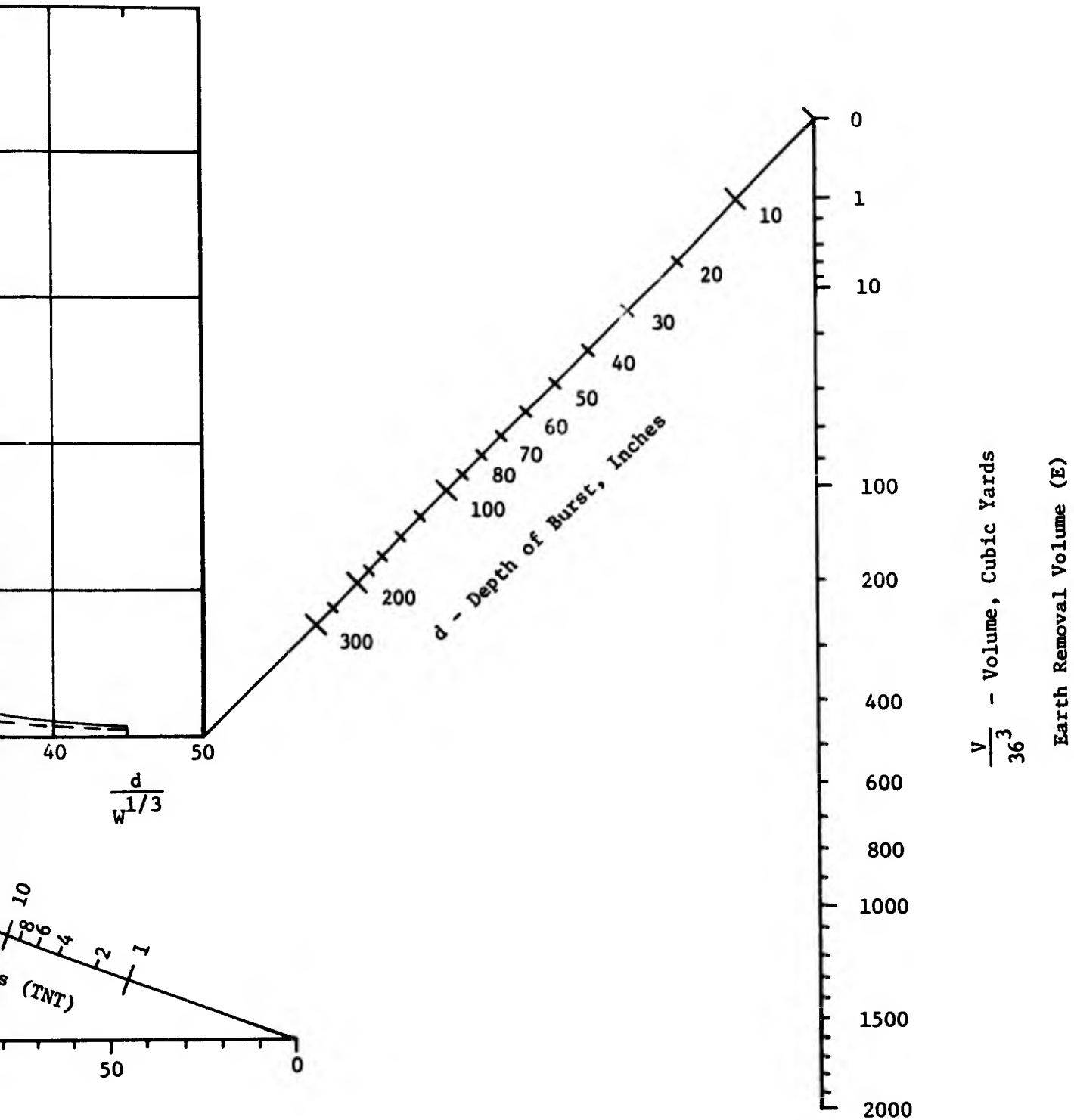


Figure 56. Bomb Damage Repair Nomograph; Earth Removal Volume,
Expedient Repair

6

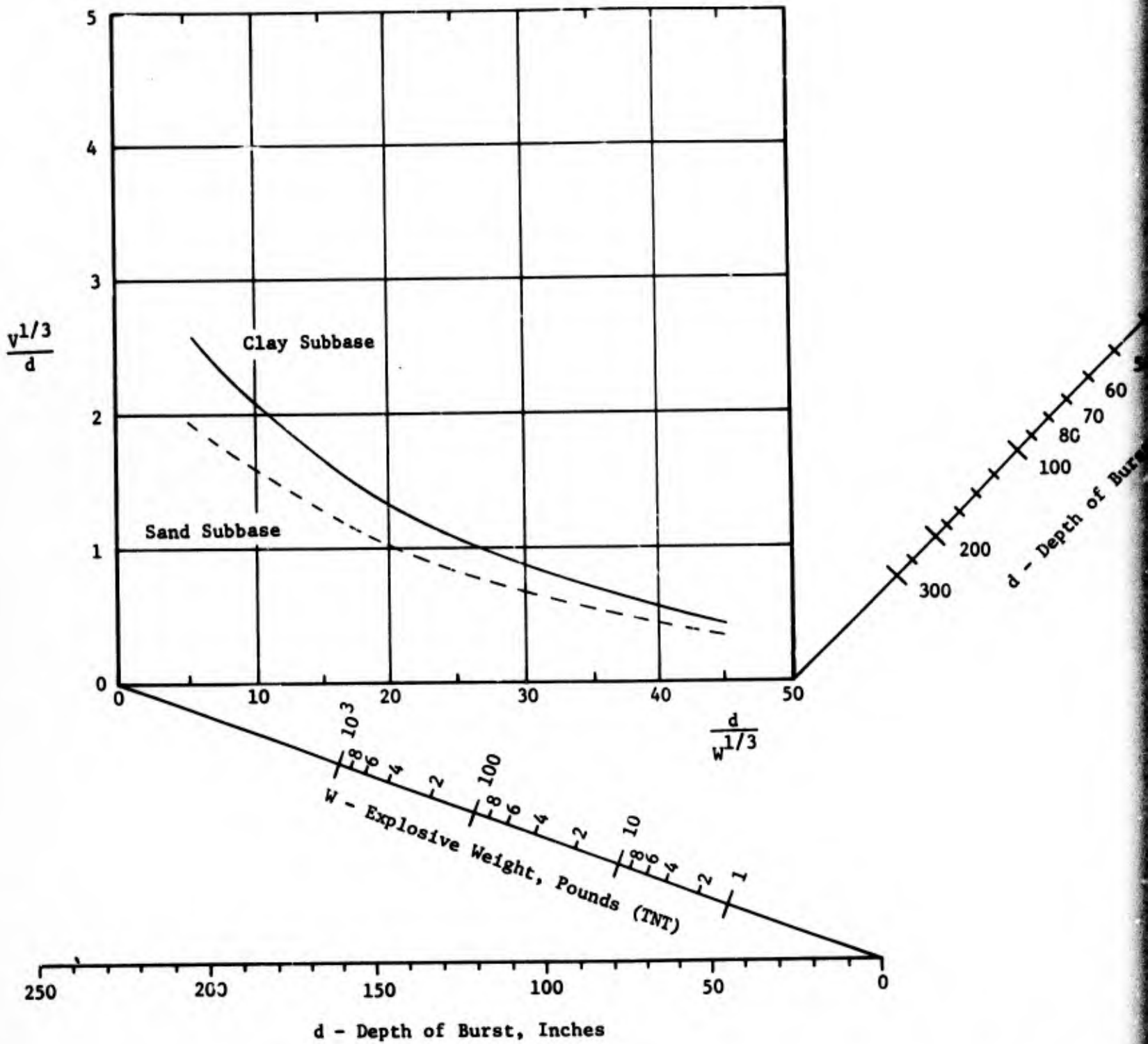


Figure 57. Bomb Damage

a

(The

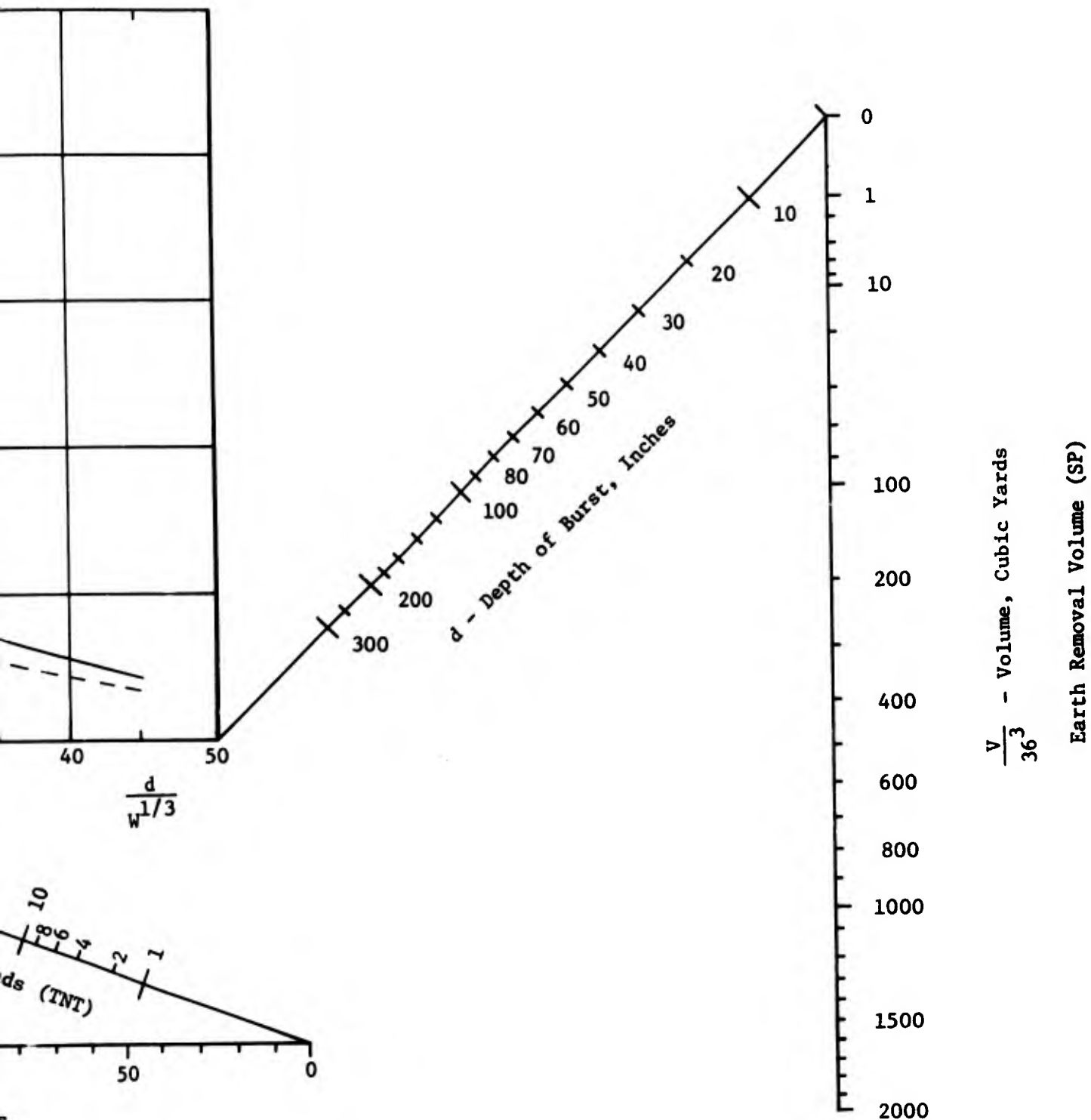


Figure 57. Bomb Damage Repair Nomograph; Earth Removal Volume, Semipermanent Repair

Preceding page blank

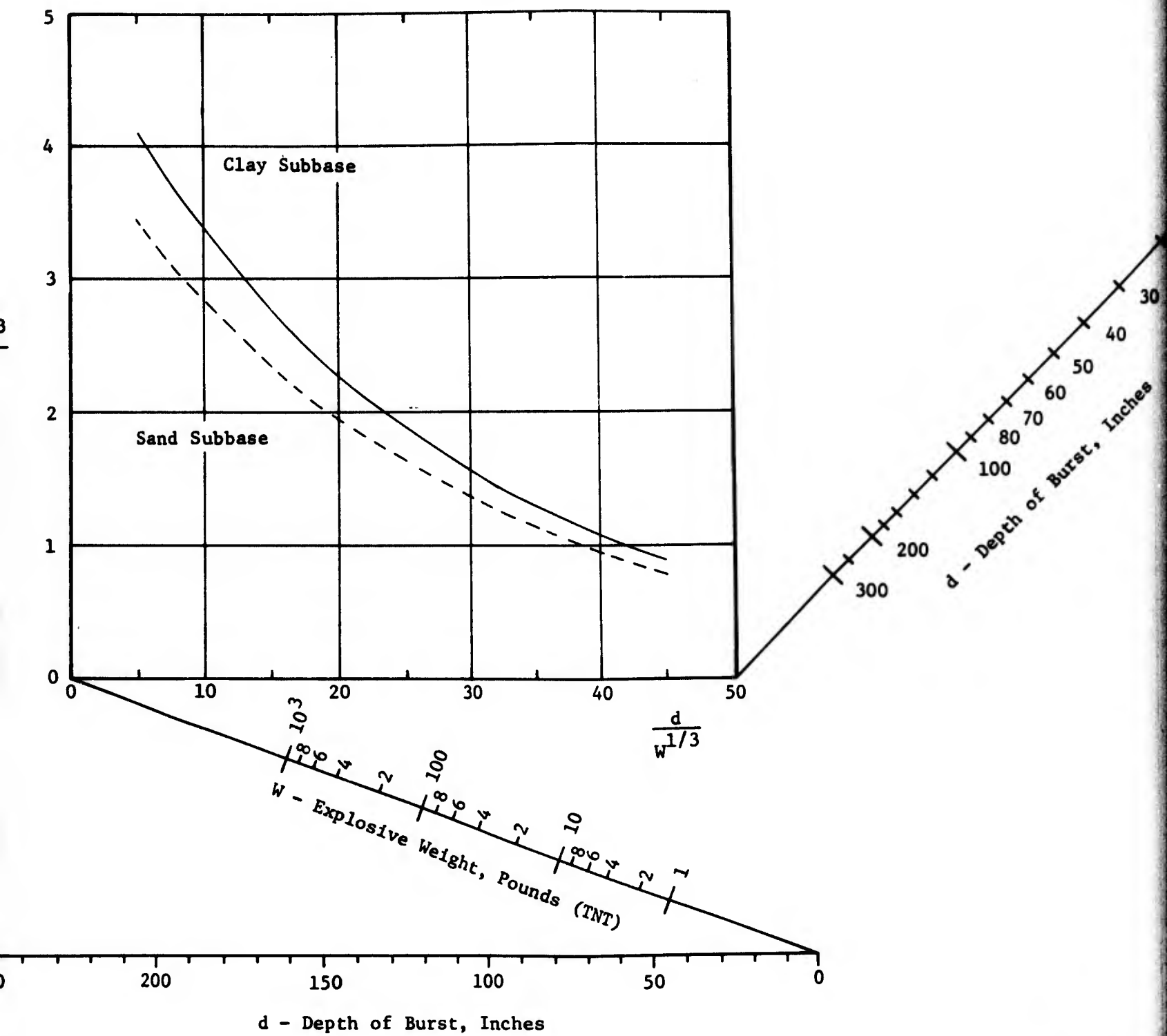


Figure 58. Bomb Damage Repair

Pe

(The reverse

a

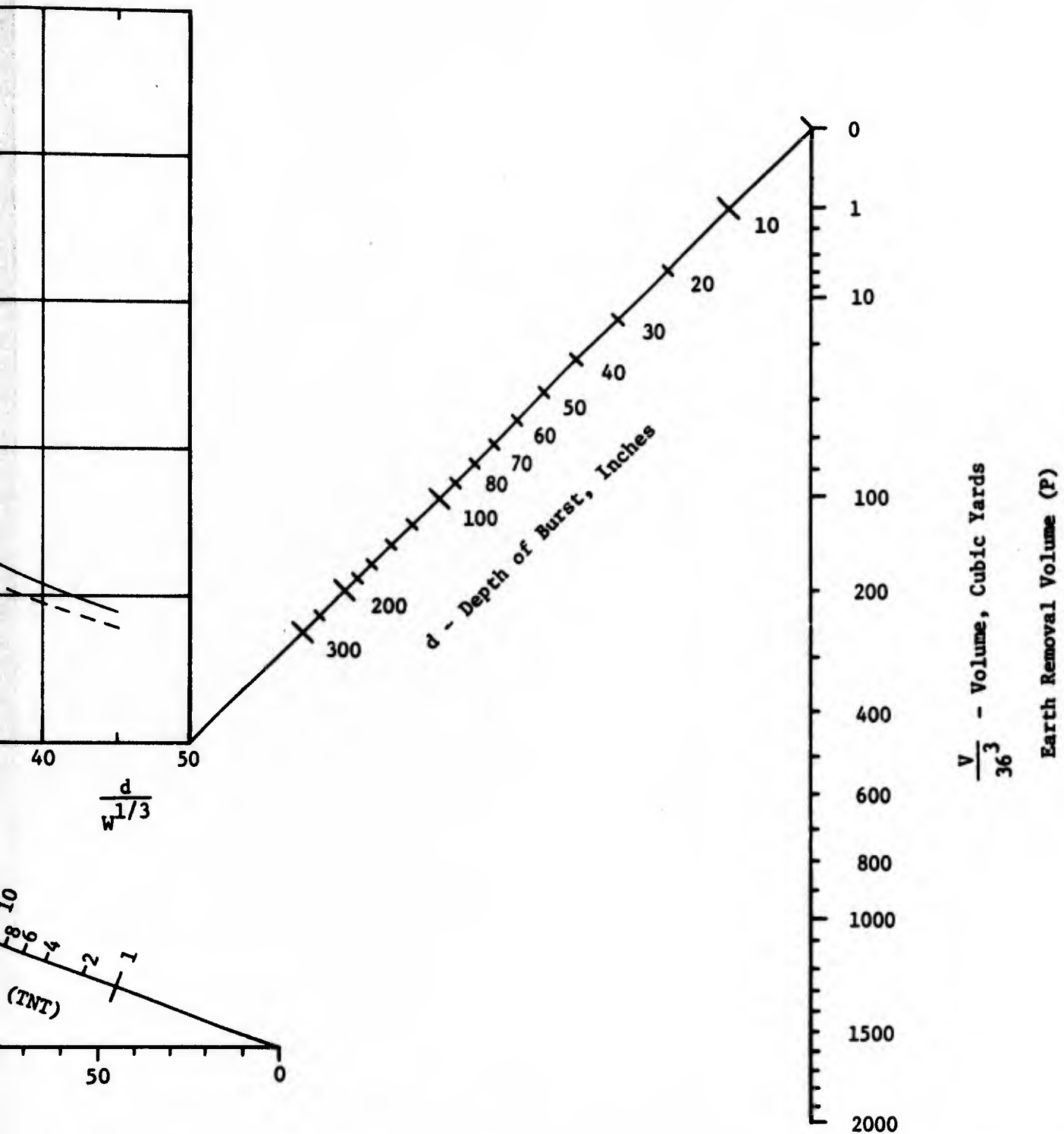


Figure 58. Bomb Damage Repair Nomograph; Earth Removal Volume, Permanent Repair

6

Preceding page blank

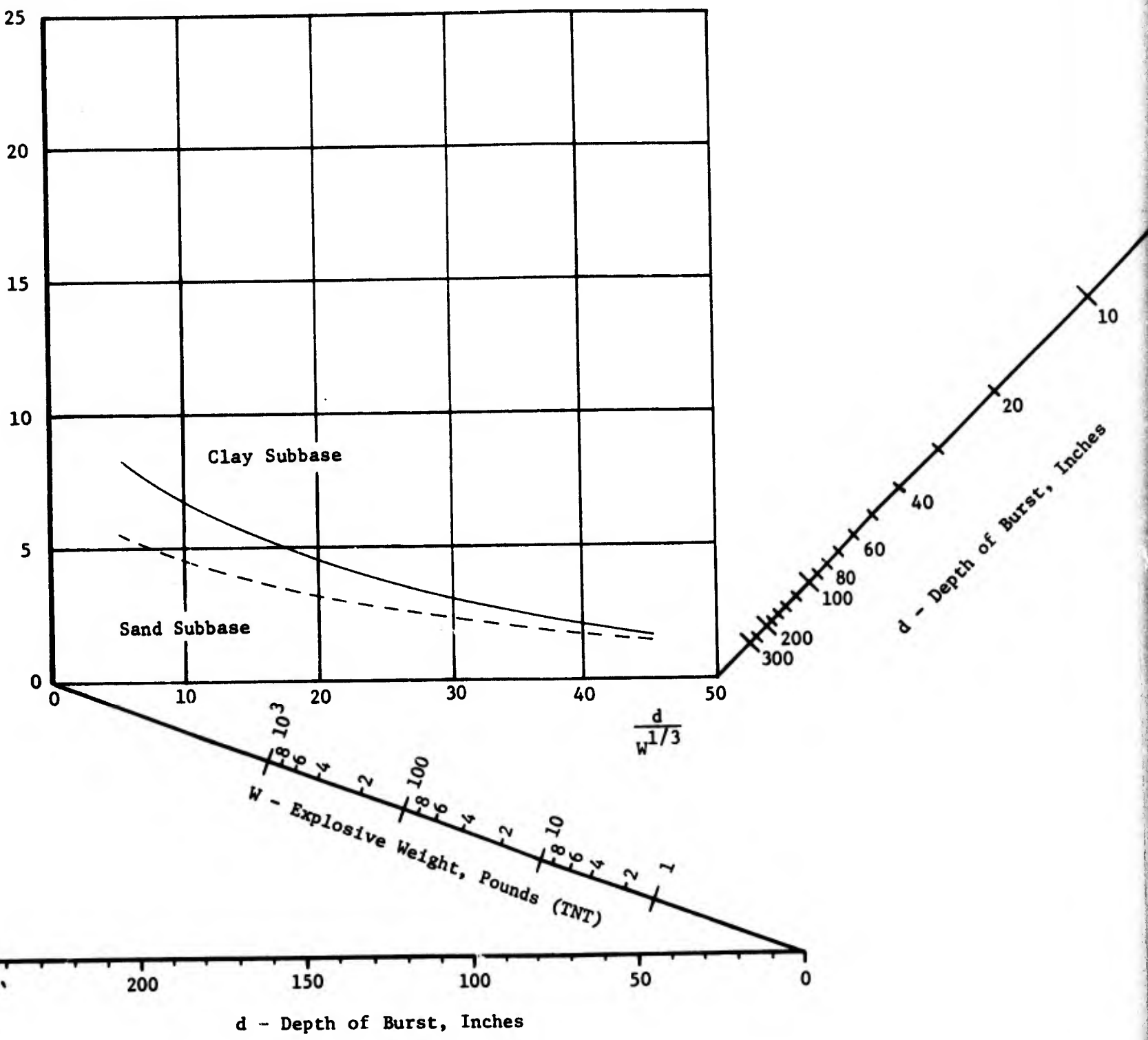


Figure 59. Bomb Damage Repair Nomogram
Expedient

a

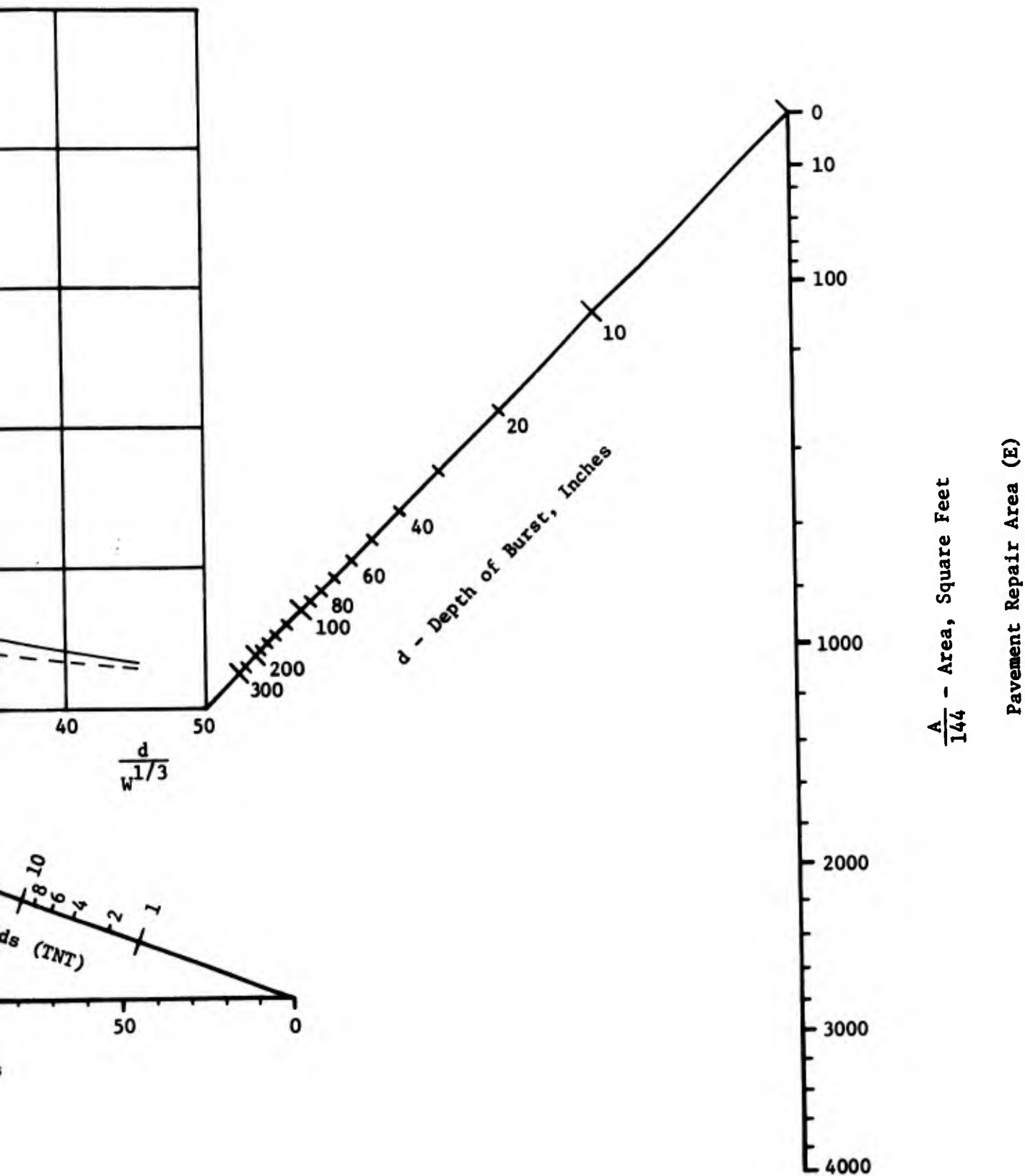


Figure 59. Bomb Damage Repair Nomograph; Pavement Repair Area,
Expedient Repair

Preceding page blank

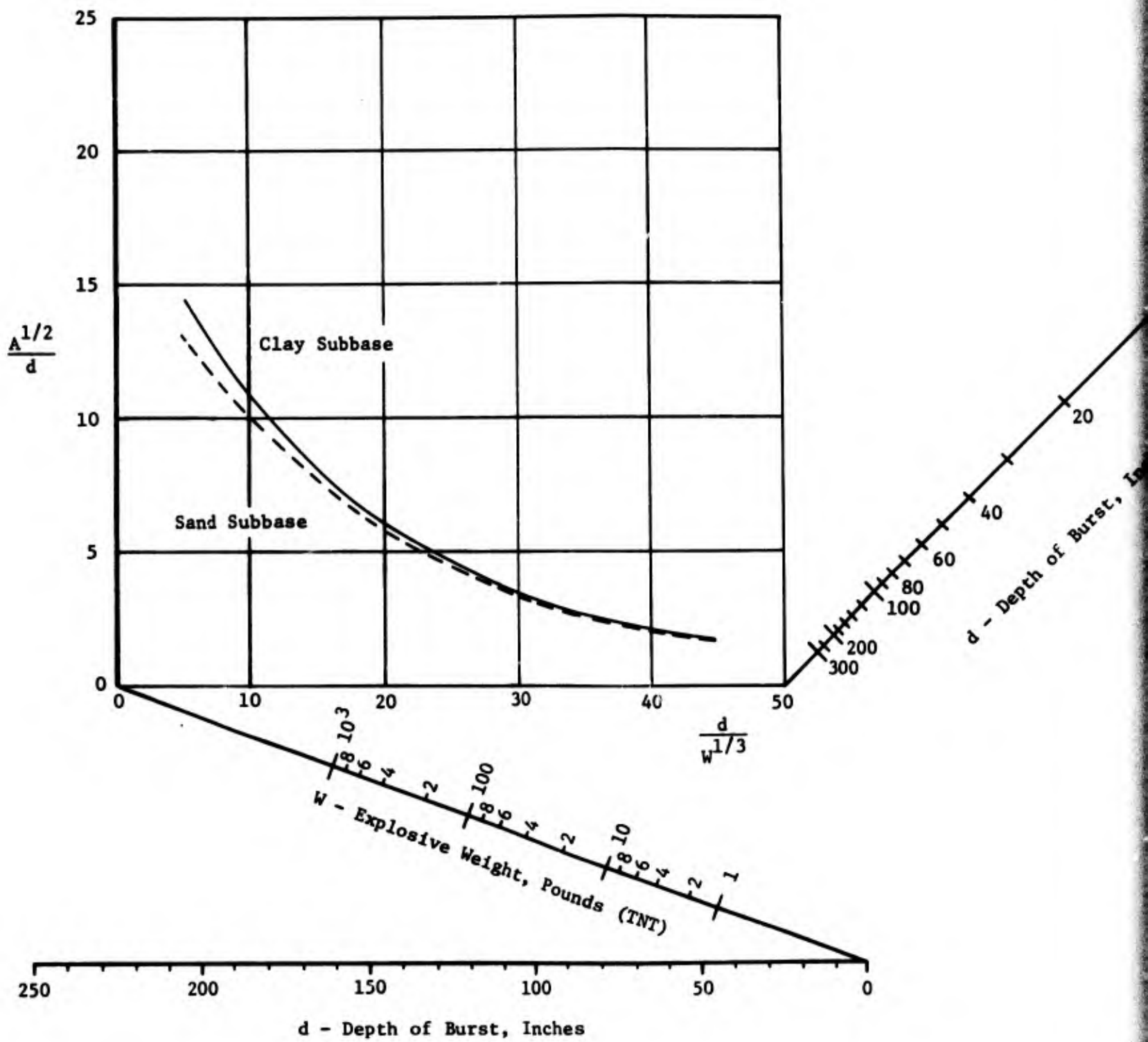


Figure 60. Bomb Damage

(The re

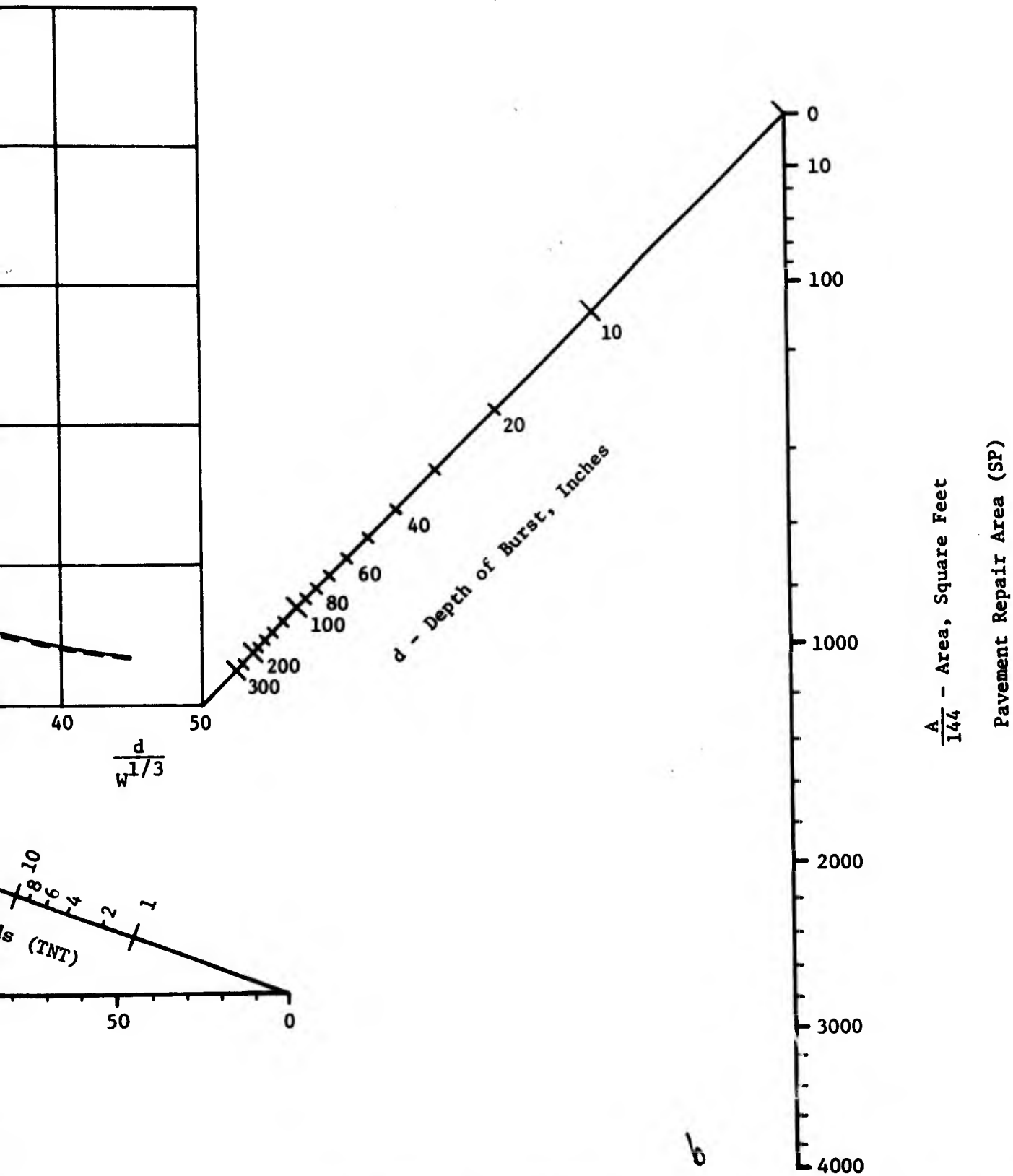


Figure 60. Bomb Damage Repair Nomograph; Pavement Repair Area, Semipermanent Repair

Preceding page blank

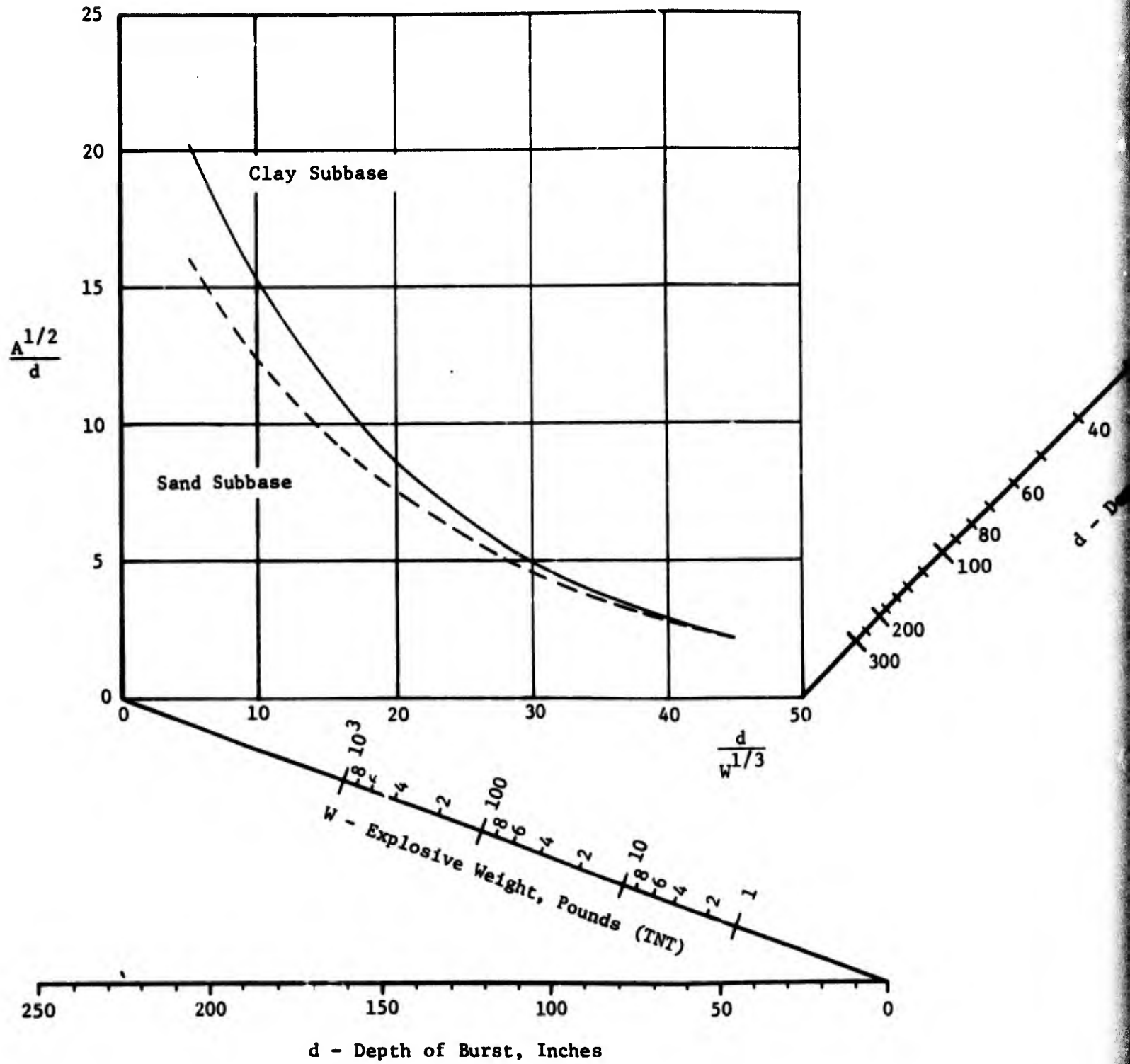


Figure 61. Bomb B

2

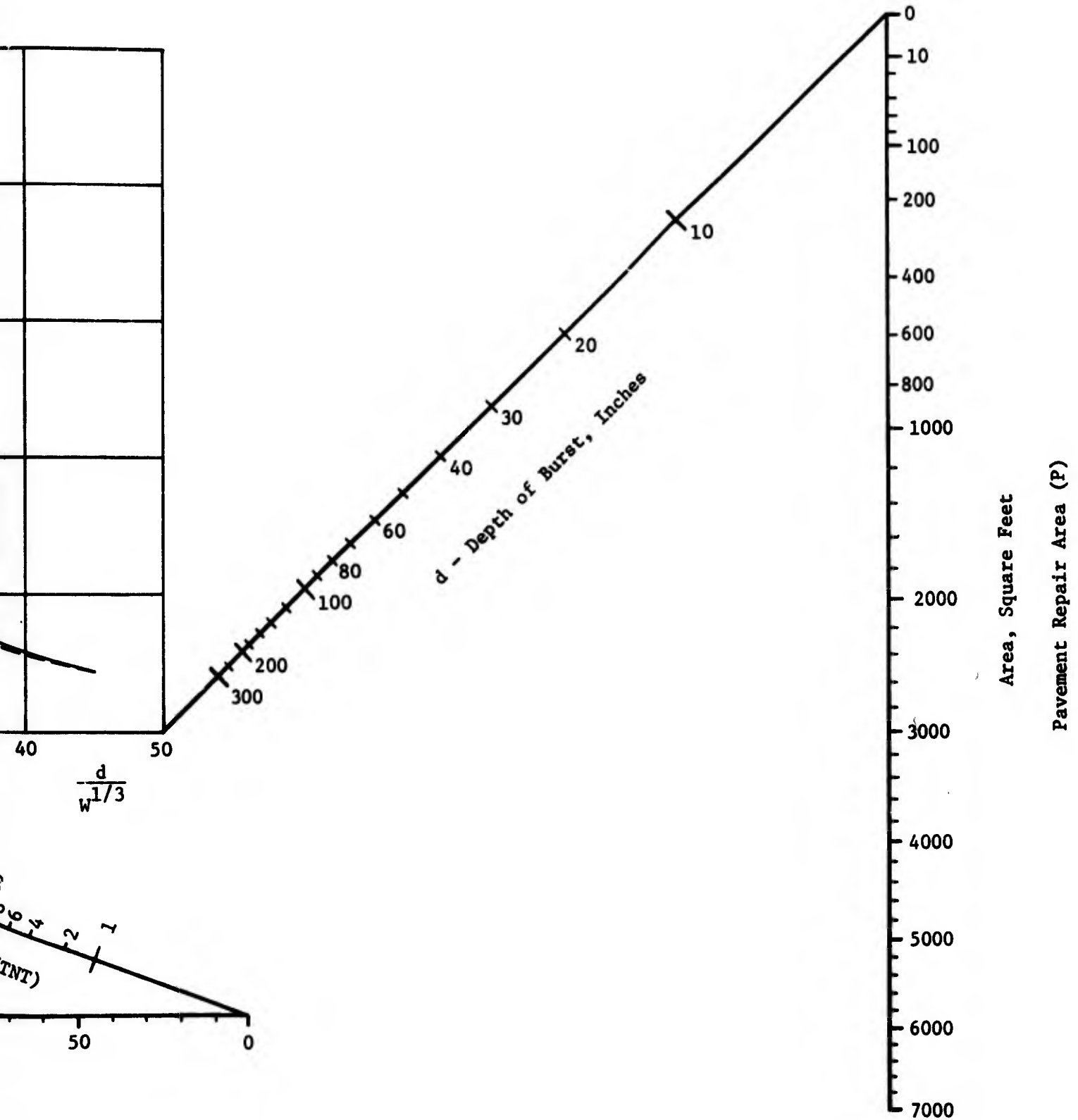


Figure 61. Bomb Damage Repair Nomograph; Pavement Repair Area, Permanent Repair

b

Preceding page blank

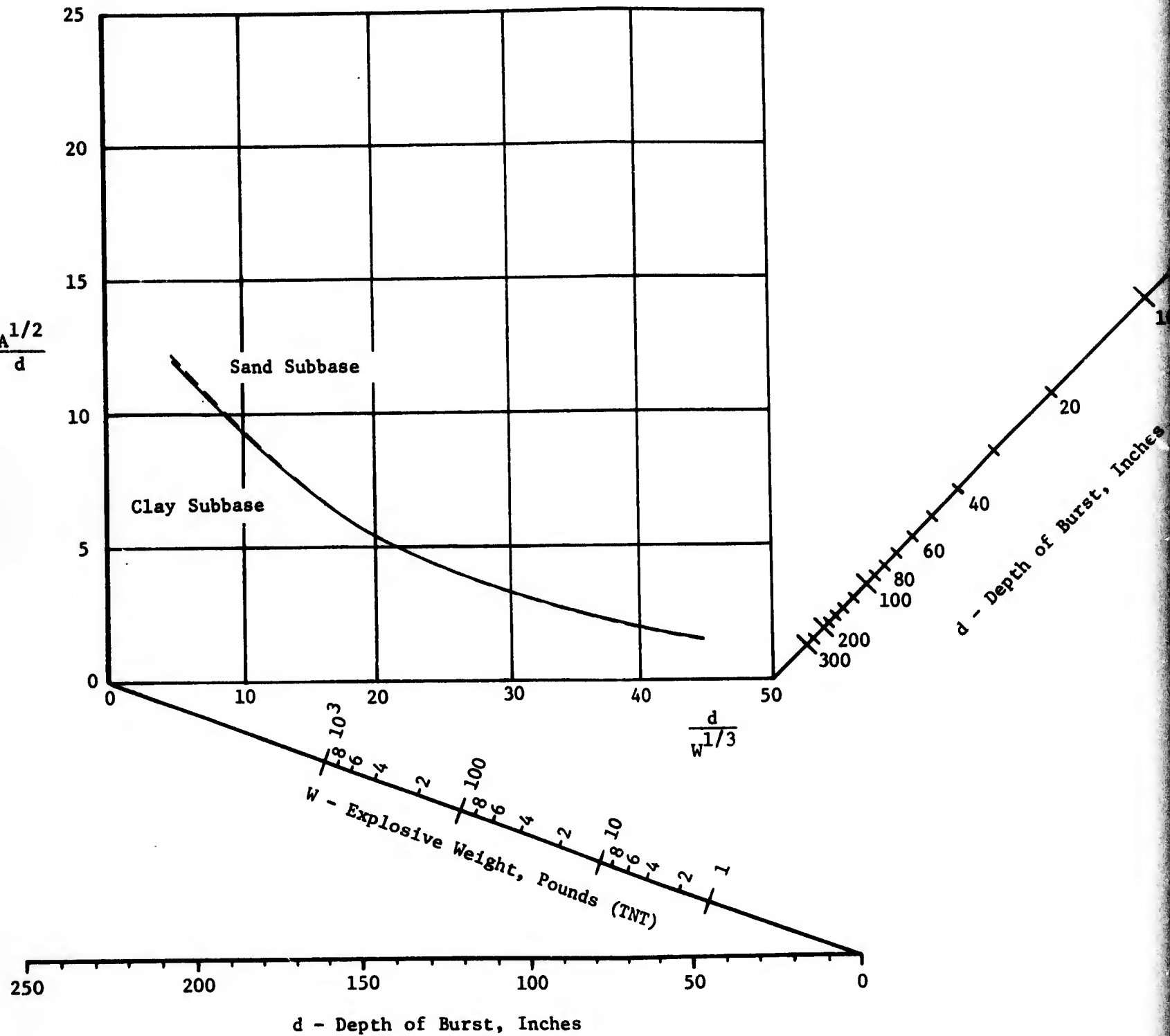


Figure 62. Bomb Damage Relationships for Sand and Clay Subbases

(The reverse side of this page shows the relationship between the depth of burst and the explosive weight for a concrete subbase.)

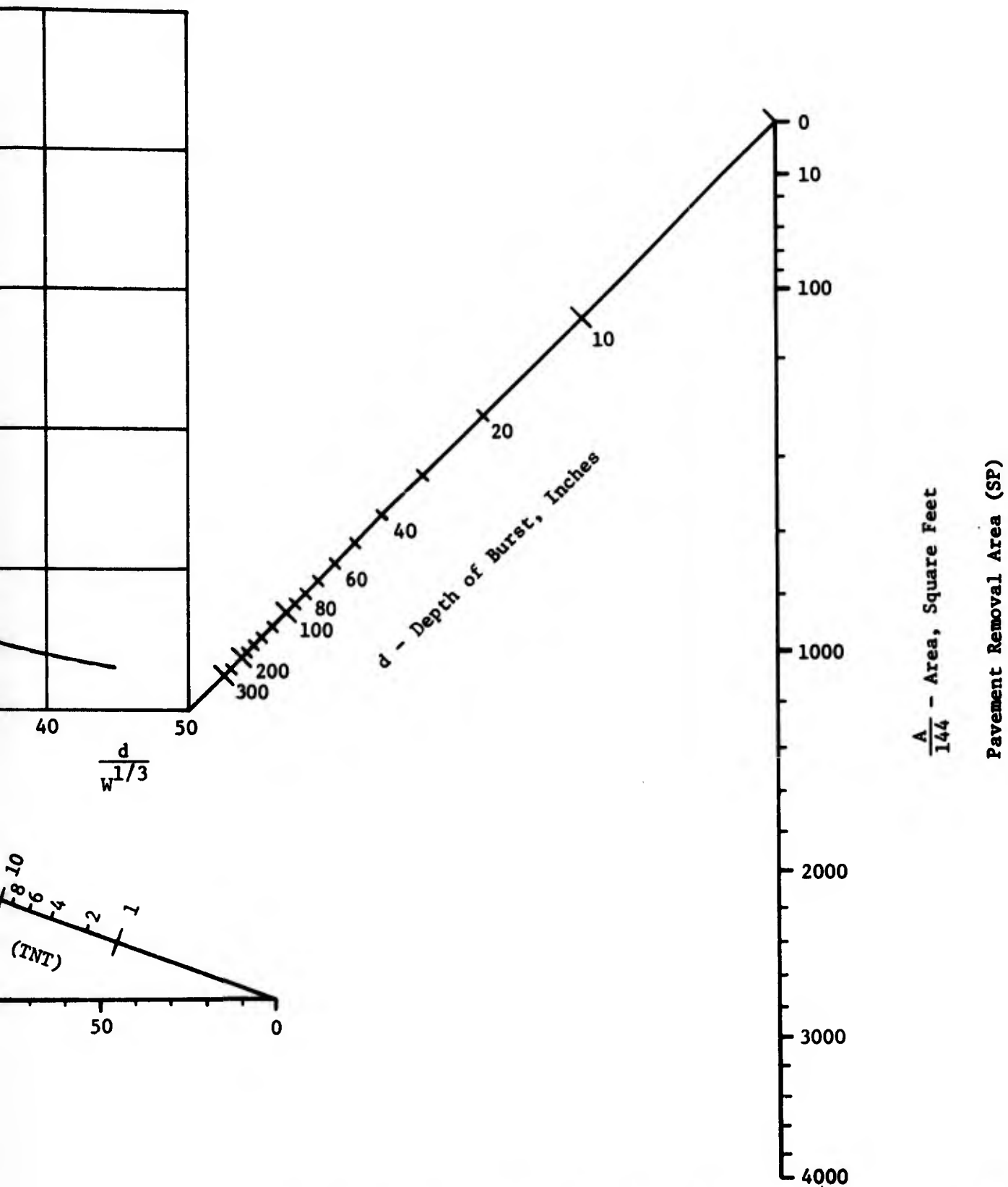


Figure 62. Bomb Damage Repair Nomograph; Pavement Repair Area, Semipermanent Repair

6 Preceding page blank

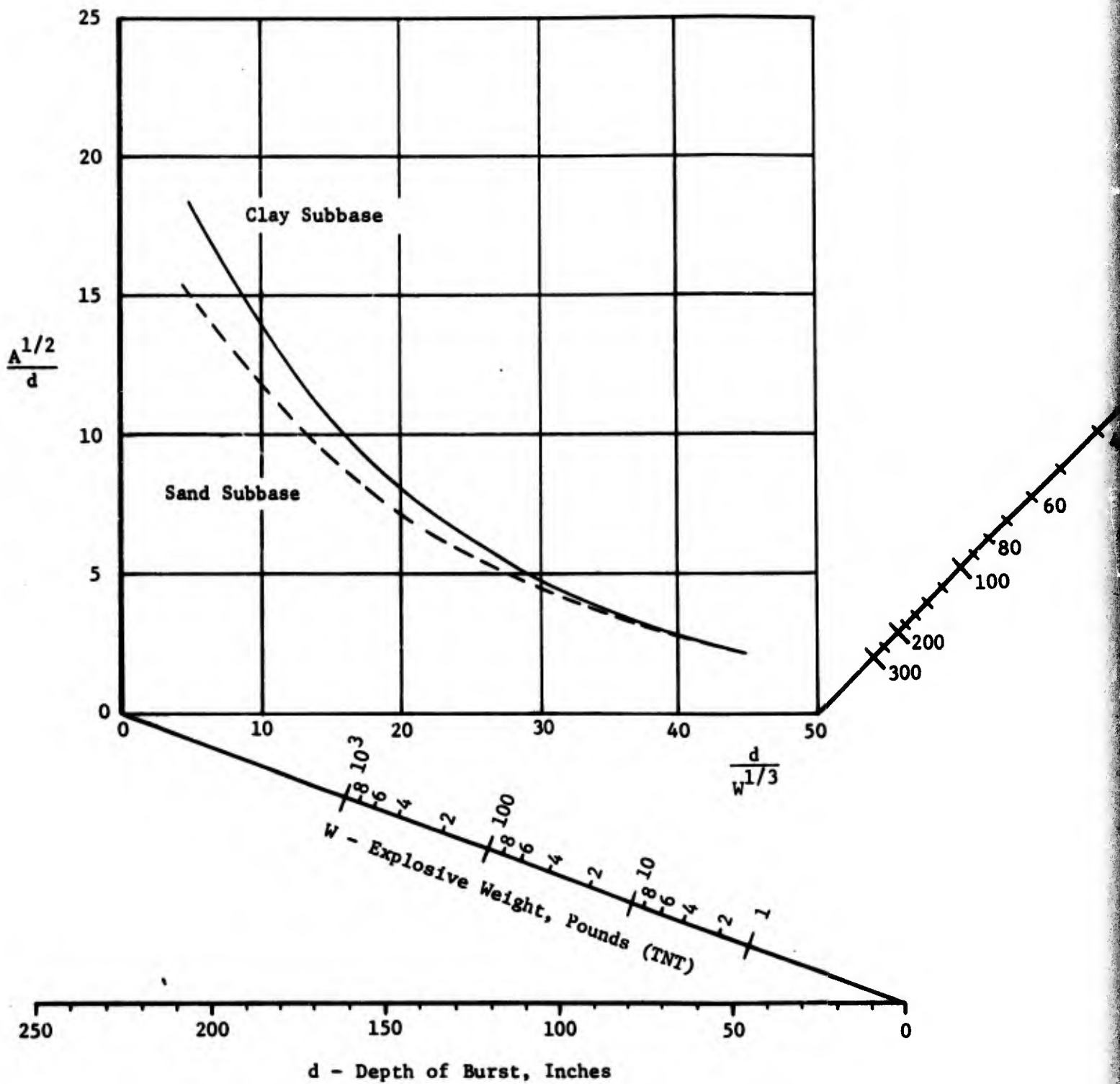


Figure 63.

2

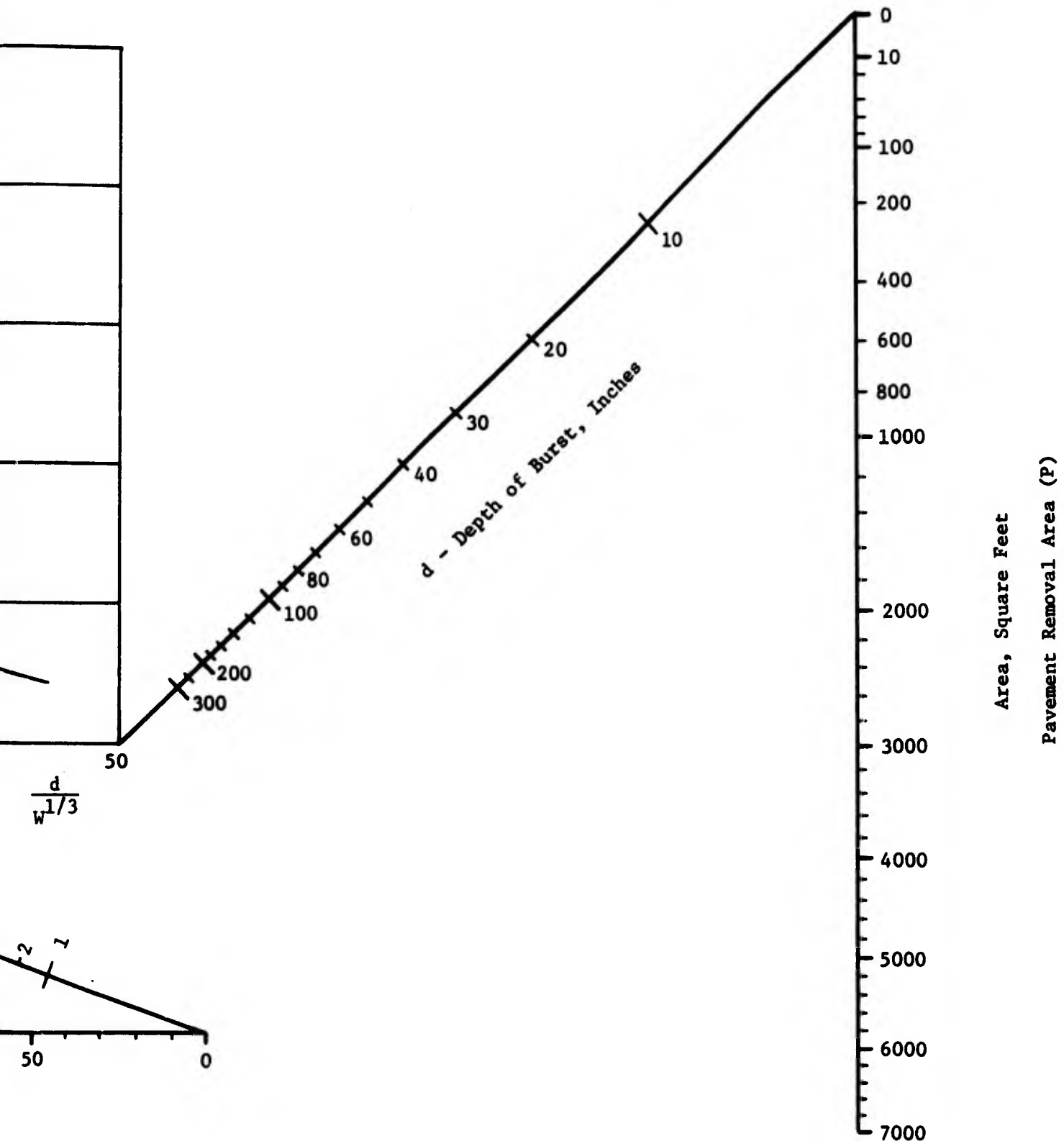


Figure 63. Bomb Damage Repair Nomograph; Pavement Removal Area,
Permanent Repair

b

Preceding page blank

SECTION VI
CONCLUSIONS AND RECOMMENDATIONS

1. CONCLUSIONS

Existing data on airfield pavement damage effects, as functions of pavement and weapon parameters, have been collected and evaluated. Those parameters identified as having a significant effect on pavement damage have received particular attention in the analysis and correlation of data. Both mathematical and graphical relationships have been developed to facilitate damage prediction calculations. All collected data were placed in a computerized data bank in consistent format and units, and various graphical data displays were created. These include plots of raw data, reduced data curve fits, and nomographs. Based on the range of repair levels defined, interpolation to predict intermediate damage levels is possible. The various data forms used provide the BDR planner (and field personnel as well) with the information needed to predict pavement damage from a wide variety of weapon types, thereby providing adequate BDR capability, methodology and expertise to prepare for rapid runway repairs. This will enable restoration of damaged pavement systems in minimal time, allowing the quickest possible resumption of air operations.

The following conclusions have resulted from completion of this effort:

- a. Large amounts of test data pertinent to the prediction of bomb damage to pavement systems can be readily and economically analyzed with computerized techniques.
- b. Raw data, rather than interpreted test results, must be used to ensure consistency in predictive relationships.
- c. Data may be analyzed by combination of basic data plots of test results and reduced functional relationships which are based on accepted statistical methods to predict expected damage parameters.
- d. Parameters relating BDR prediction requirements can be best presented in nomographic format for field application.
- e. From the information currently available on pavement cratering, the dependence of weapon weight, depth of burst,

Preceding page blank

and subbase constitution on damage can be shown functionally. Also, trends associated with other parameters, such as slab size and joint type, can be hypothesized but not substantiated mathematically.

2. RECOMMENDATIONS

As a result of the extensive data collection and analysis completed during the effort reported in this document, several recommendations are presented for future work. It is believed that completion of the recommended efforts will further enhance the damage prediction capability of those agencies concerned with BDR activities.

- a. A quantity of British test data were obtained near the end of the contract. Due to time limitations the new data could not be evaluated in the same detail as the other data. A cursory examination indicated the new data to be consistent with the other test results, in the areas where similar parameter values were tested. It is recommended that these British data be added to the BDR data base as a means to broaden its foundation and enhance its predictive capabilities.
- b. During the data collection and analysis portion of this program, several computer programs were written to aid in completing the data bank, to assist with curve fitting, and to plot data on a selective basis. These programs are available to the Air Force in the form used, but would be more useful if detailed user manuals and other documentation were prepared to enhance their utilization.
- c. Much difficulty was experienced in actually collecting data from reports and other sources because there was nothing even close to a standard format for recording test parameters and results. The data file format utilized in this effort should be made into a standard field data collection form, which would ensure collection of all needed test data, and make certain the data were consistent and readily usable in the programs mentioned in b. above.

- d. Evaluation of the capabilities of specific foreign weapons to defeat U.S. airfield pavements would be a useful effort. This would enhance the predictive capabilities of this report by having actual depths rather than speculative ones.
- e. The lack of firm roughness criteria presented some problems in completing the damage prediction analysis. It is recognized that work is in progress to generate these roughness criteria and effects on aircraft; this is mentioned here merely to emphasize the importance of this work and to encourage further effort.*
- f. No test data bank is ever completely full, and thus there is always a need for additional testing, both to explore new parameters and to enhance the data base of those parameters already addressed. Additional testing should be done to increase data for joint types, paving materials, reinforcing bars and wire, base materials, weapon obliquity angle and length-to-diameter ratio, soil moisture content, and an extended range of pavement thickness.

*The limited roughness data available were discussed in Section II. Recent efforts to define allowable roughness conditions also include the data in Reference 17, as well as analysis by CERF and analyses related to Project Essex completed by AFCEC and WES. In addition, a new program has been initiated under contract to AFCEC to develop BDR roughness guidelines. Further information in the status of these programs is available from AFCEC.

REFERENCES

1. Tucker, S. G., Bomb Crater Repair Study, Fort Bragg, NC, 23 June - 3 July 1962, WES MP 4-526, USA Engineer Waterways Experiment Station, Vicksburg, Mississippi, August 1962.
2. Menza, Dominic F., and George R. Offen, Runway Bomb Damage Repair Test, APGC-TDR-63-40, Air Proving Ground Center, Eglin Air Force Base, Florida, July 1963.
3. Yoshihara, T., Repair of Bomb Damaged Runway, NCEL-TR-297, Naval Civil Engineering Laboratory, Port Hueneme, California, June 1964.
4. Carroll, Gene E., and Paul Sutton, Development Test of Rapid Repair Technique for Bomb-Damaged Runways, APGC-TR-65-16, Eglin Air Force Base, Florida, February 1965.
5. Pichumani, Raman and James L. Dick, Effects of Small Cratering Charges on Airfield Pavements, AFWL-TR-70-66, Air Force Weapons Laboratory, Kirtland Air Force Base, New Mexico, December 1970.
6. Kvammen, Asbjorn, Jr., Raman Pichumani, and James L. Dick, Pavement Cratering Studies, AFWL-TR-72-61, Air Force Weapons Laboratory, Kirtland Air Force Base, New Mexico, December 1972.
7. Westine, Peter S., Bomb Crater Damage to Runways, AFWL-TR-72-183, Southwest Research Institute, San Antonio, Texas, February 1973.
8. Hokanson, Lawrence D., Soil Property Effects on Bomb Cratering in Pavement Systems, AFWL-TR-72-231, Air Force Weapons Laboratory, Kirtland Air Force Base, New Mexico, February 1973.
9. Cassino, Vincent, and David J. Chavez, Effects of Pavement Design on Cratering Damage From Penetrating Weapons, AFWL-TR-74-197, Air Force Weapons Laboratory, Kirtland Air Force Base, New Mexico, in publication.
10. Smith, Jimmy L., and William W. Morris, Structural Repair of Bomb Damage to Air Field Runways, AFWL-TR-73-214, Air Force Weapons Laboratory, Kirtland Air Force Base, New Mexico, February 1974.

11. Hokanson, Lawrence D., Tyndall Air Force Base Bomb Damage Repair Field Test, Documentation and Analysis, AFWL-TR-74-226, Air Force Weapons Laboratory, Kirtland Air Force Base, New Mexico, in publication.
12. Hokanson, Lawrence D., and Raymond S. Rollings, Field Test of Standard Bomb Damage Repair Techniques for Pavements, AFWL-TR-75-148, Air Force Weapons Laboratory, Kirtland Air Force Base, New Mexico, in publication.
13. Davis, L. K., Vulnerability of Runways to Conventional Warheads, Preliminary Draft, USA Engineer Waterways Experiment Station, Vicksburg, Mississippi, in publication.
14. Brooks, George W., and H. L. Davis, Development of a Concrete Runway Penetrator Munition - Simulated Runway Static Tests, AMD-ANA10408011-006, Martin Marietta Corporation, Orlando, Florida, September 1974.
15. Disaster Preparedness and Base Recovery Planning, Chapter 5 - "Rapid Runway Repair Procedures", AFR 93-2, Department of the Air Force, Washington, D. C., July 1974.
16. Harris, Terry M., Dynamic Response of an RF-4C Aircraft to a Bomb Damage Repair Patch, AFFDL-TM-73-22-FYS, Air Force Flight Dynamics Laboratory, Wright-Patterson Air Force Base, Ohio, February 1974.
17. Hokanson, Lawrence D., Analysis of Dynamic Aircraft Response to Bomb Damage Repair, AFWL-TR-75-138, Air Force Weapons Laboratory, Kirtland Air Force Base, New Mexico, in publication.
18. Gerardi, Anthony, and Adolf K. Lohwasser, Computer Program for the Prediction of Aircraft Response to Runway Roughness, Volume I Program Development and Volume II User's Manual, AFWL-TR-73-109, Air Force Weapons Laboratory, Kirtland Air Force Base, New Mexico, April 1974.
19. Whitman, R. V., The Response of Soils to Dynamic Loadings, Report 26, USA Army Engineer Waterways Experiment Station, Vicksburg, Mississippi, May 1970.

20. Rooke, A. D., B. L. Carnes and L. K. Davis, Cratering by Explosions: A Compendium and an Analysis, Technical Report N-74-1, U.S. Army Engineer Waterways Experiment Station, Vicksburg, Mississippi, January 1974.
21. Baker, W. E., and P. S. Westine, Similarity Methods in Engineering Dynamics, Hayden Book Company, Rochelle Park, New Jersey, 1973.
22. Buckingham, E., "On Physically Similar Systems; Illustrations of the Use of Dimensional Equations", Physical Review, Series II-4, October 1914.
23. Esch, Robin, "Functional Approximation", Handbook of Applied Mathematics, edited by Carl E. Pearson, Van Nostrand, Reinhold Company, New York, New York, pp. 942-998, 1974.
24. Guest, P. G., Numerical Methods of Curve Fitting, Cambridge University Press, London, England, 1961.
25. Daniel, C., and F. S. Wood, Fitting Equations to Data, Wiley - Interscience, New York, New York, 1971.
26. Young, C. W., The Development of Empirical Equations for Predicting Depth of an Earth-Penetrating Projectile, SC-DR-67-60, Sandia Laboratories, Albuquerque, New Mexico, May 1967.